

**Metamorphism and Deformation History of Precambrian Rocks of  
Sorobo, Konso Area, Southern Ethiopia**



*A Thesis Submitted to the School of Graduate Studies of Addis Ababa University in Partial Fulfillment of the Requirements for the Degree of Master of Science in Petrology*

**By: Aspirom Hangibayna**

**Advisor: Mulugeta Alene (PhD)**

**Addis Ababa University  
College of Natural Sciences  
School of Earth Sciences**

**June, 2015  
Addis Ababa, Ethiopia**

ADDIS ABABA UNIVERSITY  
COLLEGE OF NATURAL SCIENCES  
SCHOOL OF EARTH SCIENCES



METAMORPHISM AND DEFORMATION HISTORY OF PRECAMBRIAN  
ROCKS OF SOROBO, KONSO AREA, SOUTHERN ETHIOPIA

By

Aspiron Hangibayna

Approved by the Examining Board:

1. Dr. Mulugeta Alene  
Advisor \_\_\_\_\_  
Signature & Date
2. Dr. Mulugeta Alene  
Chairman, Dept Graduate committee \_\_\_\_\_  
Signature & Date
3. Dr. Asfawossen Asrat  
Examiner \_\_\_\_\_  
Signature & Date
4. Prof. Solomon Tadesse  
Examiner \_\_\_\_\_  
Signature & Date

June, 2015  
Addis Ababa, Ethiopia

## Abstract

Metamorphism and deformation evolution history of Konso Sorobo is described, which is part of the Pan-African Orogeny, Mozambique Belt of southern Ethiopia. It comprises polydeformed and metamorphosed mafic-ultramafic to felsic rocks, high grade complex gneiss rocks. Also syn- to post-tectonic intrusives that range from ultramafic to granitic in composition and various pre- to post-rift deposits are geologically described.

From field observations and petrological studies four phases of deformation and two metamorphic events are differentiated. D<sub>1</sub> predated migmatization and high grade metamorphism of the paragenesis. It has resulted large open recumbent isoclinal folds with nearly horizontal axial surface. D<sub>2</sub> phase formed open-reclined folds having NE axial surface. During D<sub>3</sub> phases, the rocks were intensively sheared creating tight flexures having NW axial surface and local mineral lineations were developed. Whereas D<sub>4</sub> was brittle-ductile deformation resulting faults owning several strike orientations.

Mineral assemblage of the area shows high grade metamorphism, which is represented by amphibolite facies to granulite facies. D<sub>1</sub> and D<sub>2</sub> phases were enhanced the progression of the M<sub>1</sub> metamorphism. Conversely, the existence of low temperature minerals in shear zones evidenced that there was retrograde metamorphism M<sub>2</sub>. This M<sub>2</sub> retrograde event was syn-D<sub>3</sub> and shows that late Pan-African Orogen-parallel shearing occurred, with the shear zones acting as important fluid conduits.

Epidotization, chloritization, serpentization alterations are common at plaes. Thin section studies evidenced (1) partial melting as the temperature raised and (2) drop in temperature led high pressure-temperature minerals to alter into low grade minerals.

**Keywords:** Metamorphism, Deformation, Progression, Retrogression

## Acknowledgements

First of all, I would like to thank the ‘Almighty God’ who made it possible to begin and finish the thesis research work successfully.

Then, I would like to thank Addis Ababa University and Department of Geology which sponsored and helped me to do the whole project. I really appreciate the department for being in collaboration during thin section preparation and microscope thin section analysis too.

I also owe heartfelt thanks to Dr. Mulugeta Alene whose grateful guidance and encouragement helped me to complete the work successfully and durably. He sacrificed his potential and time without feeling weariness apathy before and after the field work consultancy to the success of my entire project work. He also helped me by providing a lot of relevant reading materials.

Then, I am indebted deeply to Arba Minch University specifically, department of geology who helped me in field material facility including reading resources to accomplish the whole project work properly.

I am glad to thank the metrological agency bureau and the local people of Konso wereda who helped me by giving relevant secondary data of the area. I also have same heartfelt thanks to Dinote Garo who helped me in driving during field work.

Lastly, I have indebted to thank Ato Woldesilassie, Amdemikeal Z., Yemane K., and all my colleagues whose helps are unreserved to me in thin section preparation, petrographic mineral identification, software calibration, etc.

## TABLE OF CONTENTS

Contents	Page
1.1 Background .....	1
1.2 Goal and Scope of the Project.....	3
1.3 Location .....	3
1.4 Accessibility.....	5
1.5 Physiography.....	5
1.6 Climatic Condition.....	5
1.7 Ecology .....	6
1.8 Human Activity and Land Status.....	6
1.9 Objectives.....	7
1.9.1 General Objective .....	7
1.9.2 Specific Objectives .....	7
1.10 Methodology .....	7
1.10.1 Field Work and Mapping.....	7
1.10.2 Polarizing Microscope .....	8
1.11 Significance of the Study Results .....	9
2.1 Geological Description .....	10
3.1 Geological Map and Profiles.....	18
3.2 Charnockite .....	21
3.3 Amphibole Gneiss.....	22
3.4 Granulite Gneiss.....	24
3.5 Biotite-Hornblende Gneiss.....	26
3.6 Granitic Gneiss.....	28
3.7 Migmatite.....	30
3.8 Tremollite-Actinolite Schist.....	31
3.9 Tertiary Volcanics.....	33
3.10 Alluvial Deposits.....	33
3.11 Intrusion.....	34
3.11.1 Aplite Dikes .....	34
3.11.2 Pegmatite Veins and Quartz Veins/Veinlets.....	34
3.11.3 Felsite and Basalt Dikes .....	35
4.1 Geological Structures.....	36

4.1.1 S <sub>1</sub> Foliation.....	36
4.2.2 L <sub>2</sub> Lineation.....	40
4.1.3 Folds.....	40
4.1.4 Joints/Fractures .....	44
4.1.5 Faults.....	46
4.2 Equal-Area Projections .....	50
5.1 Metamorphic History.....	53
5.1.1 Metamorphism in Charnockite .....	53
5.1.2 Metamorphism in Amphibole Gneiss .....	54
5.1.3 Metamorphism in Granulite Gneiss .....	54
5.1.4 Metamorphism in Biotite-Hornblende Gneiss .....	55
5.1.5 Metamorphism in Granitic Gneiss .....	56
5.1.6 Metamorphism in Migmatite .....	56
5.1.7 Metamorphism in Tremolite-Actinolite Schist.....	57
5.2 Deformation Microstructures .....	58
6.1 Precambrian Metamorphic Assemblage .....	60
6.2 Precambrian Metamorphic Assemblage .....	60
7.1 Conclusions .....	62
7.2 Recommendation .....	63
Reference .....	65
Bibliography.....	70
Annex .....	72

## LIST OF FIGURES

Figure 1.1 Geological map of northeastern Africa, modified after Worku and Schandelmeier (1996) and Shackleton (1997), showing the Precambrian of southern Ethiopia. ....	2
Figure 1. 2 Simplified geological map of the Precambrian rock of southern Ethiopia (Asrat et al., 2001). .....	3
Figure 1.3 Location, accessibility, physiography and drainage map of the Study Area.....	4
Figure 3.1 Geological and structural map of Area of study.....	19
Figure 3.2 Geologic profiles along the lines A-A' and B-B' shown on the geologic map.....	20
Figure 3.3 Photographs of charnockite taken from Konso district .....	21

Figure 3.4 Photomicrographs mineral grains in charnockite rock .....	22
Figure 3.5 Photographs of amphibolites that show chloritization and sericitization alterations at places.....	23
Figure 3.6 Field photograph taken in amphibole gneiss showing compositional variation and banding.....	23
Figure 3.7 Photomicrographs mineral grains in amphibole gneiss.....	24
Figure 3.8 Granulite rock photographed in Konso, Sorobo .....	25
Figure 3.9 Photomicrographs mineral grains in granulite gneiss .....	26
Figure 3.10 Photomicrographs mineral grains of biotite-hornblende gneiss .....	27
Figure 3.11 (A) photograph shows exfoliation weathering in granitic gneiss. (B) Photograph shows weakly deformed xenoliths of amphibole.....	28
Figure 3.12 Microphotographs of mineral grains in granitic gneiss.....	29
Figure 3.13 Field photographs taken from migmatite patches show leucosome pods. ....	30
Figure 3.14 Microphotographs of mineral grains in migmatite rock .....	31
Figure 3.15 A thin layered amphibolite schist intruded in granite rock affected by strong deformations.....	32
Figure 3.16 Microphotograph shows mineral composition of amphibole schist. Crossed polar..	32
Figure 3.17 Pictures of soil and ash deposit taken from the area .....	33
Figure 3.18 Photographs of basalt and felsite dikes taken in field which weather to light orange. ....	35
Figure 4. 1 Photographs taken in Konso area that can depict the three ductile deformations .....	38
Figure 4. 2 Photographs taken in shear zones.....	39
Figure 4. 3 Pictures of subparallel to parallel alignment of elongated linear fabric elements in the rock.....	40
Figure 4. 4 Photographs of open-recumbent folds taken in field.....	41
Figure 4. 5 Pictures of open-reclined folds resulted by D2 deformation.....	42
Figure 4. 6 Light felsic band with very thin dark layered segregation in the granitic gneiss is folded by D3 deformation.....	42
Figure 4. 7 Photograph taken in the study area that shows boudinage in the granitic gneiss. ....	43
Figure 4. 8 Photographs of mesoscopic antiformal folds taken in the study area .....	43
Figure 4. 9 Photos taken in the field showing joints/ fractures.....	45

Figure 4. 10 Field photograph taken in amphibolite rock in granite showing the relative age of joint based on the vein cross-cut kinship .....	45
Figure 4. 11 Fault photographs taken in the field .....	48
Figure 4. 12 Structural map of the study area .....	49
Figure 4. 13 Equal-area projections for the whole data .....	50
Figure 4. 14 Best fit great circle for pole to plane of S1 foliation data using an equal-area projection .....	51
Figure 4. 15 Azimuthal poles of joint data using an equal-area projection .....	52
Figure 5. 1 Photomicrograph showing bastite texture in orthopyroxene .....	56
Figure 5.2 Micropictures resulted as temperature drop. ....	57

ABBREVIATIONS AND CONVENTIONS		
Minerals	Technical Abbreviation	Locality
Bt = biotite	MB = Mozambique Belt	KS = Konso Sample
Act = actinolite	ANS= Arabian Nubian Shield	
Cpx = clinopyroxene	EAO = East African Orogeny	
Opx = orthopyroxene	Fig = figure	
Ep = epidote	P/T= pressure temperature	
Grt = garnet	GBM = grain boundary migration	
Hbl = hornblende	UTM= universal Transverse Mercator	
Kfs = K-feldspar	AS= axial surface	
Pl = plagioclase	EIGS = Ethiopian Institute of Geological Survey	
Qtz = quartz		
Rt = rutile	PPL= Plan polarized light	
Zr = zircon	XPL= Crossed polarized light	
Chl = chlorite	N = number of data	
Op = opaque	T. Basalt = Tertiary Basalt	
	Contour Int = contour interval	

**1.1 Background**

The Arabian Nubian Shield (ANS) in the north and the Mozambique Belt (MB) in the south, together, formed the East African Orogen (EAO). These two major terranes have a paramount key to understand the geodynamic and temporal evolution of the whole Pan-African orogeny in northeast Africa (Vail, 1976; Kazmin et al., 1978; Bonavia and Chorowicz, 1992; Stern, 1994 and Asrat and Pierre, 2003) shown in the figure 1.1 below. The authors noted that Precambrian rocks of southern Ethiopian shield occupies an important position within the EAO which lies at the junction of Neoproterozoic (880–550 Ma). Two distinct tectonostratigraphic terranes, separated by repeatedly reactivated deformation zones, are recognized in the Precambrian rocks of southern Ethiopia: (1) granitic-gneiss terrane, which is classified into sub-terrane and complexes and (2) ophiolitic fold and thrust belts (Stern et al., 2012). The Konso pluton is one of the localities in Burji-Fincha Complex which in turn sub-terrane of granitic-gneiss terrane in Mozambique Belt.

The East African Orogen is formed as a complete closure of Mozambique Ocean by the assembly of crustal blocks belonging to East and West Gondwana and shows marked changes of lithology, metamorphism and tectonic style spanning the period of 800–450Ma. Pan-African tectonothermal activity in the Mozambique Belt was broadly contemporaneous with magmatism, metamorphism and deformation in the Arabian–Nubian Shield but their difference in lithology and metamorphic grade has been attributed to the difference in the level of exposure, with the Mozambican rocks interpreted as lower crustal equivalents of the juvenile rocks in the Arabian–Nubian Shield. Based on the recent geochronologic data Pan-African orogen has two major distinct series of tectonic events: 1) East Africa series: - 800–650Ma, and 2) Final suturing of the Australian and Antarctic segments of the Gondwana continent: - 550Ma (Stern, 1994; Meert, 2003 and Yibas et al., 2003b).

Precambrian rocks in Ethiopia are exposed in four major regions (Fig. 1.2): in northwest (Tigray), in the west (Gojjam, Wollega, Illubabor and Kefa), in the southwest (Sidama & Bale) and in the northeast (Hararghe) (Kazmin, 1978; Mengesha et al., 1996) as studies.

The crystalline basement rocks of southwest Ethiopia are outcropped in two main parts: in Illubabor and south west of Kafa, and in Gemu Gofa south west of Sidama. These are divided in

to three, namely the Hammar domain, the Akobo domain and the Surma domain based on the lithological, metamorphic and structural contrasts (Davison et al., 1973, Davison 1983).

The geodynamic evolution of the MB and ANS are implied based on a review of existing geochronological data on the Precambrian rocks of Ethiopia (Asrat et al., 2001 and Asrat and Pierre, 2003) indicates that three periods of granitic magmatism can be identified in both the Arabian Nubian Shield and the Mozambique Belt: 885–800, 780–700 and 660–540 Ma. In the neighbouring metamorphic terrains of Northeast Africa, Kenya, Madagascar, Sudan and Saudi Arabia similar magmatic episodes were documented (Key et al., 1989; Paquette and Nédélec, 1998; Kröner et al., 1991; Abdelsalam and Stern, 1996). The first two episodes are characterized by the emplacement of syn-tectonic granitoids, whereas the later corresponds to the emplacement of late- and post-tectonic granitoids. These ages roughly correspond to major structural and metamorphic events in Ethiopia (Ayalew et al., 1990; Teklay et al., 1998; Tadesse et al., 2000).

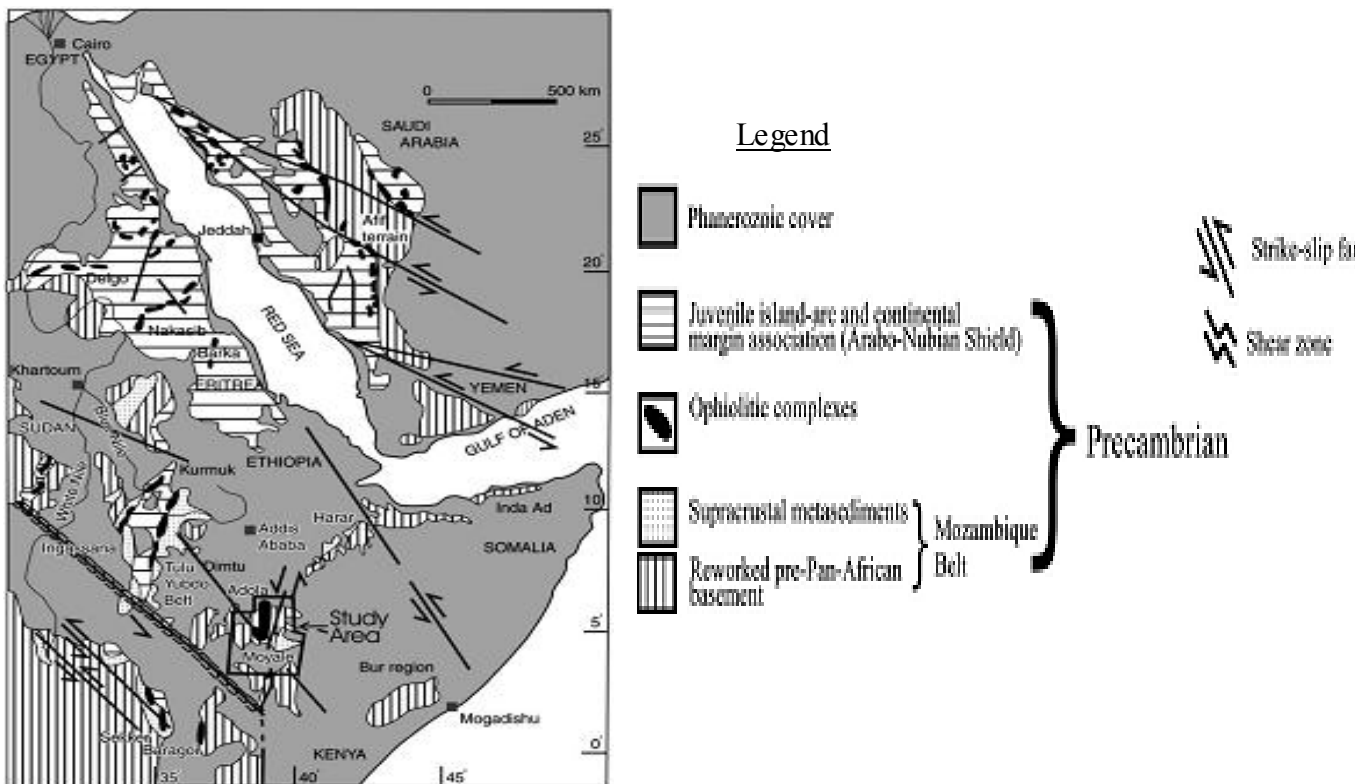


**Figure 1.1 Geological map of northeastern Africa, modified after Worku and Schandelmeier (1996) and Shackleton (1997), showing the Precambrian of southern Ethiopia.**

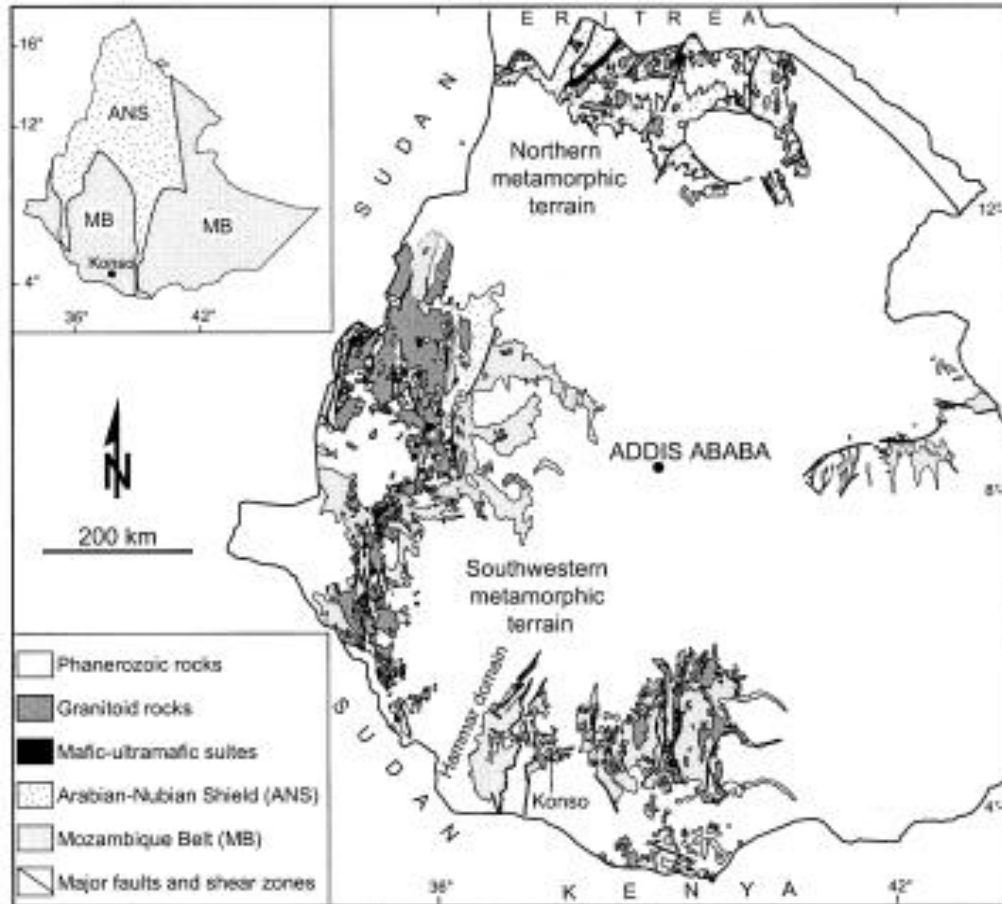


Figure 1.2 Simplified geological map of the Precambrian rock of southern Ethiopia (modified after Asrat et al., 2001).

## 1.2 Goal and Scope of the Project

The present thesis paper is a study of high-grade metamorphic rocks from Sorobo kebele stream cut outcropping in Konso district. Very thick succession of alluvial deposits lain down on the basement rock. Good exposures occur where the area is dissected by rivers and streams. Determination of joints and their infilling intrusion relative age relationship is focused.

The main purpose of this work is to study structural features and metamorphic mineral reactions which characterize the area. Retrogression processes and partial melting notably have been done under the scope of petrological studies and their occurrences documented in migmatite rock. Correlation between the large scale data, and the detail mapping performed in the area are done.

## 1.3 Location

The area of study Sorobo, is situated in southwestern part of Ethiopia within Southern Nations Nationalities and Peoples Regional State, particularly in Konso district. It is fairly about 12 km

far from the town of Konso (Fig. 1.3 below) in northwest direction. The area lies on the aerial photo imagery series ET<sub>1</sub>: 5/S/6/06:- 0451 and 0452 from Bekawile subsheet (index: 0537 C2). It is bounded between 0594000-0599000N and 318000-324000E on UTM reading covering 30 km square.

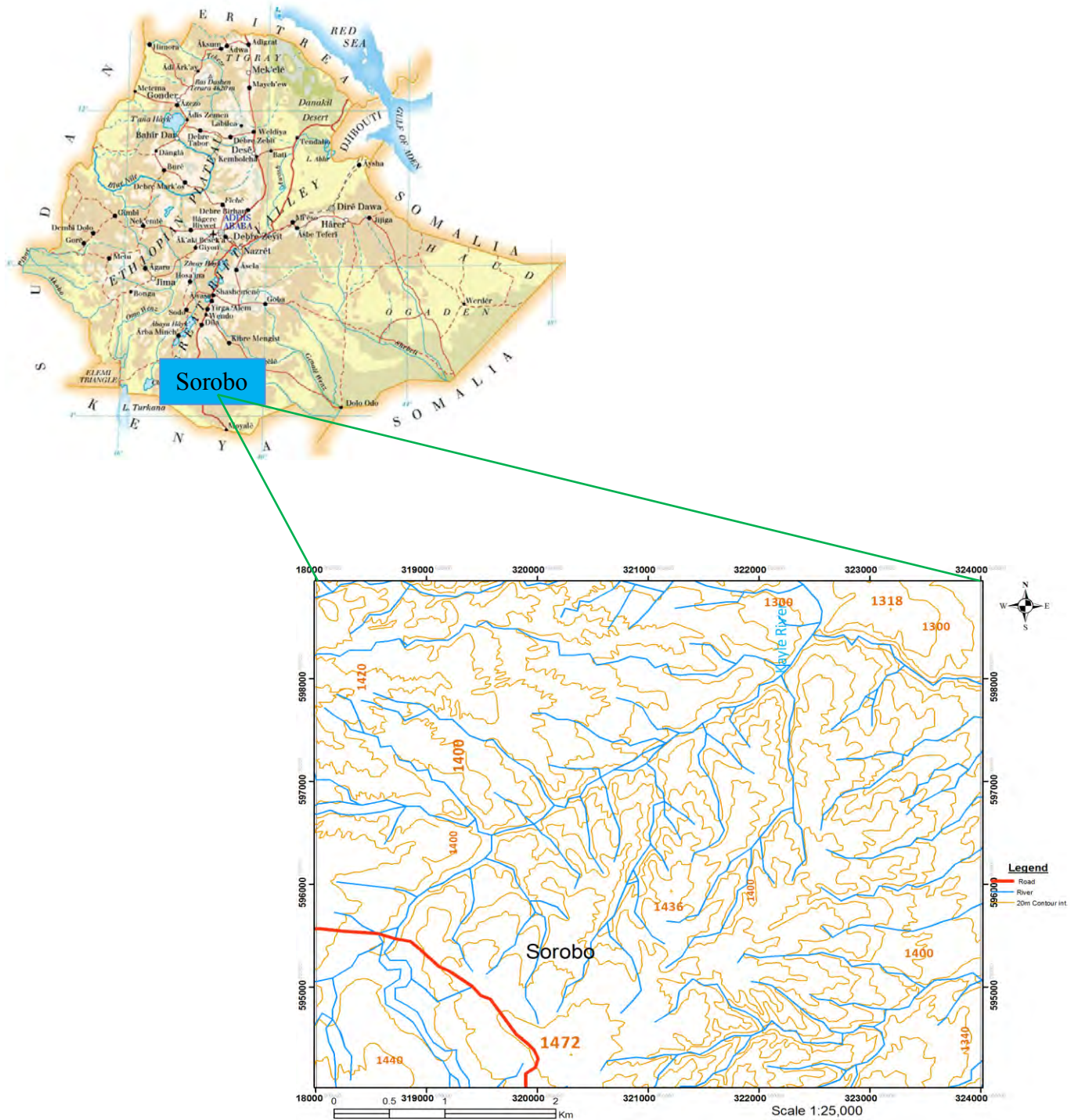


**Figure 1.3 Location, accessibility, physiography and drainage map of the Study Area**

#### **1.4 Accessibility**

Konso is located at a distance of about 564 km from Addis Ababa and can be reached from Addis Ababa through Hadiya and Arbaminch. The road from Addis Ababa through Arbaminch to the study area is asphalted, except the weathered road branching off (at about 35 km from Arbaminch) from Gidole road up to Gato which is about 25 km. The area of study can be accessed through Konso-Jinka or Konso-Arbaminch main road. There are also several foot trails to take good geologic exposure over the entire area from the main road to the target location (see figure 1.3 above).

#### **1.5 Physiography**

The local study area, Sorobo is characterized by highly to moderate rugged topography with a general elevation decreasing from south towards north and east directions. The site is typified by top soil covered highlands which are dissected by deep valleys of creeks and/or streams except some places where they have been covered up by quartz rocks. The respective highest and lowest elevations in the area are 1472 m south of study and 1247 m towards northeast above mean sea level.

The area is highly affected by geotectonic activities that paved preferred passage for the surface runoff, which formed nearly dendritic patterns (branches of segments) up to 3<sup>rd</sup> order of stream and have moderate to high density when generally looked over the whole area (Fig 1. 3 above) where most of them are drain eastward direction. But one is draining towards northwest over small portion until it turns to the east. All the streams are non-perennial in nature, but the sand in the deep valley oozes water. Even though the area is extremely exposed to erosion, a comprehensive terracing was carried out against hill terrain which helps to retain moisture and prevent fragile soil from being washed away by surface-runoff.

#### **1.6 Climatic Condition**

The Konso district is characterized by subtropical dry and hot climate in which the coldest temperature drops to 15.5<sup>0</sup> C and the hottest would raise to 32.4<sup>0</sup> C. The average annual temperature is 23.95<sup>0</sup> C. The area has two characteristic rainfall terms that range from March to May and September to mid November. The March to May one is the main rainy season in which the area receives the highest rainfall in mm and mostly accompanied by east-west blowing heavy

wind. The average annual rainfall is about 623.6 mm (source: Development Data Collection Dissemination Core Work Process- finance and economic development).

### **1.7 Ecology**

Even though the climate of area is optimal for plant growth, the vegetation cover of the area is too little. This is because of the inconsistency nature of the rock or the soil that has not been developed well in the vicinity. Another problem for the rareness of the flora is deforestation for cultivation and other purposes by the local community. As the result of these reasons, the remnants of the flora in the study area are at scrubs and bushes stage, except little acacia and few trees.

As a consequence of very puny vegetation and incited attitude of the local people for hunting, almost all of wild life higher animals in the area have been vanished. Although, the wild life of the higher animals were evicted and migrated from the area due to the above two major factors, there are yet few fauna of lower animals like gazelle, fox, rabbit, snake, apes, different kinds of lizards, different fowl and birds.

### **1.8 Human Activity and Land Status**

The inhabitants of the area, Konso people whose native language is Konsigna which belongs to Cushitic family language. The total population of the Konso district is about 250,750; from which the Sorobo kebele accounts 6330 people (year: 2005 E.C). The people are densely populated at town, whereas moderately to sparsely populated in other sites.

Religiously, the area is known for four common religions; (1) Christian (protestant, orthodox and catholic), (2) Muslim, (3) Traditional religious, and (4) Others.

They have appreciable distinctive living, feeding and wearing styles. They are known for own common food and drink known as '*Kurkufa*' and '*Cheka*', respectively.

The people depend more upon the agriculture for means of existence. The land is more privately owned by the local farmers. They cultivate both subsistence crops (like sorghum, maize, teff), and supplementary crops (like root, crops and pulse and flowering plants in places which are intensively cultivated in elevated areas). Additionally, they breed cattle, goats, hen, donkey and rarely sheep. Beehive activity is taking place in traditional way commonly in the study area.

The administration provides facilities of bank, telecommunication, postal, health (extend to hospital), schools (up to college), tap water, hotel, and shopping services.

## **1.9 Objectives**

### **1.9.1 General Objective**

The project study is generally intended to determine the nature of mineral transformation history as a result of mineral reactions which characterize the area under the influence of deformation and metamorphism processes with implication of MB in the realm of metamorphic terrain.

### **1.9.2 Specific Objectives**

In brief sense, the project research holds several particular aims but can be studied under same scheme. Thus, the specific rationales of this work are:

- ❖ To understand and identify the metamorphism and deformation relationship on the basis of field data and petrographic study.
- ❖ To identify the paragenesis of the grade of metamorphic facies at local level.
- ❖ To recognize the occurrence of partial melting and retrogression events in the area.
- ❖ To understand metamorphic and deformation history of the study area.
- ❖ Finally, to construct detailed large scale litho-structural map (scale 1:25,000) of the area.

## **1.10 Methodology**

### **1.10.1 Field Work and Mapping**

A lot of relevant literatures have reviewed to have a general overview about the geology, geochemistry, and geodynamics of the study area and surrounding regions as well. This part provides important and solid information about the area what other authors did and recommended to be done earlier. Their findings are used as an input for this research work.

Interpretation of maps, aerial photographs using table stereoscope and satellite image ries (from Google earth) were done before field work to have general outlook about the study area. Both satellite imagery and aerial photograph interpretation showed that there is northeast southwesterly trending large lineament or fault feature in the field of study; but during field tours, it is not seen.

During the field season, twelve traverse lines are selected across the geology following river routs. In each traverse, at least not less than fifteen stations are taken along the traverse line at different places. All the data were transferred onto 1:25,000 topographic maps and field geological maps prepared. In this way the entire area is accessed. Over 21 rock representative samples from each unit were taken overall the study area. The main purpose of this large scale sampling was (1) to identify the dominant rock types and (2) to collect data of foliation, planes, folds and lineation in order to determine the area's structural trend. Nevertheless, considering the difficult topography and the lack of valuable outcrops out of rivers or stream routs, most of the works have accessed along the river exposures. To construct the geological map, a systematic record of structural features and lithology has been done, with a special emphasis on the earlier nature of the rocks. High grade lenses or relics have been especially described.

Back the field laboratory studies include: the detailed petrographic and fabric/microstructural examination of 10 thin section samples of metamorphic rocks under polarizer microscope to understand the metamorphic conditions of each deformation, and to support and/or control the results of structural analysis carried out during field studies. This petrographic study was helped mineral identification which was somehow difficult in the field and in addition it aided to quantitatively percentile each mineral in a rock.

Equal-area projection software (StereoWin, version 9.0.2 software) has been used to quantitatively represent three-dimensional orientation data (such as the attitudes of linears and planes) on a two-dimensional plot to analyze the structural data and visualize the connection between the orientations of structures in the field and/or on the map and the complex patterns of lines/planes plotted on this azimuthal projection. Form this projection the general outlook of the structural pattern is attempted to be seen also. Field data were compiled using ArcGIS (version 9) software to produce the detail geological map at scale of 1:25,000, which shows lithological units, major geological structures, stratigraphic sequences and foliation orientation. The map of drainage pattern was generated together with accessibility map at the same scale.

### **1.10.2 Polarizing Microscope**

As the main analytic tool, a “Leica DM EP” petrological/transmitted light microscope has used to identify minerals beyond hand specimen scale. Microphotographs were acquired with a normal digital camera (Casio 12.1Mega pixels all pictures have taken in the dimensions 3264x2448) or not with a microphotograph. Ten thin sections have been prepared considering the limited

lithological variations in the area that have been sampled. Thin sections were prepared cut normal to foliation and parallel to lineation when possible.

Focus has given on both the deformation microstructures and the petrography. Unfortunately, still valuable microstructures are not seen except in the amphibole schist. The petrography has been studied with the help of different text books listed in the bibliography part.

### **1.11 Significance of the Study Results**

Literatures about metamorphism and deformation history of Konso district are not extensive. If the area is mentioned in many papers treating about the Konso rocks, the relationships between the deformation and metamorphism in the vicinity are usually shortly described. Some papers are found which thoroughly describing the lithological, geochemical and structural aspects of the Konso geology. According to the Melesse and Demerew (2003) detailed work report on Jinka Base Metal exploration project, local areas Orbele, Lahayte and Gelado are highly associated with economic minerals. But in the proposed area, thus far, structural and mineralization relationship has not been studied in detail where the potentially exploitable minerals are clearly unnoticed which inspired the researcher to formulate this project research.

Therefore, this research project was particularly designed to study structural-mineralization relationship and the effect of metamorphism on deformation and vice versa in the area of study in detailed scale. Furthermore, the research was come across with the relationships between the tectonic fractures and minerals transformation and availability as well. For particular emphasis was given on the assessment of the mineral potential of the Precambrian rocks on the field data and petrographic study, the result will help others to further investigate and exploit economic mineral deposits. In addition, it will serve as an important data source for mining companies as well as academic purposes. Generally, since the research was systematic study of geologic and structural relationship work, it aims to present and provide guidance throughout the different events in their interpretation of geochronological evolution which made up the Konso metamorphic rocks.

## 2.1 Geological Description

Many researchers carried out geological, exploration and research works at different scales for different (economic and academic) purposes at various geographic positions on Precambrian rocks of the Mozambique Belt and the Arabian Nubian Shield. Based on structural style, metamorphism and tectonic setting several classifications of the Precambrian rocks were proposed by different authors.

The Pan-African Orogeny in the north-east Africa consists of two major terrains: the Arabian Nubian Shield and Mozambique Belt (Vail, 1976; Kazmin et al., 1978; Bonavia and Chrowicz, 1992; Asrat and Pierre, 2003). A review of existing data (Asrat et. al., 2001) indicates that the ANS is an accretionary terrane of juvenile material (volcanic and volcano-sedimentary rocks) with dominantly subduction-related magmatism, whereas the MB involved more recycling of older crustal material (gneisses and migmatites) and dominantly post-collisional magmatism. So, several generations of granitic rocks are described in both the ANS and MB.

According to Alene and Barker (1993) study the Moyale-Agal region comprises polyphase metamorphosed and deformed mafic-ultramafic rocks, granodiorite and subordinate amount of metasedimentary rocks. As this study indicated, D<sub>1</sub> to D<sub>4</sub> phases of deformation and M<sub>1</sub> and M<sub>2</sub> metamorphic events are described in the region.

Ethiopia can be divided in to four major physiographic regions widely known as the Eastern plateau, South-east plateau, the main Ethiopian rift and Afar depression (EIGS, 2010) and the geology of Ethiopia is characterized by different rock types ranging in age from Precambrian to recent time. These rocks are categorized into three major geological formations: - Precambrian rocks, Paleozoic – Mesozoic sedimentary rocks and Cenozoic volcanic rocks and associated sediments.

Precambrian metamorphic and associated intrusive igneous rocks make up 25% of the country's landmass. They are exposed in the northern, western, southern and eastern parts of the country and have a fundamentally important tectonic position in that they occupy the interface between the MB with predominantly reworked older crust in the south and the Arabian Nubian Shield (ANS) with abundant ophiolite fragments in the northern Africa. Stern (1994) coined the term

East African Orogen (EAO) to encompass both the MB and ANS. EAO represents a plate tectonic cycle spanning a time-period of 350 Ma, beginning by about 900 Ma with rifting and continental break-up and ending by about 550 Ma subsequent to a continent-to-continent convergence collision between East and West Gondwana (Vail, 1985; Berhe, 1990; Alene and Barker, 1993; Abdelsalam and Stern, 1996; Asrat et al., 2001). Based on the reconnaissance review of geochronological, geochemical and metamorphic data, Asrat et al. (2001) concluded that the Arabian Nubian Shield and Mozambique Belt were formed coevally with the Pan-African Orogeny (950-500Ma).

The Precambrian rocks are dominantly north-trending linear belts of low-grade volcano-sedimentary rocks and mafic-ultramafic rocks, sandwiched between medium- to high-grade gneisses and migmatites. The high-grade gneisses and migmatites are referred to as Lower Complex which is part of the Mozambique Orogenic Belt and generally consist of amphibolite facies (with locally granulite facies) orthogneisses, paragneisses, migmatites, and amphibolite with bands of marble. The low-grade volcano-sedimentary rocks with associated mafic to felsic intrusives, which are referred to as Upper Complex, on the other hand, they belong to the Pan-African Arabian-Nubian Shield. The linear belts of mafic and ultramafic rocks are commonly confined to major shear zones and often mark the contacts between the high-grade gneisses and migmatites and the low-grade volcano-sedimentary rocks. Most ages obtain from these rocks range between 900 and 500 Ma with exception of older Archean and Mesoproterozoic ages obtained from some of the rock units (Yibas, 2000).

The blocks of gneissic terrains which are considered to be generally older than the volcano-sedimentary belts that they commonly enclose, consist of high grade heterogeneous orthogneisses and paragneisses, at upper, amphibolite to granulite facies metamorphism. Metamorphic facies in the low grade volcano-sedimentary succession, however, typically range from green schist to lower amphibolite facies. The most conspicuous foliation trend is N-S with deviation to NE and NW. These trends are characteristics of both the low grade volcano-sedimentary succession and the high grade rock. The boundaries between the gneissic and volcanic sedimentary-sequences up are typically of tectonic origin. Additionally, gneissic rocks are strongly deformed, steeply folded and show regional NW-SE trending foliation with its steep NE dip (Amenti et al., 1992). The Plutonic rocks occur as discrete bodies of gabbro, diorites, syn -late- and post tectonic granite accompanied with leucogranite-aplite and pegmatite dykes (Asrat and Pierre, 2003).

According to EIGS (2010) study, the Precambrian rocks have received attention in the current exploration activity for base and precious metals. The belts of mafic-ultramafic rocks and major shear zones bounding the two contrasting lithostratigraphic complexes are potential targets for gold, base metals, nickel, platinum and other mineralization.

The Precambrian rocks of southern and southwestern Ethiopia were traditionally divided into Lower, Middle and Upper Complex based on the variation in grade of metamorphism (Kazmin, 1972; Kazmin, 1978). The metamorphic grade was thought to decrease from the Lower to the Upper Complex. These authors also noted that the Lower Complex is presumably Archean whereas the Upper Complex is Neoproterozoic in age. Kazmin (1972) concluded that the high-grade gneisses and granulites of the Lower Complex may correlate with the high-grade granulites of Uganda. In southwestern Ethiopia, de Wit and Chewaka (1981) recognized that the lithological boundaries and structural trends are transected by the granulite isograd. They concluded that the granulite facies metamorphism represented a younger event in the metamorphic evolution of the region, and so challenged Kazmin (1972) suggestion that the high-grade gneiss and granulites are old Archean lithosphere similar to those found in Uganda. Moreover, geochronological data (Amenti et al., 1992; Worku, 1996b; Teklay et al., 1998; Yibas et al., 2002; Tadesse, 2003) favored the conclusion that the high-grade gneisses and granulites are not necessarily older than the low-grade volcano-sedimentary rocks.

The Precambrian rocks of south and southwestern Ethiopia comprises both high-grade gneissic terrane of the MB and low-grade metavolcano-sedimentary sequences of the Arabian-Nubian Shield. Various models have been proposed to explain the relationship between the MB and the ANS. As Kazmin et al. 1978 proposed that the high-grade rocks of the MB extend beneath the low-grade rocks of the ANS forming a basement-cover relationship. Others (de Wit and Chewaka, 1981; Vail, 1985; Berhe, 1990; Abdelsalam and Stern, 1996 and Stern, 1994) have suggested subduction-accretion processes between arc terranes of the ANS and predominantly gneissic terranes of the MB, which resulted in collisional amalgamation of lithotectonic terranes across sutures. Furthermore, Burke and Sengor (1986), Bonavia and Chorowicz (1992) and Stern (1994) invoked escape tectonics and proposed that the N-trending structures in southern Ethiopia are the roots of northward expulsion of the ANS from the MB, following a Tibetan-type continent-continent collision between east and west Gondwana along the MB after the consumption of the Mozambique Ocean. However, this model has been disproved by (Warden

and Horke1, 1984; Ghebreab,1992; and Worku and Yifa, 1992) all of whom argued that subduction has not occurred in the past time and the mafic-ultramafic rocks are intrusions into the high-grade gneissic rocks through brittle-ductile shear zones, suggesting an ensialic or intracratonic rift basin model, which did not develop into a passive plate margin (de Wit and Chewaka, 1981; Berhe, 1990; Behrmann and Woldehaimanot, 1995; Worku, 1996a; Bedru, 1999; Yibas, 2000) all advocated a Wilson cycle orogenic process to explain the evolution of the Precambrian rocks of southern Ethiopia.

The geology of southern Ethiopia has divided into two distinct folds of lithostratigraphic terranes which show separately contrasting lithological association, internal structures and grade of metamorphism: (1) the granite-gneiss terrane, consisting of high-grade paragneiss, orthogneiss and deformed and metamorphosed granitoids; and (2) the ophiolitic fold and thrust belts, consisting of low-grade, mafic-ultramafic and sedimentary assemblages each at varying proportions. Major fault/shear zones displaying multiple deformation features separate these two terrane types (Yibas, 2000; Yibas et al., 2000).

In another hand, the geology of southern Ethiopia is subdivided into three distinctive folds: Lower complex, Middle complex and Upper complex based on metamorphic grade and deformational differences (Kazmin, 1972). The Lower complex consists of Burji gneiss, Yabello gneiss, Awata gneiss, Alghe gneiss and Konso gneiss. The Middle complex comprises the terrigenous rocks of the Wadera group. The Upper complex is represented by Adola group.

The geological framework of southwest of Ethiopia is divided in to four units in this area based on age (Davidson, 1983). These are the crystalline basement (Precambrian early Paleozoic), Terrestrial sediments (Permian), pre-rift volcanic rocks (Eocene to Miocene), and post-rift deposits (late Miocene to Holocene). All the units have been separated by unconformity, except the unit between pre- and post-rift deposits.

The crystalline basement rocks are exposed in Illubabor, south west of Kafã, south west of Gamo Gofa and south west of Sidamo. These basement rocks are also further divided in to three domains; namely the Hammar domain, the Akobo domain and the Surma domain (Davidson, 1983). According to his study, the Hammar domain contains a complex of older gneiss and granulite that are highly deformed, recrystallized and in part migmatized with a suite of younger plutonic rocks that are much less to not all deformed and crystallized. He also reported that the

Akobo domain is defined by supracrustal schist and gneisses intruded by large quantities of gabbroic to granitic rocks. The metamorphic grade ranges from green schist facies to middle amphibolite facies. In the same work, the Surma domain is interlayered crystalline basement and observed being weathered. Permian terrestrial sediments occur unconformably overlying on the base rock as small tilted and mildly folded remnants. A thin red residual sandstone unit that blankets the crystalline basement beneath early tertiary flood basalt cover is of unknown age, and could be old as tertiary.

The pre-rift tertiary volcanic rocks are exposed at higher elevations in Gamo Gofa, Illubabor, South western Sidamo and Southwestern Kafa lying with profound unconformity on the crystalline basement and locally on the Permian sandstones (Davidson, 1983). He classified post rift deposits in to three types, fluvial and lacustrine stream sediments with inter related tuffs and flood basalt sheets associated with centers, not specifically controlled by rift valleys and Nile basin.

Amenti (1996) argued the Precambrian rocks of the southern Ethiopia form the northern part of the Mozambique Belt. He described the lithologic units of the southern Ethiopia into high grade gneiss, pelitic to psammitic as well as mafic to felsic that are partially migmatized. He identified  $M_1$  and  $M_2$  metamorphic events mostly middle to upper amphibolite facies, and he also indicated the occurrence of granulite facies southeast of Jinka. He suggested five phases of deformation in which  $D_1$  and  $D_2$  are related to folding and  $D_3$ ,  $D_4$  and  $D_5$  are related to strike slip shear zones.

As it is stated by Ethiopian Institute of Geological Survey (2010) rocks in Konso region are divided into three major classes based on the degree of metamorphism, structural style and mineralogical composition. These are Precambrian metamorphic rocks, Tertiary-Quaternary volcanic rocks and Quaternary deposits.

The Konso gneiss was initially interpreted as the lowest lithostratigraphic unit in the Lower Complex because of its similarity to relict high-grade Archean terrains in the Ugandan basement. However, this unit which shows no comparable evidence of reworking probably represents a localized geothermal peak of the terminatory Mozambiquean metamorphism whose isograds transgressively overprint the primary layering (Warden, 1981; Davidson, 1983). If the foregoing interpretation is correct, the lowest structural unit is the Alge gneiss which comprises a rather monotonous biotite-amphibole gneiss-migmatite-granodiorite gneiss sequence possibly

equivalent to the grey gneiss of the Sudan (Vail, 1976). It is overlain by the more variable Awata gneiss mainly consisting of mafic gneiss with pelitic and psammitic units, and banded magnetite quartzite. Tectonised lenses of talc-tremolite schist within the mafic gneisses represent a disrupted ultramafic unit. The Konso pluton is an amalgamated intrusion of peraluminous and ferro-potassic granites and subordinate coeval metaluminous monzodiorites, intruded into high-grade gneiss–migmatite associations of the MB where the whole suites display chemical features of A-type granites (Asrat and Pierre, 2003). In this report it is concluded, Konso pluton is the witness of an Ordovician A-type magmatic event, which marks a change from convergence, related to the Pan-African collision, to extension in the Mozambique Belt of southern Ethiopia.

Metamorphic and deformation processes have brought several characteristic features of whole rocks like banding and alterations in Konso area (Brodie and Rutter, 1985; Melesse and Demerew, 2003). As their discussion results of the report, the high grade metamorphic rock was retrograded by regional shearing and presumably fluid activity, resulting adequate deposits of mineralization in the region associated particularly with the amphibole gneiss.

The metamorphic complex with its associated plutonic rocks that make up the crystalline basement rock of Ethiopia is part of the Mozambique Belt, itself part of the Pan-African Orogenic System of late Precambrian to earliest Palaeozoic age. The Mozambique Belt is a Neoproterozoic, polycyclic, collisional belt that extends along and underlies the eastern margin of much of the African continent (Shackleton, 1997). It is characterised by folds and metamorphic fabrics that trend between NNE and NNW and consists of high-grade, amphibolite- to granulite-facies rocks (Gichile, 1992) forming a gneissic-migmatitic complex. In Ethiopia, the MB is exposed in the south and south-west and forms a front with the ANS, a lower grade (greenschist facies) calc-alkaline volcano-sedimentary terrain to the north.

The studies of de Wit and Chewaka (1981), Davidson (1983) and Gichile (1992) indicated that the evolution of the south-western metamorphic terrain forms part of the whole evolution of the Precambrian of Ethiopia, which involved early rifting that gave way to an ocean basin at ~1,100–1,000 Ma. Compression resulted in a west-dipping subduction zone and associated volcanic arcs at ~900–750 Ma. Later, at ~750–650 Ma, the island arc crust was extended. Gneissic-granulitic formation complex is considered to have involved periodic closure of the inter-arc basins through subduction, uplift and Himalayan-type continental collision and associated metamorphism followed by retrogression at ~650–450 Ma. Plutonic suites emplacement started

prior or subsequent to the first metamorphic event (syntectonic plutons), and possibly continued up to tens of millions of years after the closing stages of collision (post-tectonic plutons).

The Hammar domain, which corresponds to the eastern sector of the south-western metamorphic terrain of Ethiopia, contains two major rock groups: an older gneissic complex and several generations of plutonic suites of which the Konso pluton is the one (Davidson, 1983). The gneissic complex comprises mafic, intermediate, felsic as well as metasedimentary gneisses and granulites, which were metamorphosed to middle-upper amphibolite and locally to granulite facies conditions. The gneissic rocks are strongly and steeply folded, and show regional NNW–SSE-trending foliations with steep NE dips. The plutonic rocks occur as discrete bodies of gabbros, diorites, syn-, late- and post-tectonic granites accompanied with leucogranite, aplite and pegmatite dikes. The emplacement of intraplate alkali-granite ring complexes and associated volcanic rocks started at 450 Ma and continued till 20 Ma in the surrounding Pan-African terranes in Sudan and Somalia (de Wit and Chewaka, 1981; Vail, 1985; 1989).

The geodynamic evolution of the MB and ANS is implied based on a review of existing geochronological data on the Precambrian of Ethiopia (Asrat et al., 2001 and Asrat and Pierre, 2003) indicates that three periods of granitic magmatism can be identified in both the Arabian Nubian Shield and the Mozambique Belt: 885–800, 780–700 and 660–540 Ma. In the neighbouring metamorphic terrains of Northeast Africa, Kenya, Madagascar, Sudan and Saudi Arabia similar magmatic episodes were documented (Key et al., 1989; Paquette and Nedelec, 1998; Kroner et al., 1991; Abdelsalam and Stern, 1998). The first two episodes are characterised by the emplacement of syn-tectonic granitoids, whereas the later corresponds to the emplacement of late- and post-tectonic granitoids. These ages roughly correspond to major structural and metamorphic events in Ethiopia (Ayalew et al., 1990; Teklay et al., 1998; Tadesse et al., 2000).

According to (Vail 1985, 1989; Ayalew and Gichile, 1990; Kuster, 1993; Hohndorf et al., 1994) studies; there were two episodes of granitoids emplaced during the closing events of the Mozambique Belt; post-collisional granitoids emplaced at 580–540 Ma by the emplacement of an orogenic granitoids in the period between ca. 470 and 20 Ma. The Rb–Sr isochron and the zircon U–Pb isotopic data placed the Konso pluton at ca. 450 Ma implying that it is post-tectonic in the MB where all these granites are not Pan- African (Asrat and Pierre, 2003). Furthermore, the emplacement of ferro-potassic, metaluminous to peraluminous Konso granites in MB

displays the properties of anorogenic suites marking a change from convergence to crustal extension (Eby, 1992).

The lower initial Sr ratios (Asrat and Pierre, 2003) and other similar studies (Kuster and Harms, 1998; Teklay et al., 1998; Asrat et al., 2001) show that the MB is not simply a zone of reworking of older crustal materials (as a result of subduction and collisional processes), but was also a zone of accretion at around 0.8 to 1.0 Ga in southern Ethiopia. On the other hand, ANS (north east Africa and western Arabia) is predominantly composed of juvenile continental crust materials that were formed when smaller arc terranes were generated within and around the margins of a large oceanic tract known as Mozambique Ocean, associated with closure of the ocean basin due to subduction and also its calc-alkaline nature of the granitic rocks and their derivation from a primitive source (Ayalew et al., 1990; Stern and Dawoud, 1991; Stern, 1994; Asrat, 1997; Teklay et al., 1998; Tadesse et al., 2000; Asrat et al., 2001, 2002). Both MB and ANS were sites of subduction processes related, but an old continental crustal involvement is limited to MB. A chronological relationship has made between intrusion of post-collisional, potassic granites and late Pan-African high-grade metamorphism. Therefore, the emplacement of the Konso pluton at ca. 450 Ma largely post-dates the latest granulite-facies metamorphism (580–545 Ma); which was nearly contemporaneous to post-collisional uplift and to the most intense period of granitic magmatism (580 to 540 Ma) in the Mozambique Belt of southern Ethiopia (Kuster and Harms 1998; Ayalew and Gichile, 1990).

According to the Temtme (1955) report there is an occurrence of copper mineralization in the Surma region in the southern Ethiopia. The geologies of southern and southwestern Ethiopia have described in detail Mohr (1960), Jelenc (1966), Gilboy (1970), and Chater (1971). The southern region is mapped, the granulite rocks description, lithostratigraphic discussion and evolution of the Precambrian rocks by Kazmin (1972). Amenti (1996) compiled the Precambrian rocks of southern Ethiopia encompassing the area of study. There are occurrences of minerals such as base metal sulfides like copper, cobalt and nickel as well as kaolin have been reported (Davidson, 1983). This report also included the occurrence of alluvial gold deposit south of Maji that lies within the high grade gneisses of the Hamar domain.

Melesse and Demerew (2003) reported that geologically, the Konso Special Wereda is characterized by complex of gneisses, syn-post tectonic intrusive that range from ultramafic to granitic in composition and various pre-post rift deposits.

The area of study is covered by high grade metamorphic rocks. Most part of the area is covered by amphibole, granitic, granulite and biotite-hornblende gneisses. The rest small part of the area is covered by charnockitic rock suite, alluvial deposits and Tertiary volcanics. There are veins and veinlets like pegmatite and quartz, as well as dykes and/or sills of felsite, aplite and basaltic intrusions are also associated with these high grade metamorphic rocks. The area is also highly affected by tectonic deformations which resulted different structures like foliation, faults/lineaments, folds, joints and/or fractures and even shear deformation.

In addition, there are alterations at places in all mapped rock suites such as chloritization, sericitization, serpentization. Weathering effect is very high where the color of the rocks changed greatly and somehow difficult to identify the rock in field.

Each rock unit has gradational contact with the vicinity litho-units even very difficult to decide the exact boundary between adjacent rocks. Some rock types like migmatites were appeared in granulite, and amphibole gneisses as patches.

### **3.1 Geological Map and Profiles**

Based on investigations carried out in the Sorobo area, a geological and structural map was constructed (Fig.3.1). Foliation planes and lineations measurements collected from field. Two geologic cross-sectional profiles (Fig. 3.2) have been constructed from the geological map.

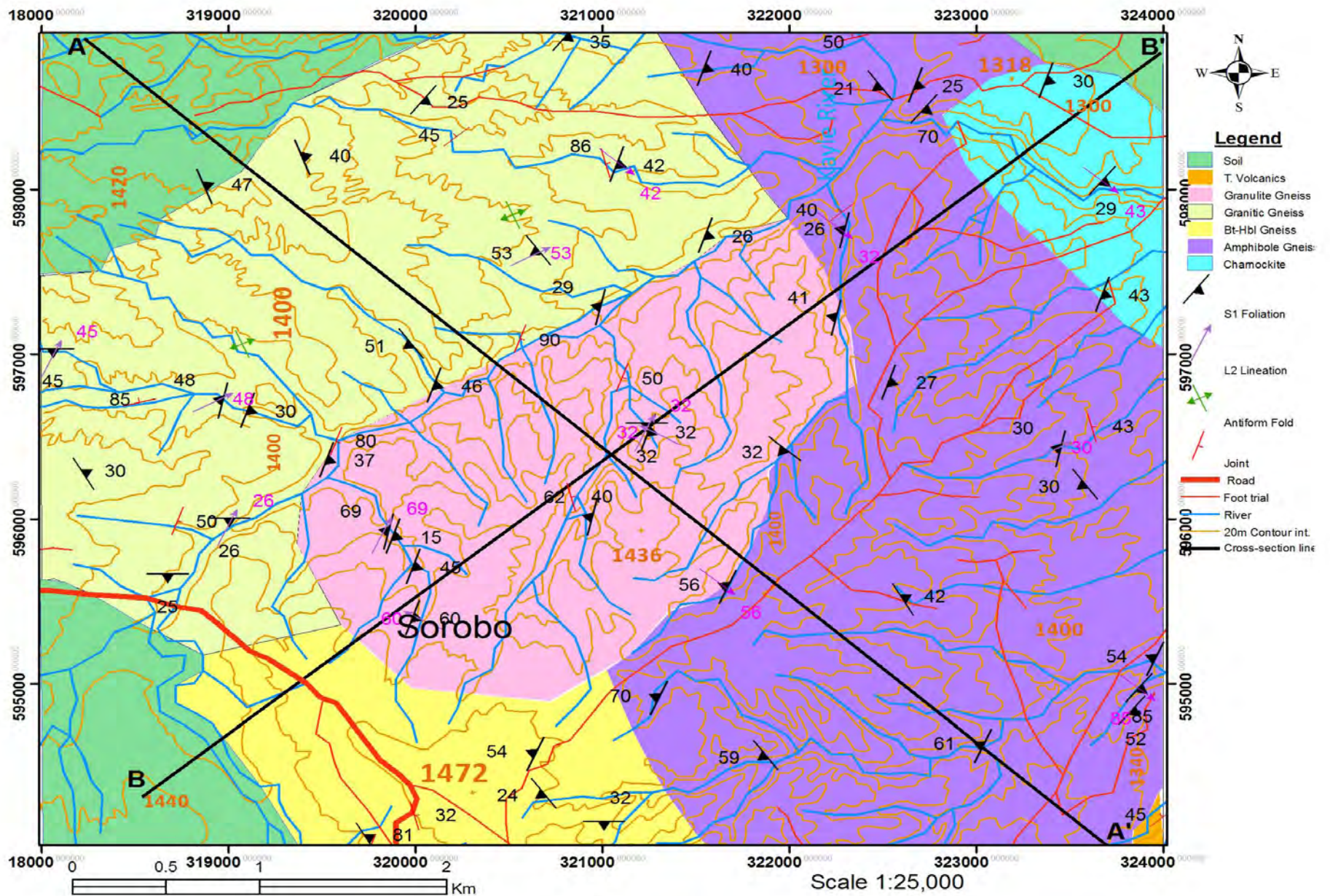


Figure 3.1 Geological and structural map of Area of study

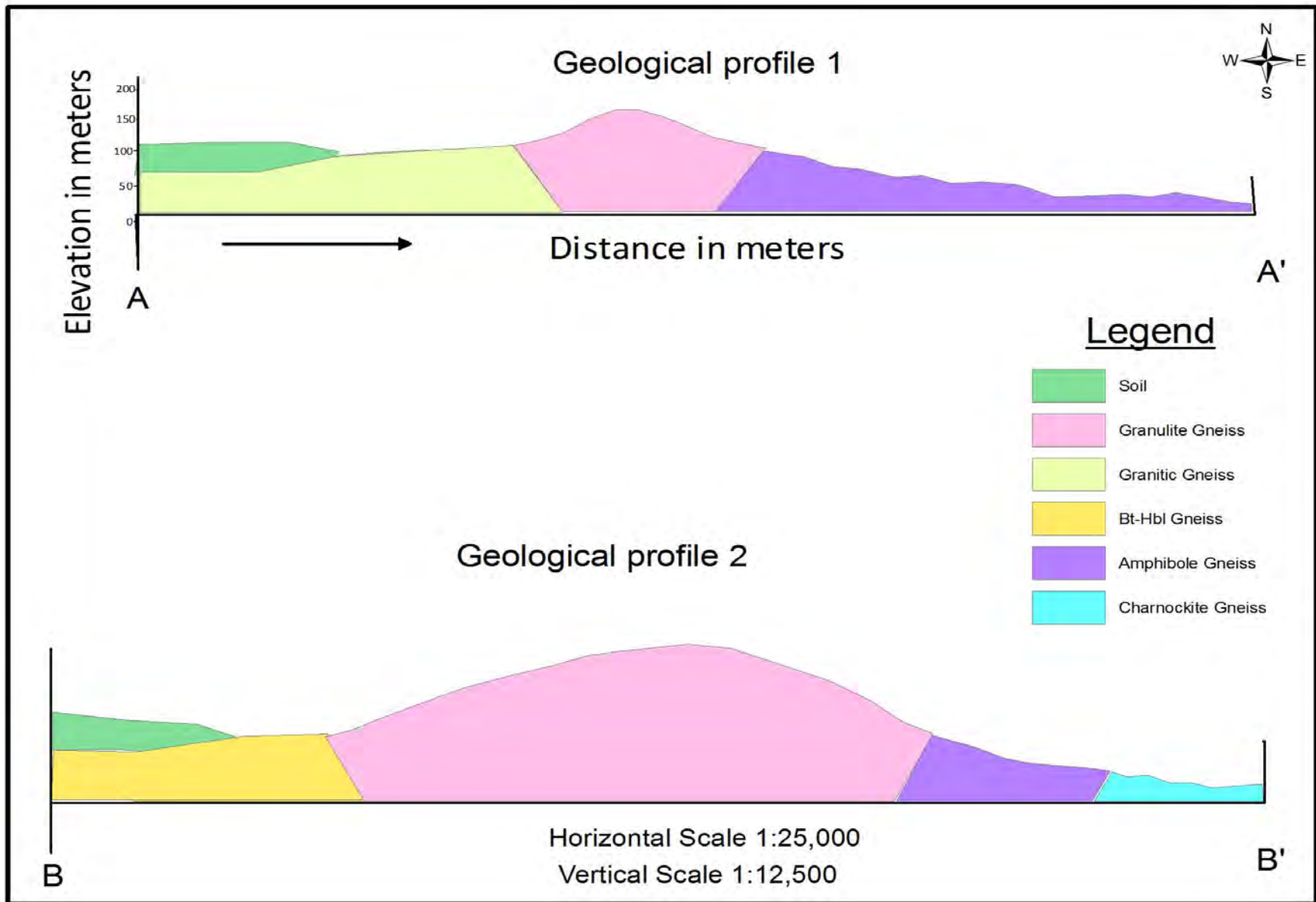


Figure 3.2 Geologic profiles along the lines A-A' and B-B' shown on the geologic map.

### 3.2 Charnockite (KS<sub>2</sub> sample)

Charnockite is any orthopyroxene-bearing quartz-feldspar rock, composed mainly of coesite, perthite or antiperthite and orthopyroxene (usually hypersthene) formed at high temperature and pressure, commonly found in granulite facies metamorphic terrain.

This rock unit covers relatively a small part of the study area. It is exposed in the NE of the study area, mostly by river cut exposure and shows a gradational contact with the other units and is predominantly composed of orthopyroxene.

The rock exhibits granulite gneiss or layers. It occurs as big boulders which have pale pink to gray in color, hard and compacted. Some of the boulders are also containing garnet restite in their composition. The rock is permeated by quartzo-feldspathic veins. These veins also contain tourmaline and garnet (Fig. 3.3). The rock is also highly fractured and jointed. These fractures are occupied by quartz and pegmatite intrusions. In some of the joint openings, there are epidote, tourmaline, garnet and amphibole mineral developments observed.

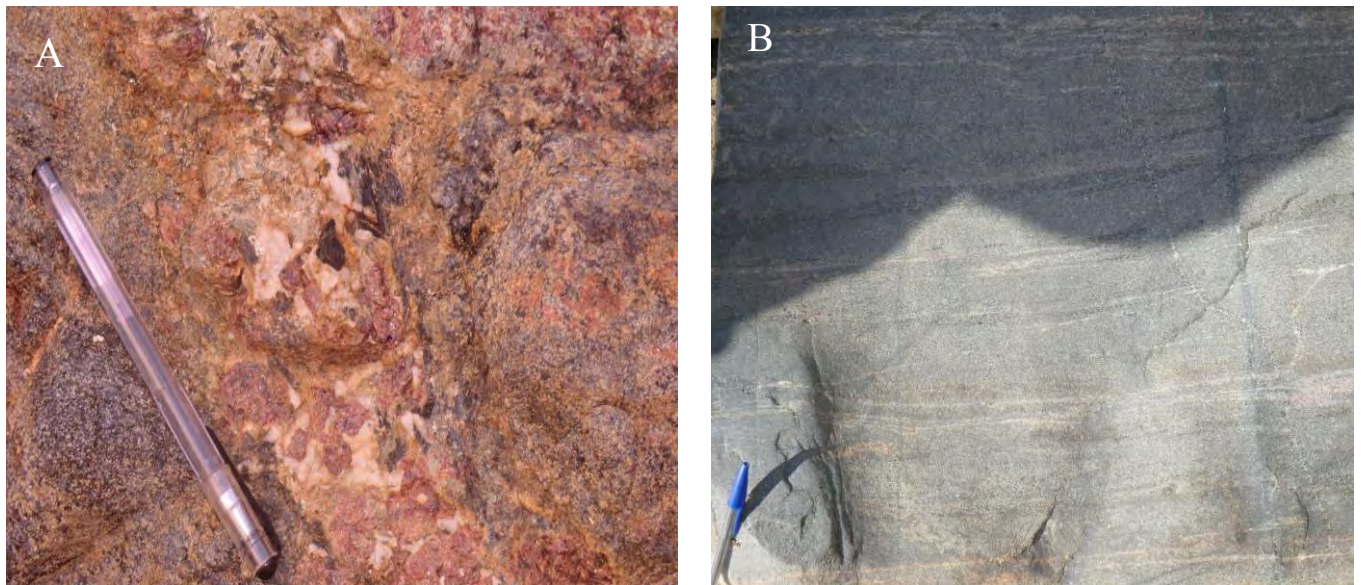


**Figure 3.3** Photographs of charnockite taken from Konso district. (A) Restates of large garnet crystals embedded in the charnockitic rock. (B) Charnockite with compositional layers.

Thin section study of the sample shows that the rock is composed of 30% Plagioclase, 16% orthopyroxene, 15% k-feldspar, 14% quartz, 14% clinopyroxene, 5% hornblende, 4% opaque, and 2% garnet (Fig. 3.4B-E).



**Figure 3.4** Photomicrographs mineral grains in charnockite rock. (A) Clinopyroxene shows serpentinization as well as being replaced by hornblende. (B) Broad grain of clinopyroxene surrounded by k- and plagioclase felds pars. (C) Small grain of sanidine (D) Broad twisted biotite with opaque inclusions. (E) Small euhedral garnet grain. All are seen under crossed polars.

### 3.3 Amphibole Gneiss (KS<sub>8</sub>, KS<sub>9</sub> samples)

Amphibolite rock is exposed by river cut and hill site exposure and covers approximately 30% of the study area exposed to the east in the map (Fig 3.1). It shows dark grey weathered color and mixture of dark with minor light at fresh color and it also shows heterogeneity with other rock like migmatite rock.

The rock is composed of alternative light and dark colored minerals where the dark minerals are dominant. This compositional variation and banding (Fig. 3.6) in this rock unit is due to metamorphic differentiation which is formed in the progressive deformations of high grade metamorphism. It shows a general striking orientation between  $N5^{\circ}E$  to  $N20^{\circ}E$  and dips westerly. It has gradational contact with the other all adjacent units as well as migmatite rock within it except the tertiary volcanic rock right bottom in the map (Fig. 3.1).



**Figure 3.5 Photographs of amphibolites that show chloritization and sericitization alterations at places .**

The rock unit is composed of hornblende, plagioclase, k-feldspar, pyroxene (minor), quartz, and garnet. At places, it shows gneissose texture; the rock also shows chloritization and sericitization (see Fig. 3.5). These alteration features are resulting from late retrograde meta morphism.



**Figure 3.6 Field photograph taken in amphibole gneiss showing compositional variation and banding.**

Thin section study of the samples shows the rock is composed of 40% hornblende, 25% Plagioclase, 12% quartz, 6% k-feldspar, 6% clinopyroxene, 5% biotite, 4% chlorite, and minor amounts of opaque and zircon (Fig. 3.7A-D).

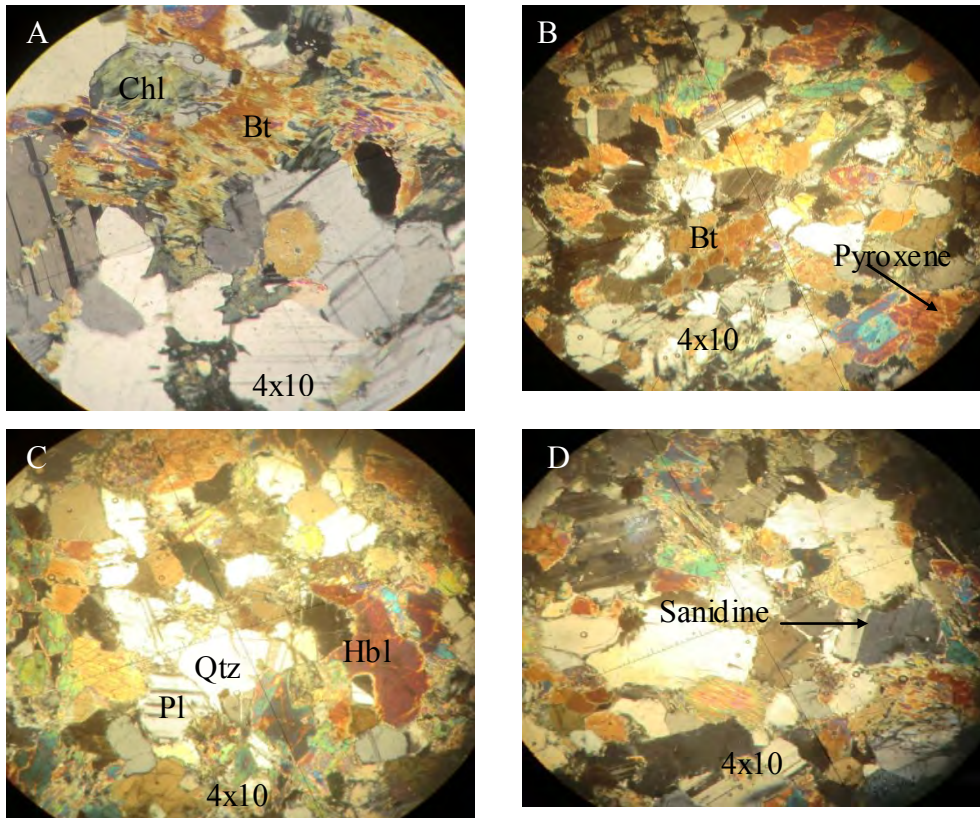


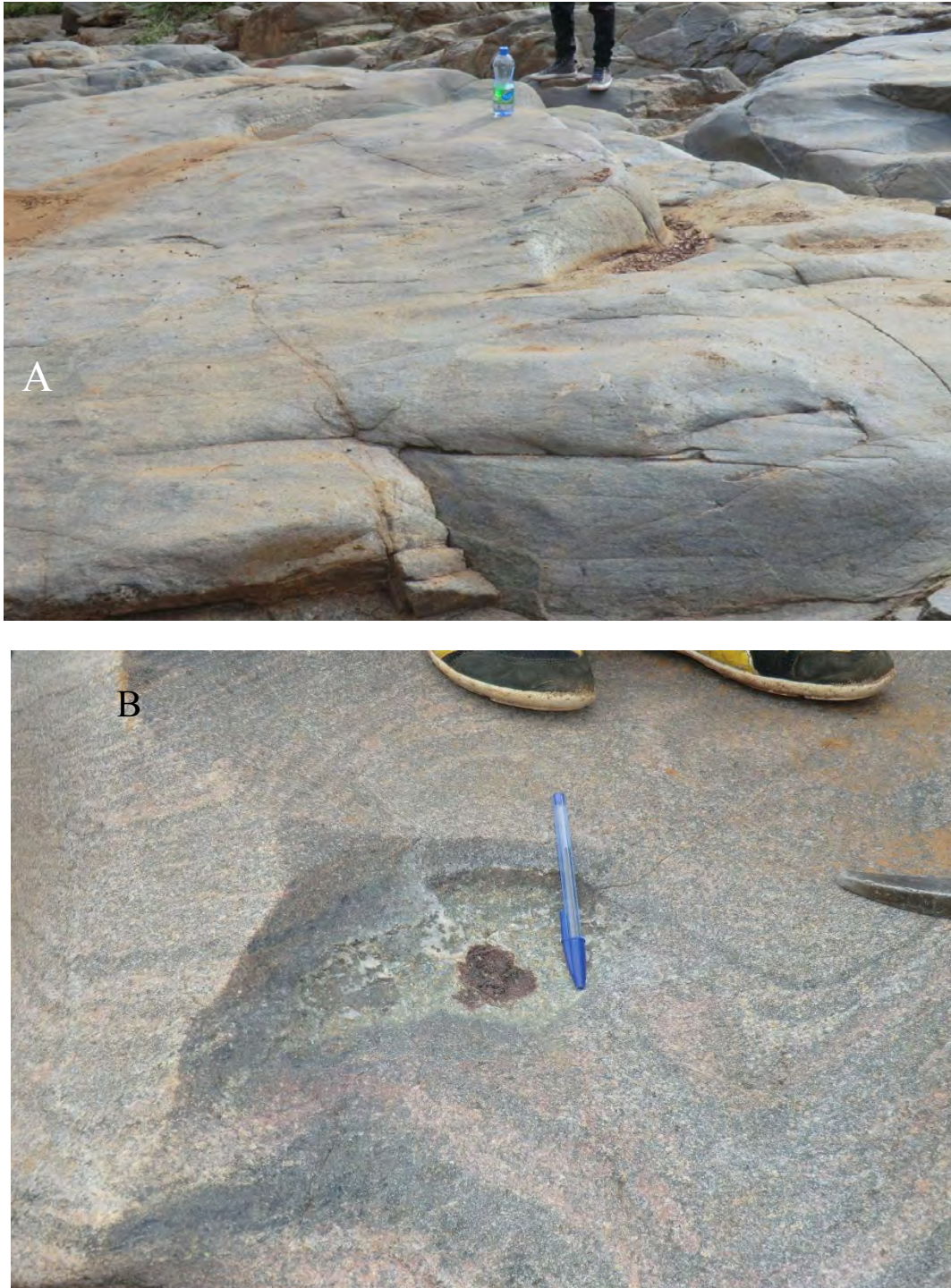
**Figure 3.7 Photomicrographs mineral grains in amphibole gneiss. (A) Chlorite is retrogradically formed from biotite. (B) Clinopyroxene shows color zonation at some part. (C) Hornblende mineral that shows retrograde process at its rims. (D) Sanidine k-feldspar mineral surrounded by strongly altering amphibole. All are in crossed polars.**

### 3.4 Granulite Gneiss (KS<sub>4</sub>, KS<sub>10</sub> samples)

A mappable metamorphic rock consisting of uniformly sized unit granulite is exposed at centre of study area (Fig. 3.1), covering about 20% of the total. There are amphibole gneiss and granitic gneiss laterally intercalated with it to south and north respectively. At exposures patches of migmatitic rocks are recognized in the unit. It also shows a gradational contact with its adjacent rocks. It is mostly granular in texture and at places gneissose, and is exposed as lensoid bodies, as patches and as continuous outcrop.

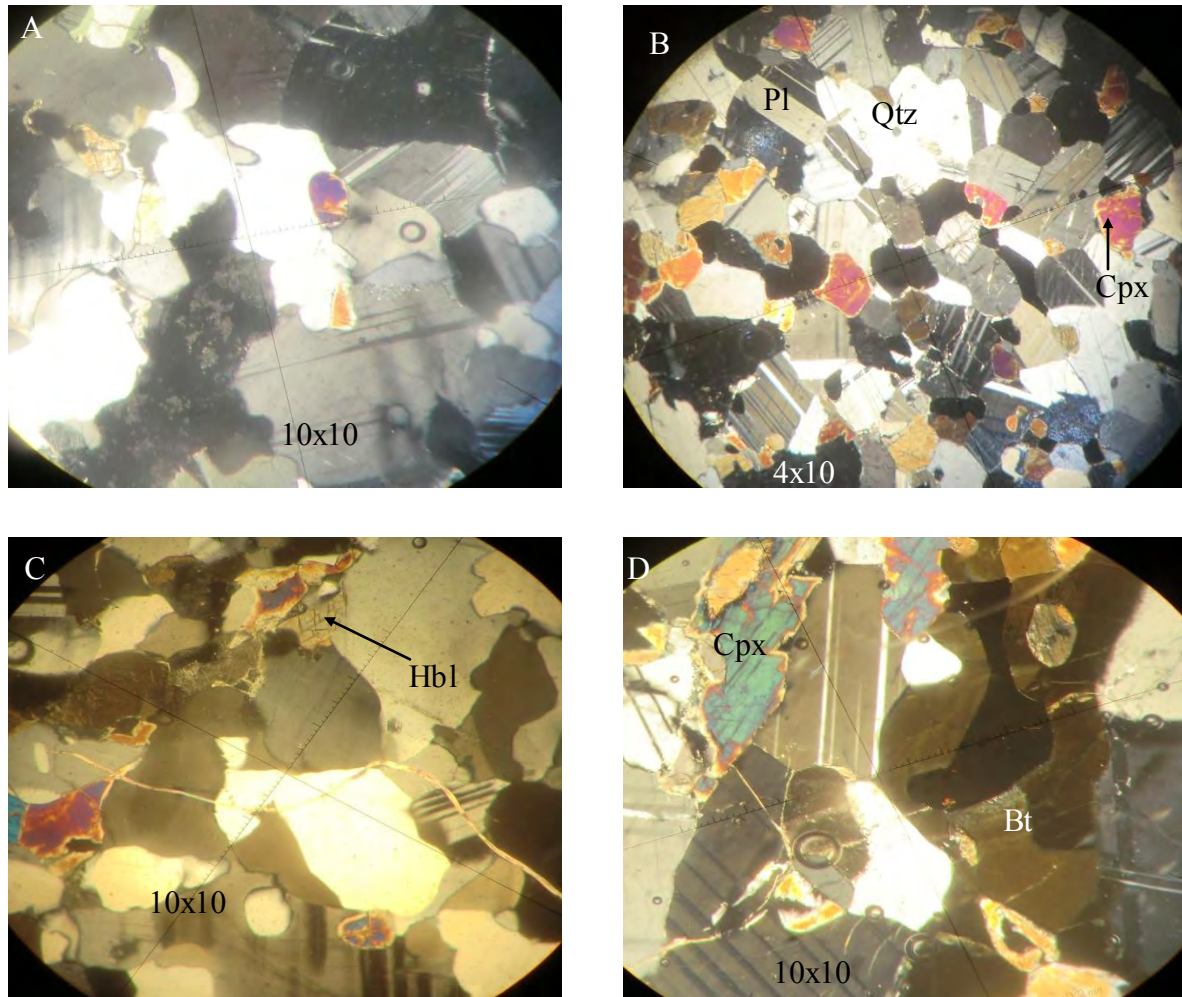
It is dark green to gray in color; medium to coarse grained composed of pyroxenes, quartz, biotite, hornblende, +/- k- feldspar, plagioclase feldspar and +/- garnet minerals which exhibited granulose texture. Pyroxene minerals show granular shape, anhedral, brown in color, which

exhibit bronze luster; and the plagioclase minerals occur as subordinate quantities and are characterized by anhedral to subhedral in shape. Chloritization and serpentization alterations are also noted (Fig. 3.8B).



**Figure 3.8 Granulite rock photographed in Konso, Sorobo. (A) Hard non-foliated granulite rock (B) A typical granulite contains serpentine around garnet mineral.**

Thin section study of the samples shows the rock is composed of 40% Plagioclase, 35% quartz, 10% biotite, 8% clinopyroxene, 6% hornblende, and minor amount of epidote, rutile and garnet (Fig. 3.9A-D).



**Figure 3.9** Photomicrographs mineral grains in granulite gneiss. (A) Clinopyroxene in leucosomes grains. (B) Clinopyroxene grains show bastite textures. (C) Hornblende forming from clinopyroxene because of temperature drop. (D) Larger shades of biotite being dissolved. All are in crossed polars.

### 3.5 Biotite-Hornblende Gneiss (KS<sub>7</sub> sample)

This rock unit is another rock suite which covers approximately 10% of the whole study area. It is exposed by river cut exposure. It mostly characterized by friable coarse grains and shows light gray and dark color, medium to coarse grained and foliated fabric. The dark colored minerals are slightly flaky and are oriented in different fashion and elongated. But the light color minerals are not oriented and are granular. Chloritization and sericitization processes are commonly observed at places during field work. The rock has alternating bands of dark green to light green mafic

minerals and light to grayish felsic minerals. It exhibits both the compositional variation and banding which is presumably due to metamorphic differentiation. Generally, this rock shows foliation with strike of  $N80^{\circ}E$  to  $90^{\circ}E$  and is cross-cut by quartz veins with several strike directions. It also affected by pegmatite intrusions. It is highly fractured and jointed of which the most part of the rock is highly sheared. It is mainly composed of plagioclase, quartz, hornblende, biotite minerals.

Petrographically, it is composed of 30% hornblende, 21% biotite, 14% plagioclase, 10% k-feldspar, 10% quartz, 4% opaque, 10% clinopyroxene and accessory minerals which are shown in figure 3.10.

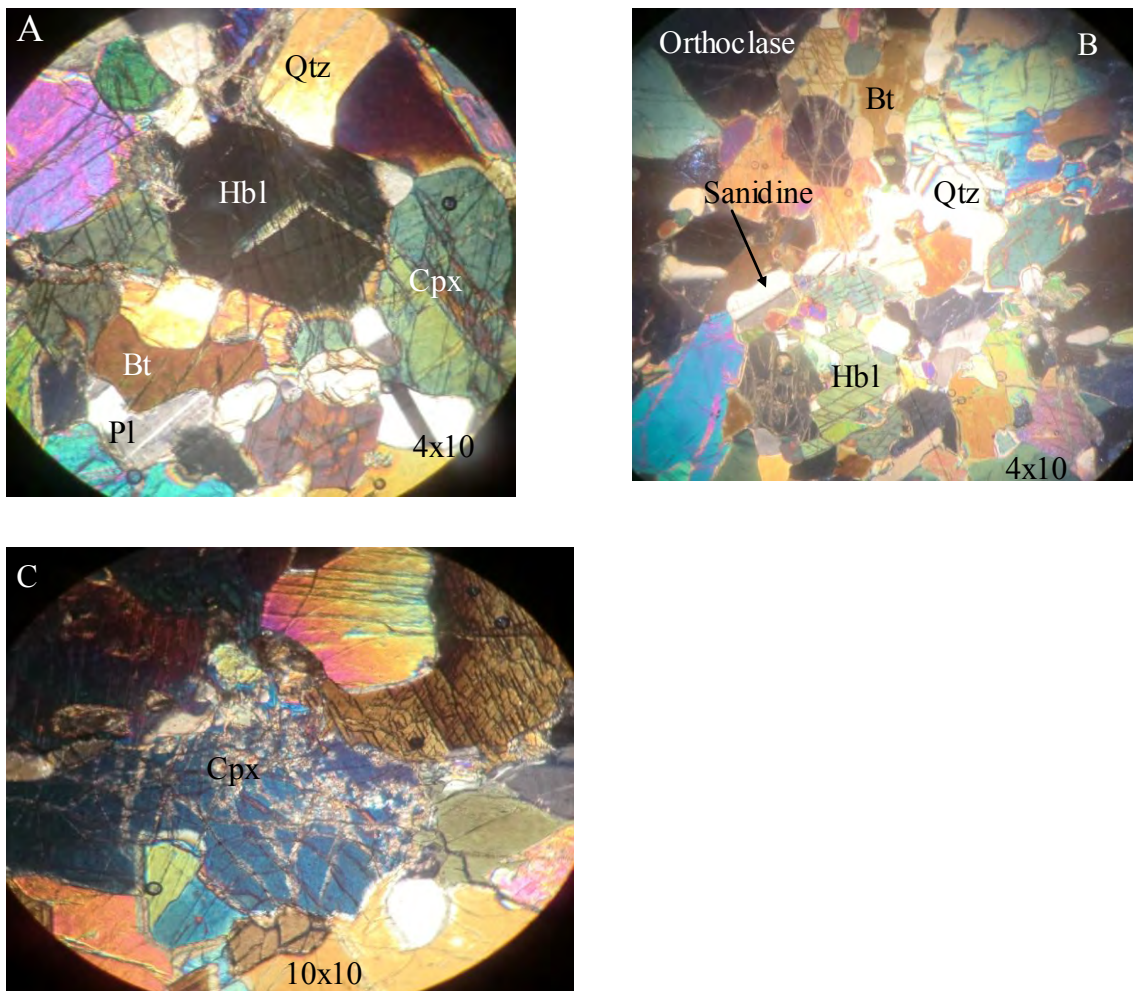


**Figure 3.10** Photomicrographs mineral grains of biotite-hornblende gneiss. (A) Hornblende at extinction position. (B) Orthoclase feldspar exhibits perthitic texture. (C) Clinopyroxene retrograding to serpentine shows bastite texture. All are in crossed polars.

### 3.6 Granitic Gneiss (KS<sub>3</sub>, KS<sub>6</sub> samples)

It is exposed in the northwest of the study area (Fig.3.1); associated with the amphibolite rock. It is characterized by white fresh color, highly coarse grain size, with lenticular shape minerals and its foliations. It is mainly composed of plagioclase feldspar, quartz, k-feldspar, hornblende, biotite, and +/- pyroxene. Plagioclase feldspars are major components in the rock and characterized by gray color, elongated and foliated. K-feldspar is also characterized by slightly light or pink color and lenticular shape. Generally, the rock shows gneiss texture and the outcrops possess different sets of joints. This rock also shows a tour topography in which big boulders are observed.

At places, exfoliation and xenoliths of lensoid amphibole in composition are commonly observed in the rock unit and which may indicate its igneous origin (shown in figure 3.11). Sericitization, chloritization and epidotization are seen.

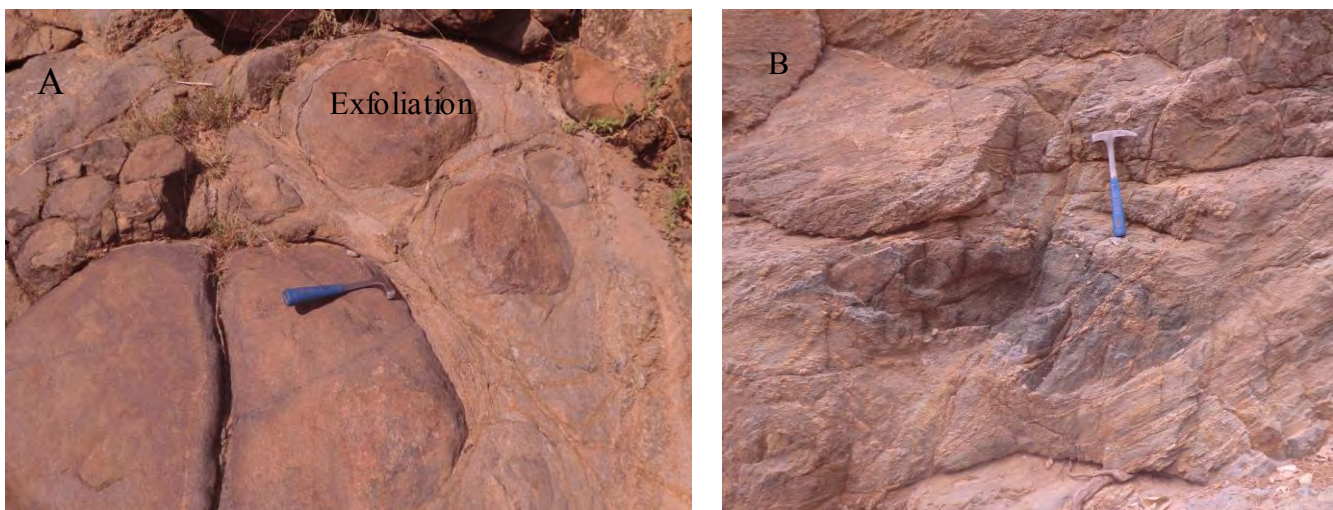


**Figure 3.11 (A) photograph shows exfoliation weathering in granitic gneiss. (B) Photograph shows weakly deformed xenoliths of amphibole.**

Thin section study of these samples shows the rock is composed of 38% Plagioclase, 28% quartz, 5% biotite, 10% clinopyroxene, 11% hornblende, 7% k-feldspar and minor amount of chlorite, epidote, rutile and garnet (Fig. 3.12A-E).

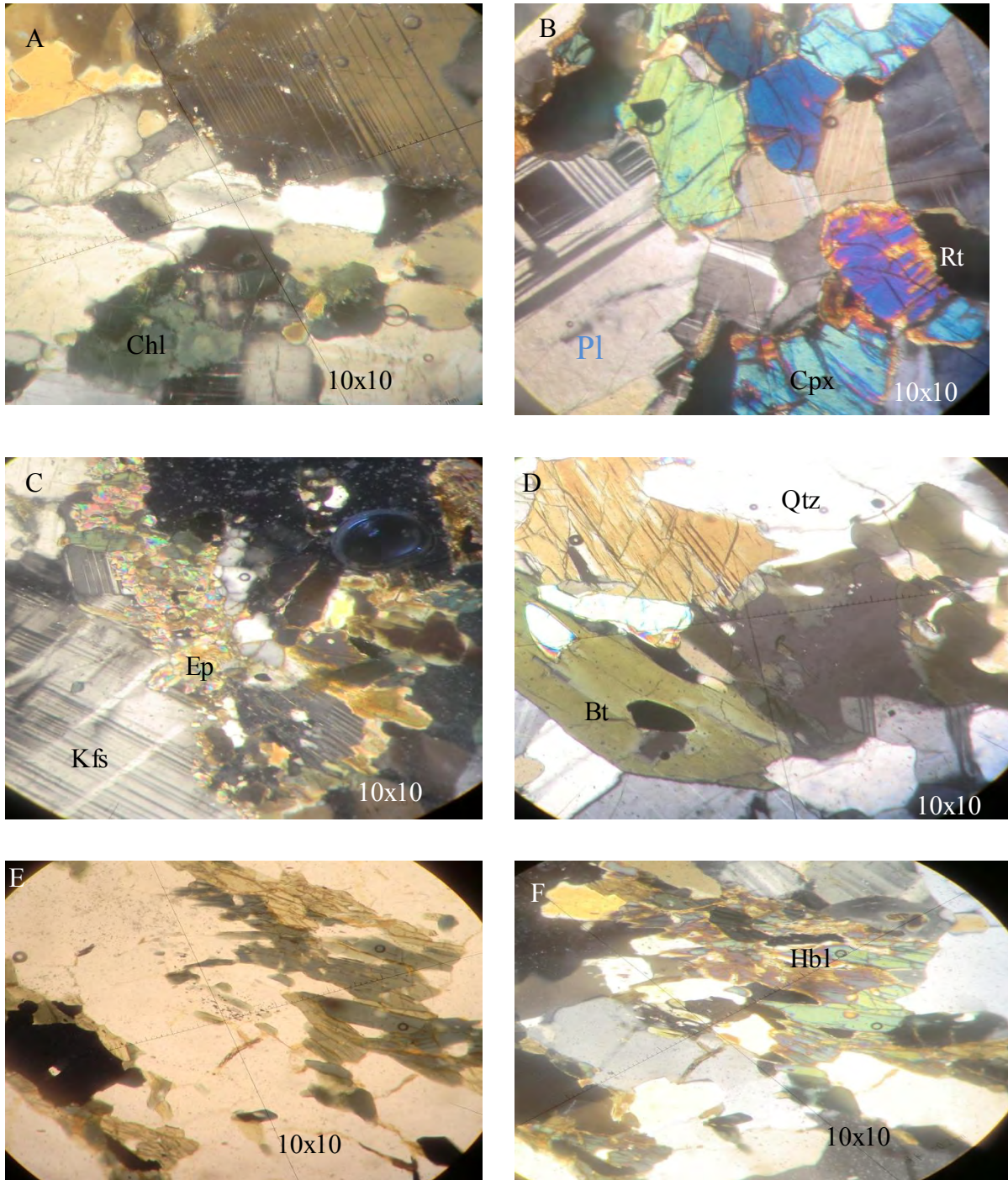


**Figure 3.12** Microphotographs of mineral grains in granitic gneiss. (A) Chlorite with relic of biotite mica (Crossed polar). (B) Olivine mineral surrounded by rutile and pyroxene (Crossed polar). (C) The grain shows epidotization and exsolution (Crossed polar). (D) Broad grain of biotite concomitance with opaque (Crossed polar). (E) Opaque minerals precipitate from biotite laths (plane polarized light). (F) Laths of hornblende contain opaque inclusions (Crossed polars).

### 3.7 Migmatite (KS<sub>5</sub> sample)

A migmatite is a particular rock body that has been heated so much that some of the minerals in it have started to melt and segregate from other minerals with a higher melting temperature. Thus, it is macroscopically composite rock, most of which consists of dark coloured minerals intimately mixed with light coloured minerals.

Gneisses from the Sorobo have sometimes undergone partial melting. The resulting melt is mostly found as thin layers or elongated lenses of quartzo-feldspathic leucosomes, which display chaotic and intricate folded patterns that contrasts with the fabric of the host rock (Fig 3.13). It is exposed by river cut exposure and has slightly flat morphology. The rock body is commonly seen at antiform of large folds suggestible, it has been brought to the surface by thrust folding. This migmatite rock appears within granulite, granitic and amphibolite units and not independently mapped in the study area.

It is characterized by composite layer of mafic and felsic bands with fragments of earlier rock relics. It also exhibits partly gneissose and partly granulose structures which are composed of light coloured minerals such as quartz, plagioclase feldspar and dark coloured minerals like biotite, hornblende, and pink coloured mineral k-feldspar. This rock also contains porphyroblastic garnet which is pink reddish in color and it is also characterized by coarse grained hard and highly compacted rock at places.

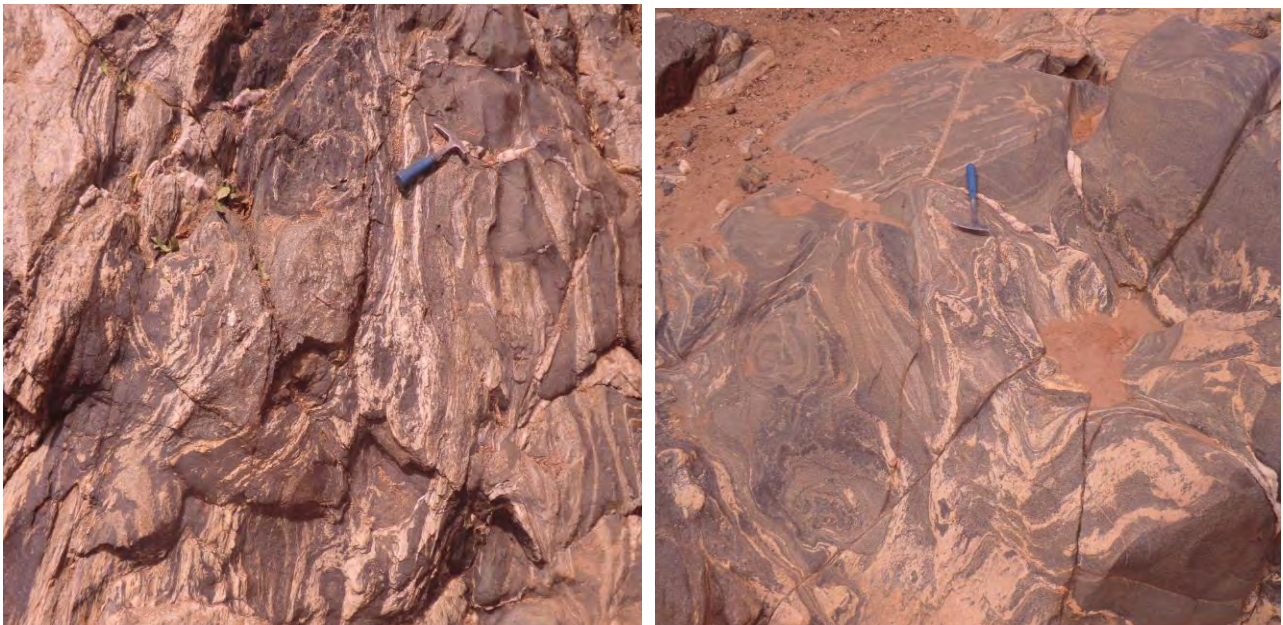
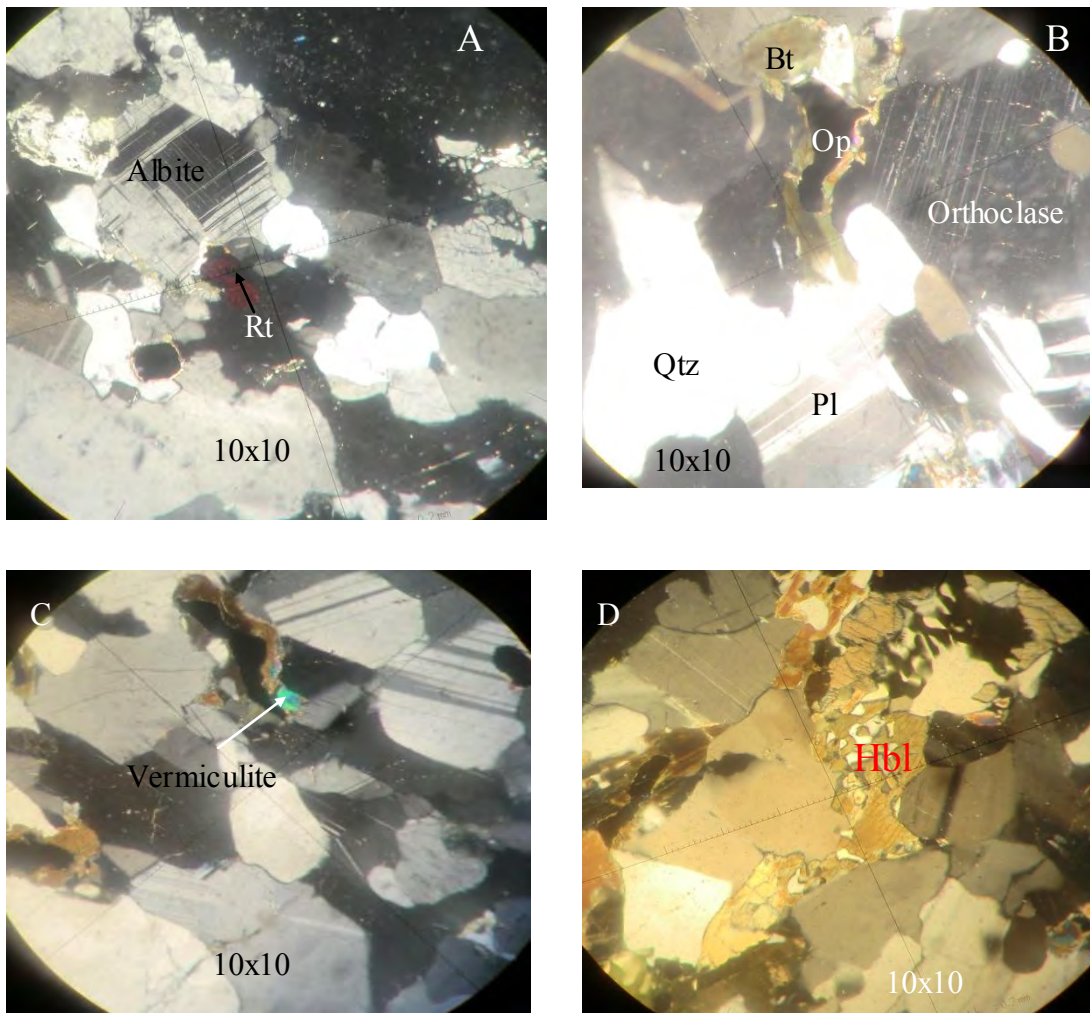


Figure 3.13 Field photographs taken from migmatite patches show leucosome pods.

It has been affected by structures like joints, folds and faults. The folds include: ptygmatic folds (zigzag-like features) which are the most typical characteristics of migmatite rock. The folded patterns occur because migmatite forms when there is partial melting of pre-existing rock.

Thin section study shows that the rock is composed of 26% quartz, 24 % k-feldspar, 16 % biotite, 12% hornblende, 16% Plagioclase, 6% opaque and 1% epidote (Fig. 3.14A-D).



**Figure 3.14** Microphotographs of mineral grains in migmatite rock. (A) Deep red rutile mineral embedded in leucosome. (B) Biotite contains opaque precipitation and k-feldspar showing perthitic texture as a result of dissolution. (C) Blue colored vermiculite mineral associated with biotite. (D) Hornblende exhibits graphic intergrowth with quartz. All are in crossed polars.

### 3.8 Tremollite-Actinolite Schist (KS<sub>1</sub> sample)

This rock unit is a thin and small outcrop exposed in western part of the study area in the Kayle River and its northwest tributary stream. At this scale is not mappable having 5 m thick in south and 50 cm pinching towards north generally trending southeast and dips 30° south west on

average. Although, the unit has the same striking direction in the two exposures they are misplaced at about 700 meter. A small scale light bands in the unit are folded and refolded even very complex to identify the foliation phases at the outcrop (Fig. 3.15). It is observed as thin layer sandwiched between coarse grained thick layers in granitic gneiss unit. It is schistose, soft, and fine to medium grained, dark in color composed mainly of amphibole, quartz and chlorite.



**Figure 3.15** A thin layered amphibolite schist intruded in granite rock affected by strong deformations.

In thin section, the rock consists of 52% actinolite, 20% quartz, 17% tremolite, 6% epidote and 5% chlorite (Fig. 3.16).

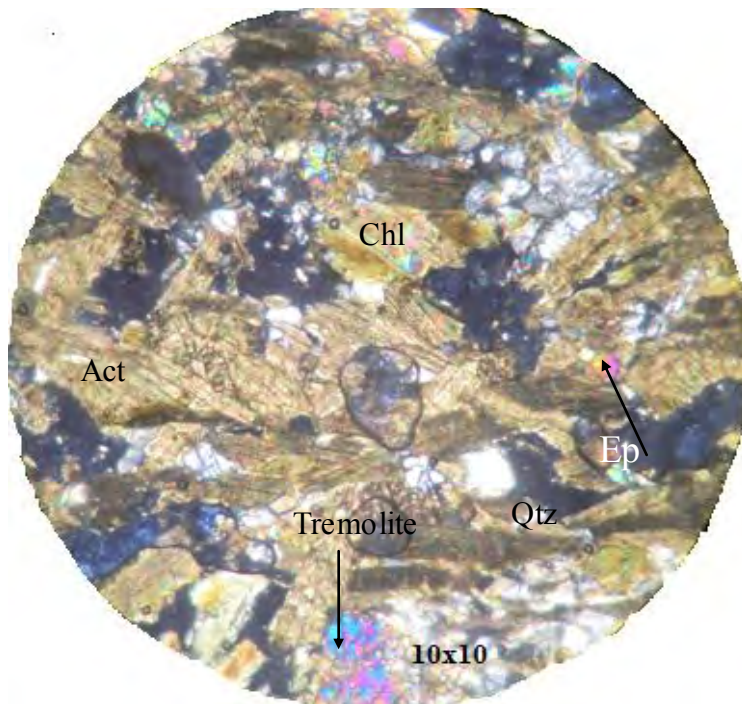


**Figure 3.16** Microphotograph shows mineral composition of amphibole schist. Crossed polar.

### 3.9 Tertiary Volcanics

This rock appeared in the area at the most lower corner of right hand covering very small portion from the total studied area. The rock unit is mainly basalt, which is massive fine grained, melanocratic in color. Columnar joints are observed at places. In hand specimen, it is mainly composed of amphibole, plagioclase and minor quartz minerals. It has a general strike of NNE at contacts with amphibole gneisses. At the contact, the baking effect of the volcanic pulse affected about 74 meter of the gneiss causing its color to become reddish and at the contact the rock has highly weathered having white color.

### 3.10 Alluvial Deposits

About 10 per cent of the study area is covered by alluvial deposits mapped as soil. These deposits are found in the top and bottom corners in the west as well as top corner of the right in the map. It is loose sediments of dark brown to gray, mainly sands, clayey/silty sands with some gravelly layers. It also contains voluminous clastic detritus materials.

At the place top corner of left map, the soil thickness reaches about 30 meter (Fig. 3.17A). In the top right corner of the map above the charnockite rock unit, the black cotton soil layers from bottom and above are separated by a 1.25 meter horizontally mantling very fine layer of ash deposit (Fig. 3.17B).

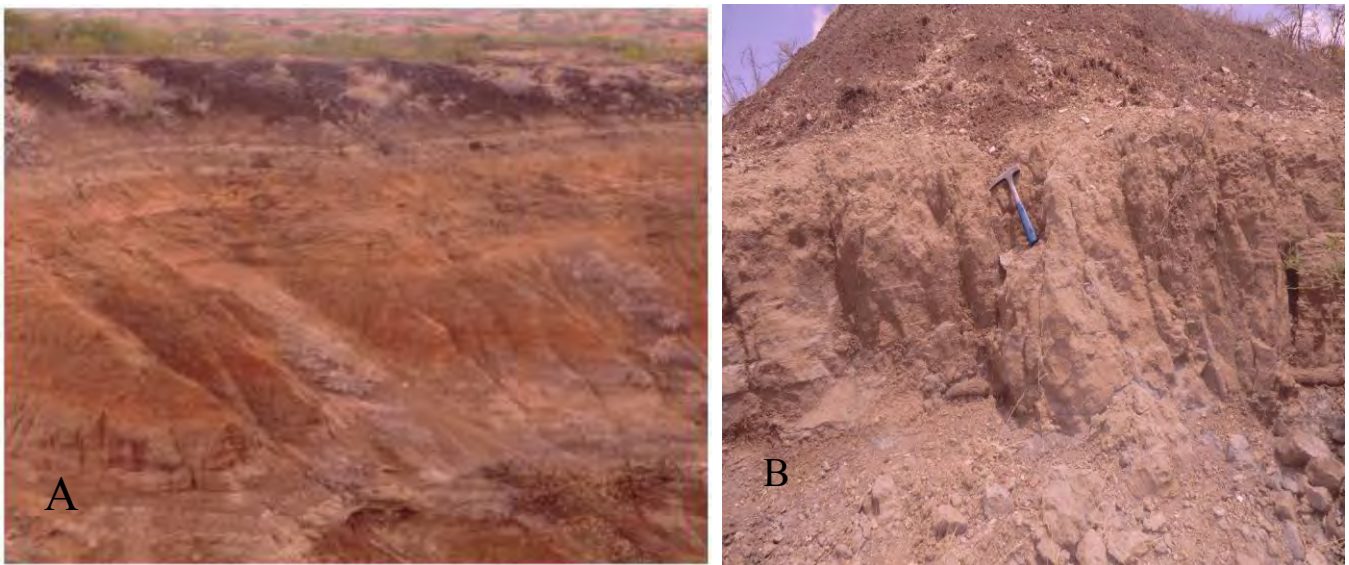


**Figure 3.17 Pictures of soil and ash deposit taken from the area. (A) About 30 m thick alluvial deposit. (B) Fine grained layer of ash deposit that separates black cotton soil in the area.**

### **3.11 Intrusion**

In the study area different types of intrusion are observed: concordant or discordant to the host rock strata. Detail petrographic description of them is as follow:

#### **3.11.1 Aplite Dikes**

It is characterized by gray to brown weathered and white fresh color with vitreous luster. At hand specimen, it is fine to medium grained, is composed of quartz, plagioclase feldspar, k-feldspar (minor amount). It also contains few black color minerals which occur as small veins with parallel to the foliation direction. At the exposure they are highly fractured at different orientations.

All the aplite intrusions observed in the field are discordant to the foliation in which they are hosted. Their width ranges from 1 meter to 4 meter. They all have trending orientation of 20° NE to 45° NE. The one that laterally exposed over 30 meter is folded locally.

Microscopic study shows that the aplites are composed of 50% quartz, 30% microcline, 15% muscovite, 2% plagioclase, 2% garnet and 1% opaque minerals most likely sulfides (Melesse and Demerew, 2003).

#### **3.11.2 Pegmatite Veins and Quartz Veins/Veinlets**

Pegmatite and quartz veins are occurring in each of metamorphic rocks. They are medium- to coarse-grained, mainly composed of plagioclase, k-feldspar, quartz, small amount of garnet, magnetite, muscovite, biotite mica and sulfide minerals are observed in a minor amount. Both pegmatite and quartz veins/veinlets range from a cm to 4 meter width with various lengths are seen in the area arranged either discordant or concordant to the plane. From the intrusion veins relationship to each other that they suggested to have different episodes of occurrence. The quartz veins and veinlets are abundant and some of them are associated with sulfide oxides like pyrites.

Thin section investigations show that these veins are composed of 85% quartz, 8% opaque, 5% garnet, 3% biotite and trace amount of hornblende. On the other hand, the pegmatite veins are petrographically composed of 35% quartz, 30% plagioclase, 10% k-feldspar, 10% sericite, 10% epidote, and 5% muscovite (Melesse and Demerew, 2003).

### 3.11.3 Felsite and Basalt Dikes

Several fine grained dikes of felsites as well as basalt dikes are observed in the area coupled with all the rock units. The felsite is very fine grained with light in fresh and has brownish black weathered color. It possesses dissimilar joint patterns which are brick joints, polygonal joints and spheroidal joints (Fig. 3.18). On some felsite intrusions joints arrayed about  $110^{\circ}$  from the strike.



**Figure 3.18** Photographs of basalt and felsite dikes taken in field which weather to light orange.

The crystalline basement rocks exposed in Sorobo exhibit many structures varying in size from large scale to microscopic which indicate that these rocks have been subjected to polyphase deformation. Preliminary work including field description of the structures and stereographic plotting was carried out by Davidson (1983) for the Hamar Domain in which the present study area is included. According to his stereoplots, all the domains except subdomain in Akobo reveal small characteristic differences. The Hamar domain gneisses show a certain variation in attitude about a line extending from the Segen River south of Konso northwest towards Bala River valley even though they have general east-northeast dipping direction. Six deformation events were identified in Agere Maryam area (Nesir et al., 1991). Konso area is subjected to at least five phases of deformation by Melesse and Demerew (2003) report.

The present study has taken into consideration the work carried so far in light of the data available and an attempt has made on the bases of structures to classify the deformation into four phases.

#### **4.1 Geological Structures**

Metamorphic rocks of an area in general exhibit a variety of deformation structures. These can range from structural features similar to the original protolith at low grades of metamorphism, to structures that are purely produced during metamorphism and leave the rock with little resemblance to the original protolith.

The study area is affected by tectonic activities that resulted different geologic macrostructures like folds, faults/lineaments, foliations, lineation, boudins and joints and/or fractures. These structures are associated with all the major five litho-units such as amphibole gneiss, granitic gneiss, granulite, biotite-hornblende gneiss and charnockitic rocks in the area. Foliation structures are the most dominant one following folds and brittle deformation fractures in the entire area.

##### **4.1.1 S<sub>1</sub> Foliation**

Foliation (S<sub>1</sub>) is a typical characteristic of the metamorphic rock in the study area. These foliation surfaces allowed defining the three ductile deformations D<sub>1</sub> to D<sub>3</sub>. The first phase of deformation surface (F<sub>1</sub>) was resulted due to north-south compressional stress letting the

foliation to have west- east trending (Fig. 4.1A). This surface is also refolded by late E-W ductile deformations  $D_2$  forming  $F_2$  and another NE-SW oriented force ( $D_3$ ) sheared the foliation  $S_1$  resulted  $F_3$  surfaces (figure 4.1B), but cannot be clearly understood from foliation data. This  $D_3$  deformation event is traced from the axial planes of fold data which is next discussion. Generally,  $S_1$  foliation was only presented in this paper because it was refolded by  $D_2$  deformation trending it between NW and NE; and  $D_3$  force was applied in northeast direction and no more foliation is observed which resulted as  $D_3$  deformation i.e. these late ductile deformation episodes were not enough to rearrange the foliation direction rather than resulting smaller local folds. During foliation data collection, the shear foliations were marked by “S” to the west and “Z” shaped folds to east (see Fig. 4.2). Therefore, this simple shear (as a result of  $D_3$ ) foliation was formed as a consequence of sinistral shear and dextral shear (found along the opposite limbs of antiform fold at regional wide which is not seen in the field) showed rotation of mineral grains at about  $15^\circ$  to  $35^\circ$  in the rocks. This deformation also increased the foliation dipping degree.

The shear foliation shows translation movement (one rock plane slides over the other bed) under applied compressive stress or pressure. Most of these shear foliations show northeast southwesterly and northwest southeasterly trending direction with dip amount ranging from  $21^\circ$  to  $82^\circ$ . Those trending NE and SE direction have covered maximum range of dip amount from  $22^\circ$ -  $82^\circ$  degree meaning while they dip shallowly to too steeply. Others those striking N-S and E-W have experienced moderate dipping ( $26^\circ$ -  $48^\circ$ ) amount. Sigmoidal features and lenticular shapes of amphibole xenoliths and quartz minerals as well as strong penetrative foliations were observed in the amphibole and granitic gneisses in sheared zone show that there were series of shearing in the area and are the most identification features of the sense of movement. Also the ‘Z’ and ‘S’ are recognized in the rocks show dextral (right hand lateral) and sinistral (left hand lateral) shear sense of movement (Fig. 4. 2).

Both the bed and foliation change their dipping direction after approximately a kilometer distance. Therefore, a systematized tracing of these foliation dip direction data was made to wisely observe the general morphology of the fold shape at regional wide.

Gneissose foliation is mostly associated with granite, amphibole gneiss and migmatite rocks forming separate layer or bands of white and dark minerals (Fig. 4.1B). They have similar orientation with beds.

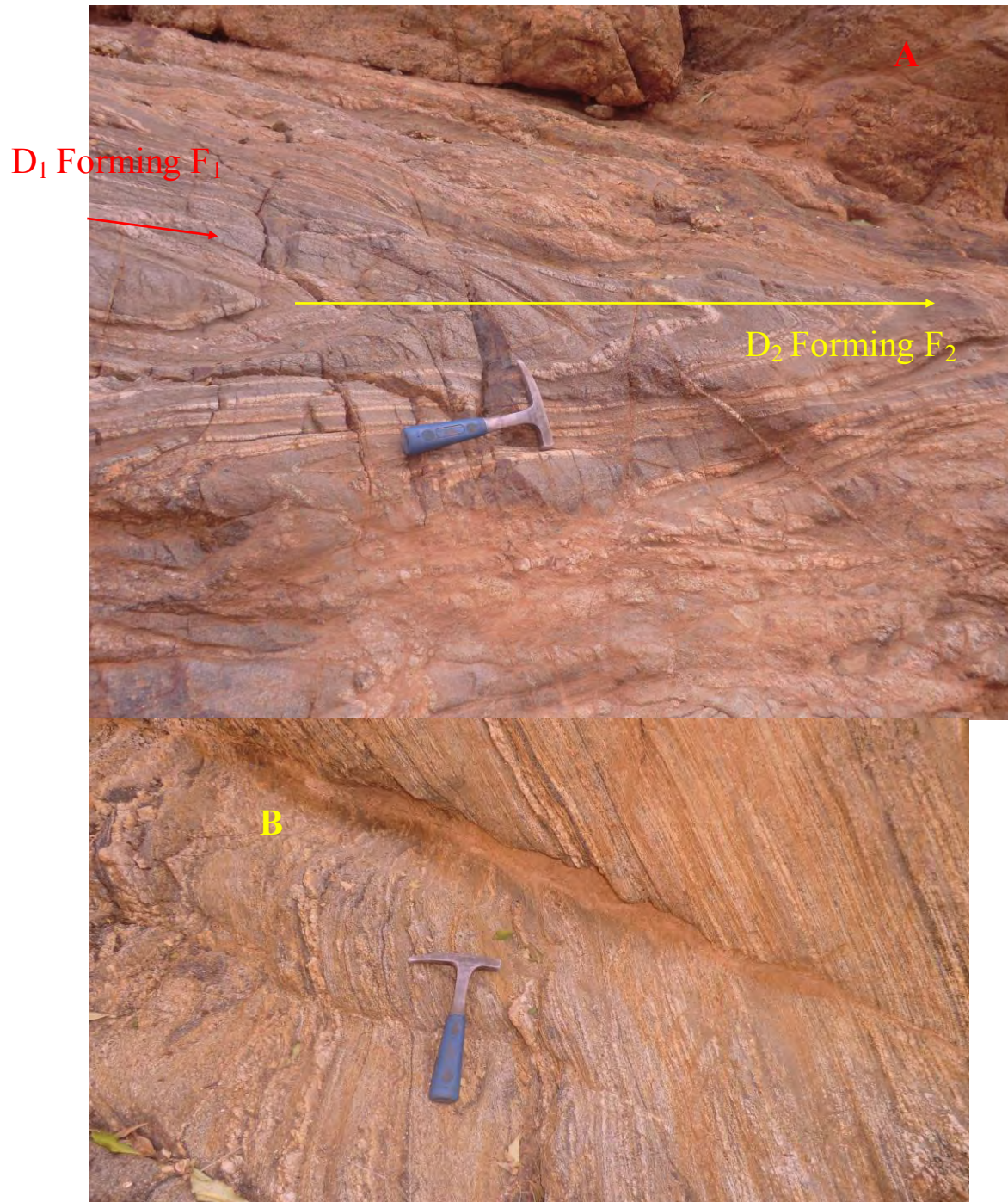
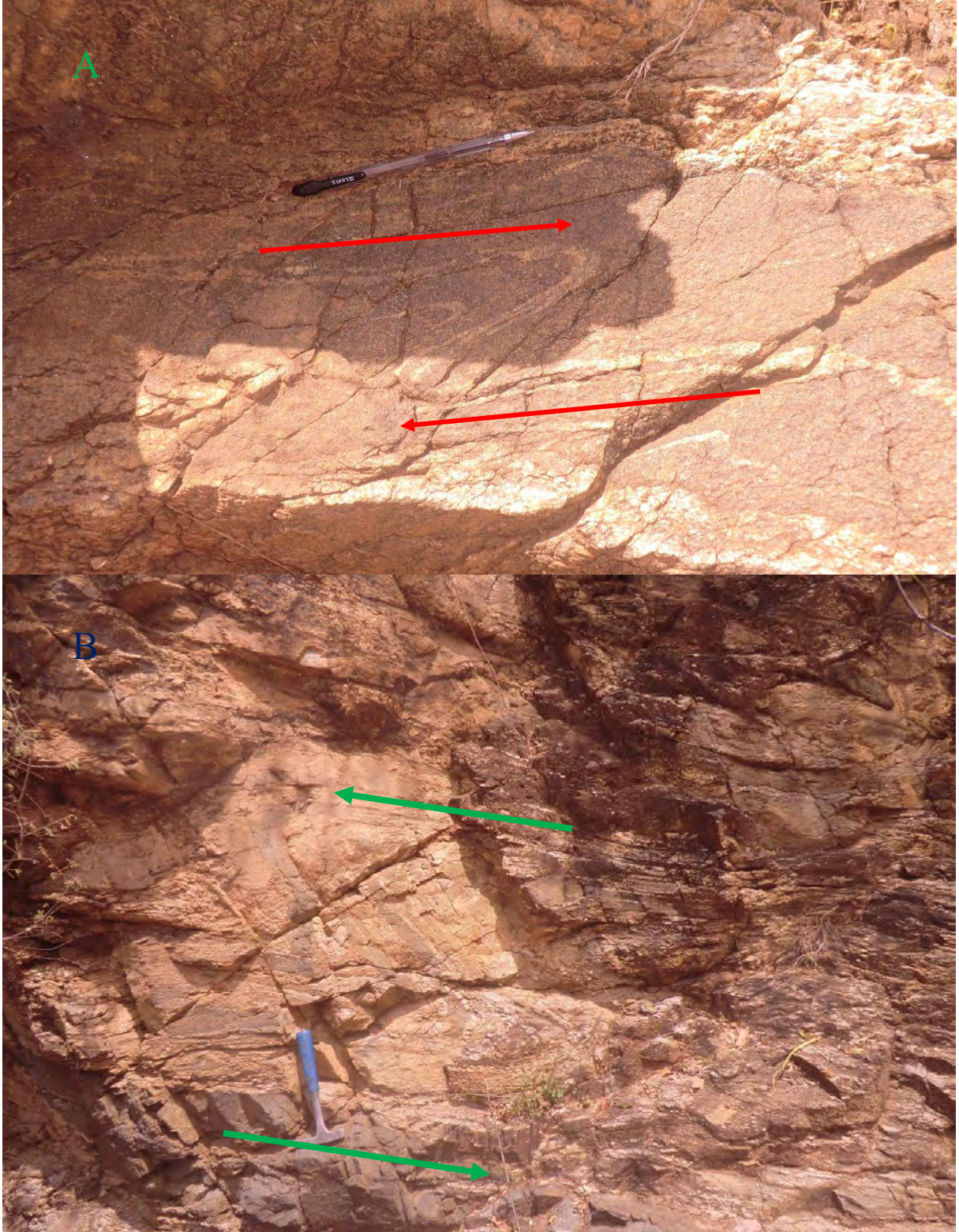


Figure 4. 1 Photographs taken in Konso area that can depict the three ductile deformations. (A) A typical Photograph which shows foliation  $S_1$  that is folded and refolded by early ductile  $D_1$  and  $D_2$  deformations, respectively. Photo is taken facing E direction. (B) Photograph taken in granitic rock showing a typical gneissosity resulted by shearing.



**Figure 4. 2** Photographs taken in shear zones. (A) A “Z” like fold that depicts dextral sense of shear. (B) Sinistral shearing deformation forming “S” shape. Note these deformation figures are results of  $D_3$  shear deformation.

#### 4.2.2 L<sub>2</sub> Lamination

In the study area there are numerous linear structures (L<sub>2</sub>) associated with all lithologies. They typified as preferred orientation of mineral grains and small elongated lenticular features perpendicular to the foliation (see Fig. 4.3). Lineations occurred in granitic rock have plunge of 070° and trend of 050°. In the granite rock light coloured mineral probably plagioclase feldspar and quartz are preferably oriented in a line form which is parallel to each other. Some of those occurred in the amphibole gneiss rock units have parallel orientation with foliation and others are at an angle (pitch 15° to 20°) to the foliation. Their general plunging and trend are 62°/41° NE.



**Figure 4.3 Pictures of subparallel to parallel alignment of elongated linear fabric elements in the rock.**

#### 4.1.3 Folds

The many folded structures observed in the study area are classified as minor crinkle and major folds based on their scale of size. The minor folds are recognized on the rock body within the major folded rock units. Ptygmatic fold features (Fig. 3.13) which mostly have chaotic orientations are observed in the dominion of migmatitic rock suite. Other folds are commonly seen in all lithologic units as similar, disharmonic curved double, and parallel-concentric folds because they resulted from different ductile compressional forces applied in different directions. Two major (mesoscopic folds) folds in the area observed (Fig. 4.8). These folds may be small

second-order parasitic features in the regional large megascopic fold. All the folds observed in the field are laid within three groups taking in account their axial-surface (AS).

#### 4.1.3.1 D<sub>1</sub> Folds

From these fold data it is believed to define the first three ductile deformations D<sub>1</sub> to D<sub>3</sub> in the study area. The first category of folds recognized as open-recumbent folds having a nearly horizontal axial surface (AS oriented in the east-west shown in Fig. 4.4). They have trend and plunge in the range of 260°/0° to 270°/7° and show vergence southward. This class of folds is a result of D<sub>1</sub> deformation event because they showed the same characteristics and structures orientations as it has been described in the literature.

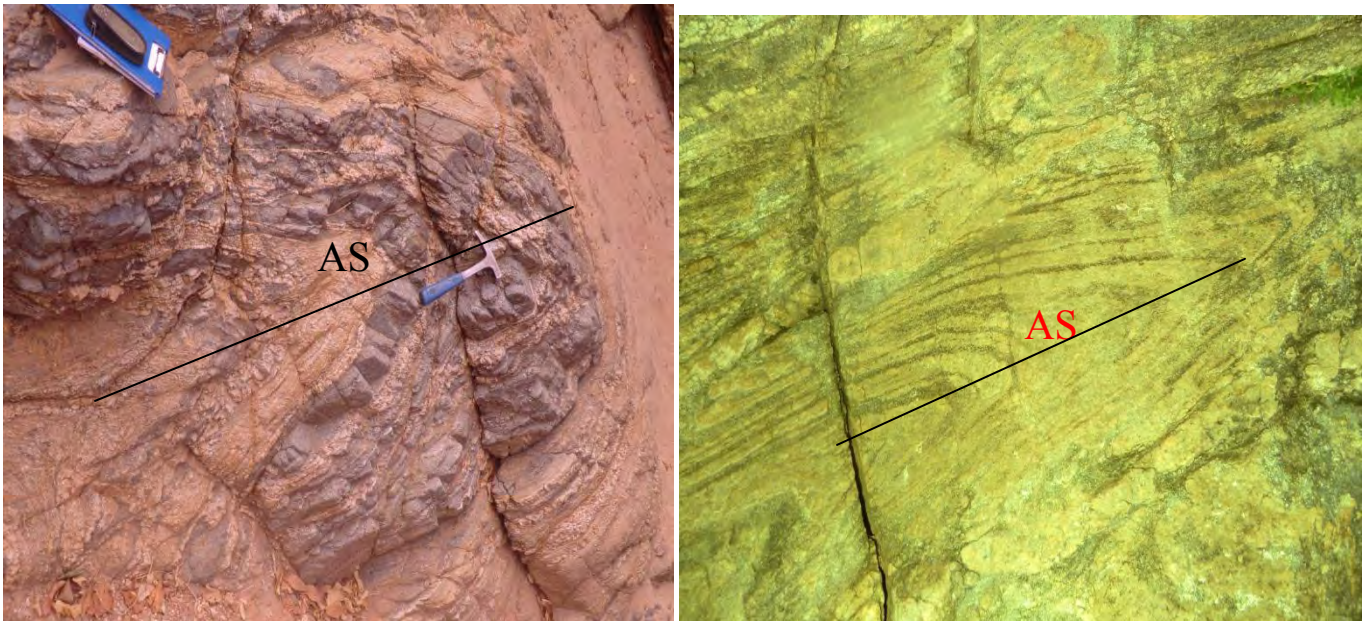


**Figure 4. 4 Photographs of open-recumbent folds taken in field. Felsic and amphibolitic layers folded as a result of D<sub>1</sub> deformation. Their axial plane is nearly horizontal.**

#### 4.1.3.2 D<sub>2</sub> Folds

The second fold class has NE axial surface and average trend/plunge 60°/40°. They are generally open-reclined folds verging to east. The responsible deformation phase for the creation of these folds is D<sub>2</sub> deformation (Fig. 4.5).

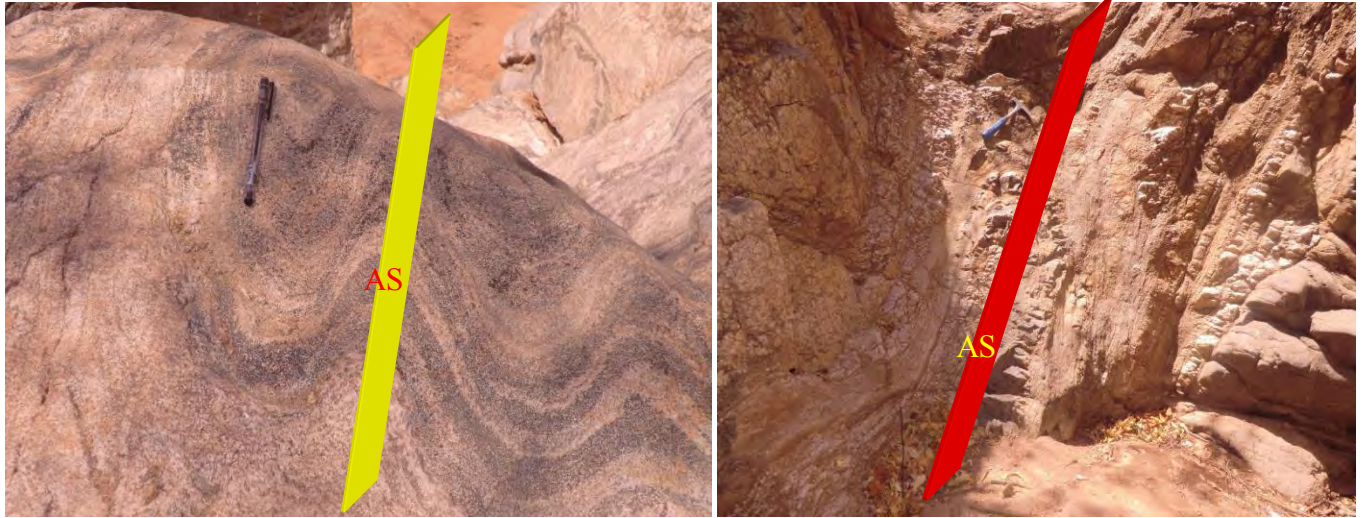


**Figure 4.5** Pictures of open-reclined folds resulted by D2 deformation. Their axial surface=NE trending.

#### 4.1.3.3 D<sub>3</sub> Folds

The last third class is those folds having NW axial surface which are resulted as D<sub>3</sub> at high T and low pressure. In nature, they are tight, vertical folds and have southwest vergence where the force was oriented from NE. The average trend and plunge of these folds are 320<sup>0</sup> and 90<sup>0</sup>, respectively (Fig. 4.6).

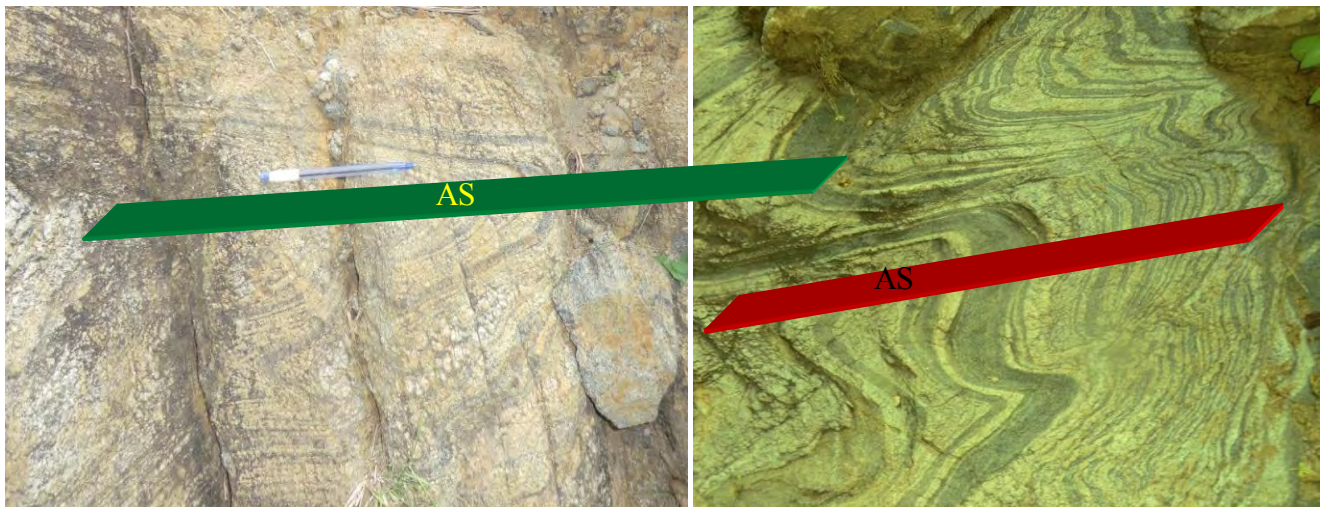


**Figure 4.6** Light felsic band with very thin dark layered segregation in the granitic gneiss is folded by D3 deformation.

There is fracturing of planar competent layers into rectangular fragments called boudins found in the area. They have similar sense of movement direction with the shear. Therefore, they are A-slip type boudinages showing that the ductile deformation condition is pertained to shear deformation (Fig. 4.7).



**Figure 4. 7** Photograph taken in the study area that shows boudinage in the granitic gneiss.



UTM 319012E  
0596837N



UTM 320423E  
0597685N

**Figure 4. 8** Photographs of mesoscopic anti-formal folds taken in the study area. (A) Flattened amphibole relic in granitic rock is mesoscopically folded. (B) An open fold is observed in the migmatitic rock suite.

#### 4.1.4 Joints/Fractures

The study area is also highly affected by joints and/or fractures (Fig. 4.9) evidencing the existence of brittle D<sub>4</sub> deformation. Therefore, several types of joints have been recognized in the different rock units like polysynthetic joints, brick joints/basket like, polygonal joints and parallel joints. Based on their alignment they are classified in to systematic and non systematic joints. Most the joints have relatively perpendicular alignment to the foliation direction within which they have been developed. Some of them are parallel and others are neither of the two orientations to the foliation trend.

The striking as well as the dipping direction of the joints/fractures is different either in the same place or in different places. The major trending directions measured in the field are NE, NW, NE, and N-S with their respective dipping directions NW, NE, SE, and E. Thus, depending on the striking- dipping relationship they were grouped into four sets (Fig. 4.16A) and the entire area data of them was presented in figure 4.16B. Most of the joints are slightly persistent and others are non- penetrative. They have dip amount between the ranges of 31<sup>0</sup> to 90<sup>0</sup>. The average joint spacing for most joints is about 20 cm-1 m and aperture ranges from 2 cm to 4 m and mostly filled with fine sediments and coarse materials like quartz veins, pegmatite veins and mica rare as well as felsites aplite dyke/sill. Some fractures are very recent where the apertures opened lacking infilling materials (see figure 4.10C & D).

As it has investigated from field data and equal-area plots of joints, there are three major sets of joints. These are generalized as those trending NE, NW and nearly E-W (Fig. 4.16B). In all cases, some of the joints are filled with felsites and aplite intrusions and quartz and pegmatite vein and some are not. Form the cross-cut relationship point of view of veins, relative aging has done for the fractures. So that veins oriented NE have been cut by those oriented NW ones in the field (Fig. 4.11F). This relation is also evidenced the aplite trending NE cut by NW trending felsite dike. Again from the vein relation, E-W trending fractures have been cut by NW trending joints meaning the formers are older in age than later ones (Fig. 4.10 and Fig.4.11G). But the age relationship between the NW and E-W trending joints are not evidenced during field work. So their relative aging is left to the next research.

As it has stated above, some joints are very recent and not filled by anything having trending either of three joint sets mentioned earlier. Without vein cross-cut relationship, it is somehow difficult to date their relative age and therefore their existence is merely noted (Fig.4.9).

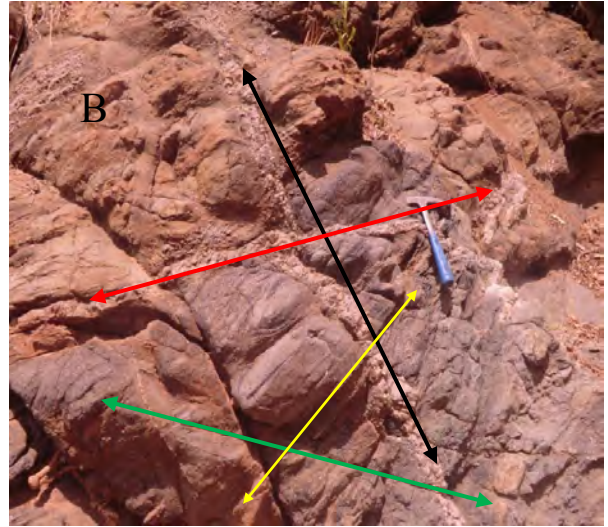


**Figure 4. 9** Photos taken in the field showing joints/ fractures. Picture (A & B) taken in the area showing four sets of joint. Pictures (C & D) taken from the study area showing that the area is being highly affected by earth dynamism in brittle environment where some areas are fractured in different directions ranging from mm to tens of centimeters. As it has shown in these photographs above (C & D), most probably there must be a very recent tectonic activity.



**Figure 4. 10** Field photograph taken in amphibolite rock in granite showing the relative age of joint based on the vein cross-cut kinship. Photo is taken facing E.

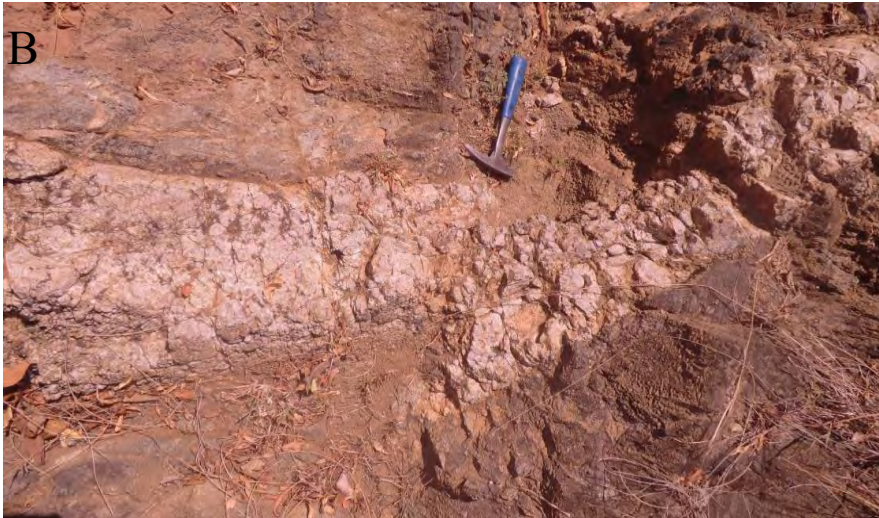
#### 4.1.5 Faults

All of the faults observed in the study area are minor faults; i.e. small scale slipped faults which are associated with all the different rock units. During the field survey, eight minor faults recognized in same place or different places. They all have a displacement ranging from 17 cm to 50 cm.

There is an east west striking sinistral-reverse/trust dip slip faults (see Fig. 4.11A). These faults gave rise a plausible clue that there was a sinistral shear deformation taken place most probably soon after  $D_3$  when the rock behaves brittle-ductile nature. This idea is reported by Geological Survey of Ethiopia (2003). The other category of deformation phase is the pure brittle deformation  $D_4^1$ . It resulted: (1) Northwest trending dextral-reverse/trust or -normal dip-slip and oblique faults; (2) Northeast trending dextral-normal dip slip faults and (3) Northwest trending sinistral-normal dip slip fault (see figure 4.11B-G below). These brittle deformation faults have NE and NW strike orientations and dip amount between the ranges of  $32^0$  to  $70^0$  and  $30^0$  to  $52^0$ , respectively.



*$D_4^1$  = In this deformation there are more than one phases of brittle deformation collectively put together as  $D_4$  for the sake of simplicity*



320647E

UTM 0595725N

Strike= $90^{\circ}$

Dip= $32^{\circ}$ S

Slip=17cm

Type: dextral reverse dip-slip fault

This photo is taken facing N



320717E

UTM 0595849N

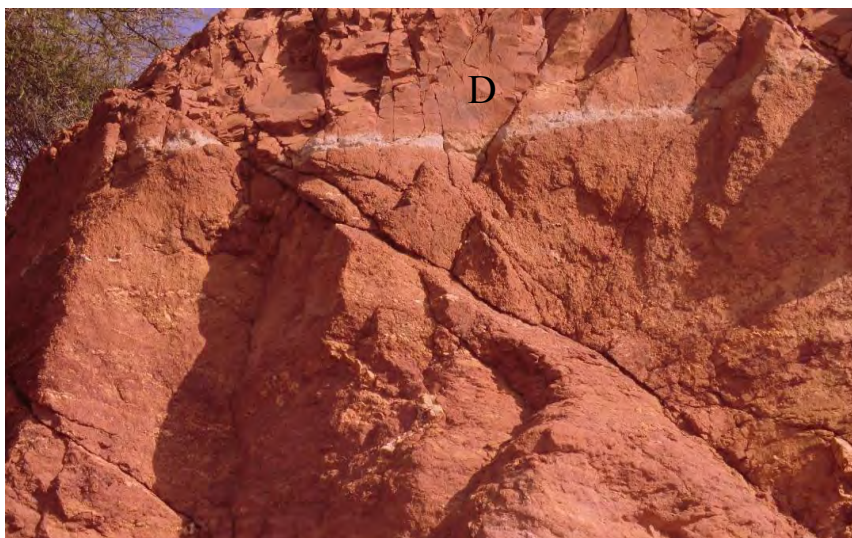
Strike= $340^{\circ}$

Dip= $30^{\circ}$ SW

Slip=35cm

Type: dextral reverse oblique fault

This photo is taken facing N



323976E

UTM 0595079N

Strike= $66^{\circ}$

Dip= $70^{\circ}$ SE

Slip=50cm

Type: dextral normal dip-slip fault

This photo is taken facing E



UTM 319840E  
 0597936N  
 Strike= $90^{\circ}$   
 Dip= $28^{\circ}$ S  
 Slip=7cm  
 Type: sinistral reverse dip-slip fault  
 Photo is taken facing NE



UTM 321105E  
 0598147N  
 Strike= $345^{\circ}$   
 Dip= $52^{\circ}$ E  
 Slip=29cm  
 Type: dextral reverse dip-slip fault  
 Photo is taken facing N

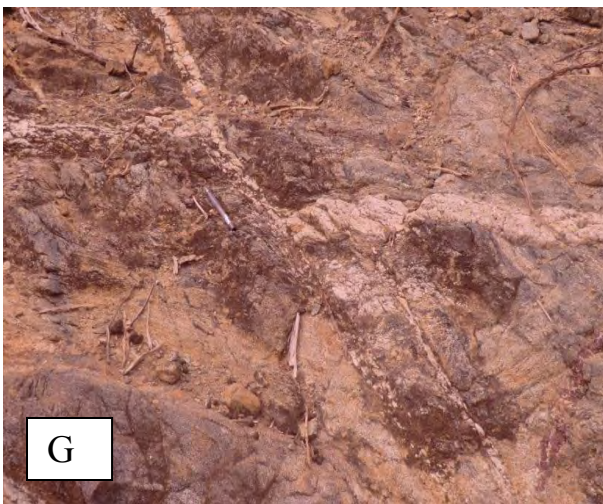


**Figure 4. 11** Fault photographs taken in the field. (A) A sinistral shear deformation taken in amphibolite rock which reveals brittle-ductile environment. (B) A dextral reverse dip-slip fault seen in granulite rock. (C) A dextral reverse oblique fault observed in granulite rock. (D) A dextral normal dip-slip fault taken in migmatite where the rock is baked by Tertiary volcanic pulse. (E) A sinistral reverse dip-slip fault photographed in granite. (F) A dextral reverse dip-slip fault taken in amphibolite. (G) Dextral normal. (H) Sinistral normal in amphibolite rock. Photo is taken facing S.

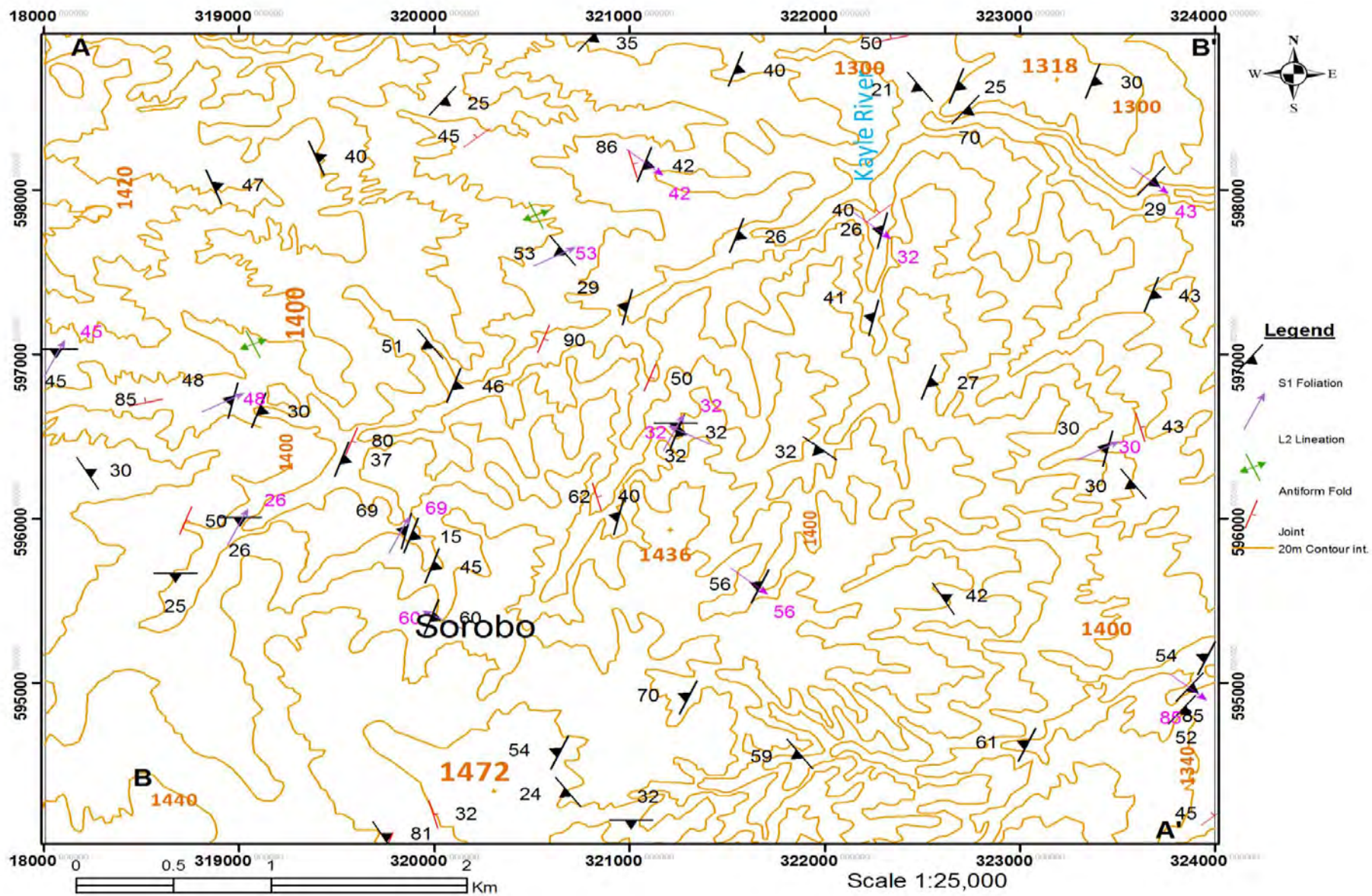
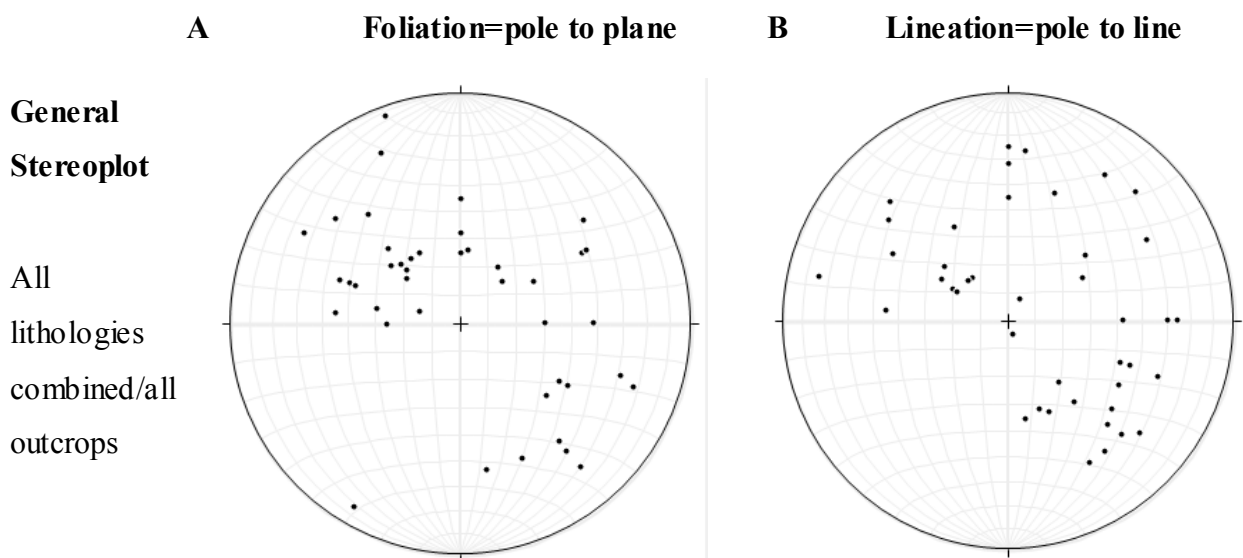


Figure 4. 12 Structural map of the study area

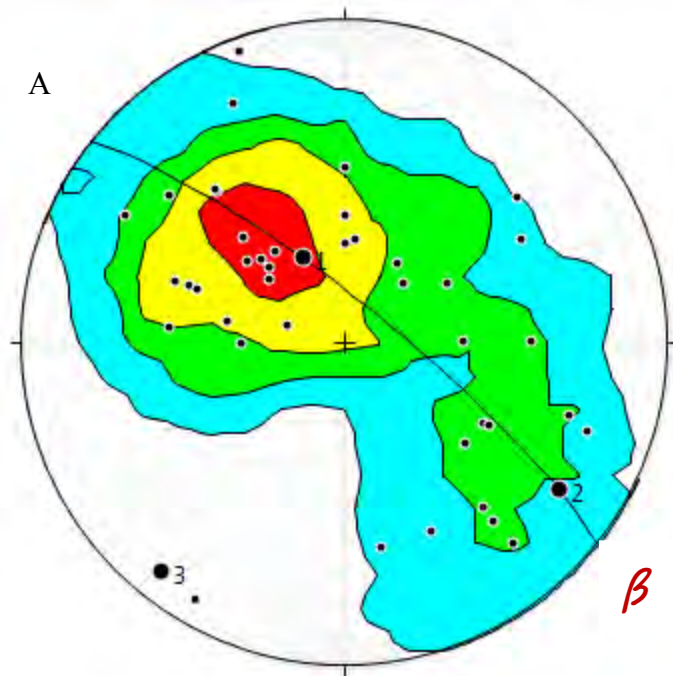
## 4.2 Equal-Area Projections

Two types of measurements were carried out in the Sorobo. Secondary foliation which is referred as  $S_1$  and stretching mineral lineations are defined as  $L_2$  are used in this research. Foliation and stretching lineations were both plotted in stereoplots, generated for amphibole and granitic gneisses, biotite-hornblende gneiss, granulite and charnockite high grade rocks as presented on the geological map (Fig. 3.1).

Because measurements were also taken in the entire area of study, a general Schmidt net is constructed with all data, including those from the mapped area. These stereoplots are generated for foliation planes and stretched mineral lineations, all lithologies combined (Fig. 4.14). Measurements used to generate these azimuthal projections are those used in the geological map. A combined pole to plane and rose diagram (Fig.4.16) are presented from the equal-area plot. Kamb and Mellis methods (Fig. 4.15 A & B below) are used among the four contouring methods (Schmidt, Mellis, Kalsbeek and kamb) since they are convenient for small number of data set (<100). Besides these, kamb method of contouring permits graphic analysis of the statistical significance of point concentrations on an equal-area plot. In addition it has alternative choice for area of contouring circle at any fraction from total area. The observed densities of foliation data are contoured at intervals of  $2\sigma$  (standard deviation) on the equal-area plot of kamb method of contouring that the population points have preferred orientation in the area of study.

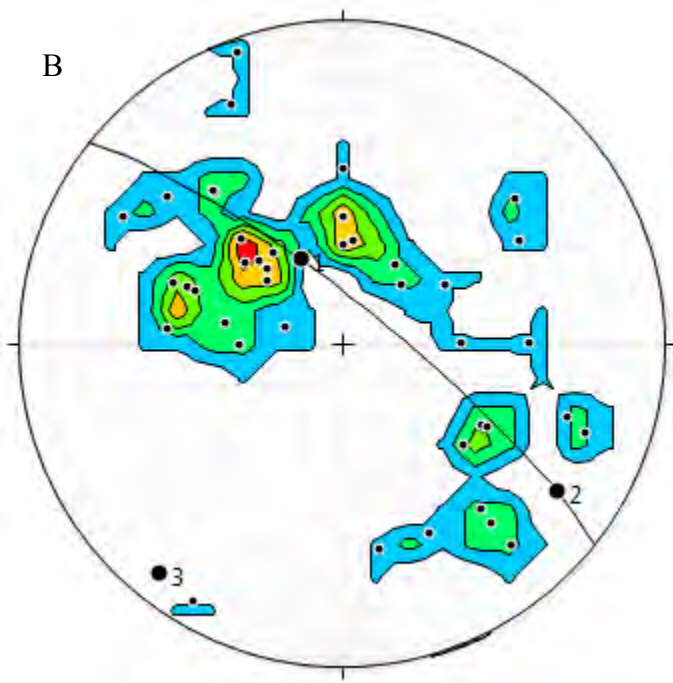


**Figure 4. 13 Equal-area projections for the whole data. (A) Stereoplots using an equal-area projection for the foliation data of different rock types observed in the entire area. Data combined measurements from the geological map. (B) Stereoplot for the lination data collected from the entire area. Number of data is 42.**



■ ---->2%  
 ■ ---->4%  
 ■ ---->8%  
 ■ ---->16%  
 (Max=17.6%)

№ Data= 42  
 Contour Interval = 2 sigma;  
 Calculated beta (mean principal orientation) axis  $129-309^0$   
 Best fit great circle (strike, dip RHR) = 308.5, 79.5



■ ---->1%  
 ■ ---->2%  
 ■ ---->4%  
 ■ ---->8%  
 (Max=1%)

№ of Data=42  
 Contour Interval = 2 %  
 Calculated beta (mean principal orientation) axis  $129-309^0$   
 Best fit great circle (strike, dip RHR) = 308.5, 79.5

Equal-area projection

Generated with

file:///Users/rwa/Desktop/Stereonet\_Windows/Stereonet%20Help/differences- with previous.html[11/14/2013, 8:50:43 PM]

**Figure 4. 14 Best fit great circle for pole to plane of S1 foliation data using an equal-area projection. (A) Kamb Contouring method. (B) Mellis (1%) Area Contouring method. The pole to plane shows that the rock is folded about a deeply S-W-plunging axis.**

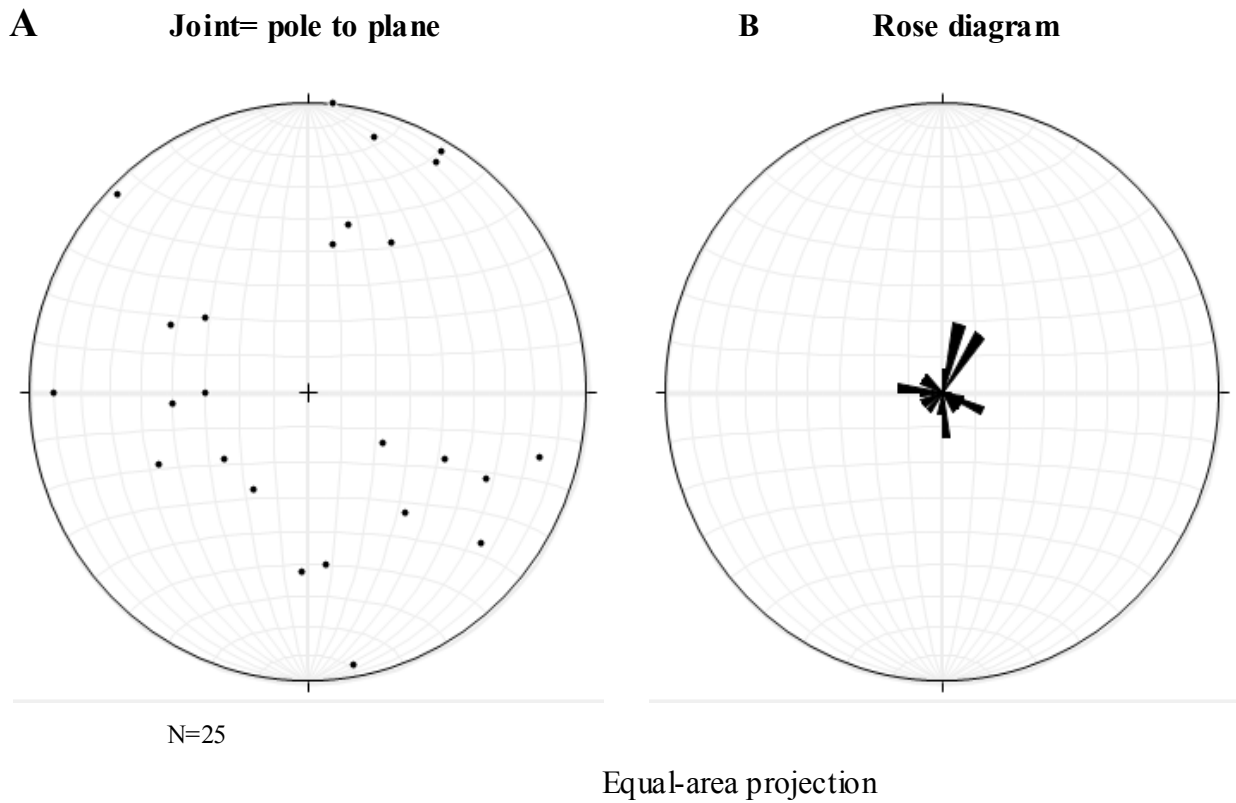


**Figure 4. 15** Azimuthal poles of joint data using an equal-area projection. (A) Pole to plane for the whole data of joint systems. (B) Rose diagram for the different sets of joint types observed in the entire area.

## **CHAPTER-V METAMORPHISM AND DEFORMATION HISTORY**

Petrographic observations of the rock samples of the Sorobo area have led to the identification of two different stages of “metamorphism events” which are defined as  $M_1$  and  $M_2$ .  $M_1$  is defined as the metamorphic peak assemblage reached during the deformation event of the Mozambique Belt Orogeny. It has reached up to upper granulite facies during the first two phases of deformation.  $M_2$  is defined as the metamorphic retrogression mineral assemblage reached back during the late deformation ( $D_3$ ) event. It is associated to a retrograde path where late crystallizations of granulite facies to amphibolite facies in granulite and charnockite.

### **5.1 Metamorphic History**

As far as only the metamorphic units are concerned, the rocks in the area consist of gneissose bands showing that they were faced high grade metamorphism. At least two phases of metamorphism are identified in the study area and they are designated as  $M_1$  and  $M_2$ . The first phase of metamorphism ( $M_1$ ) is associated with prograde of regional metamorphism resulted as the first two progressive deformations ( $D_1$  and  $D_2$ ), whereas the second metamorphic phase ( $M_2$ ) is characterized by local retrograde metamorphism presumably during end Pan-African shear deformation phase ( $D_3$ ) that had favored important condition for fluids conduit.

#### **5.1.1 Metamorphism in Charnockite**

##### **Prograde Metamorphism ( $M_1$ )**

The metamorphic peak assemblage is observed in the sample  $KS_2$ , notably because the mineral characteristics of the metamorphic peak facies (Cpx + Pl + Grt, +Opx). The assemblage Qtz + Grt + Kfs + Opx + Pl + Cpx + Hbl + opaque describes the average rocks composition (Fig. 3.4). The granulite facies assemblage Cpx + Pl + Grt + Opx (higher pressure) used as a characteristic assemblage of a granulite facies ( $M_1$ ). Again, the presence of orthopyroxene, clinopyroxene, hornblende and plagioclase together in the facies assemblage indicates the metamorphic rock has root of igneous protolith. The appearances of both pyroxenes (orthopyroxene and clinopyroxene) together indicate a complete dehydrated assemblage (Bucher and Frey, 1994) is taken place  $M_1$ .

## Retrograde Metamorphism ( $M_2$ )

In the charnockitic rock, retrograde is also reported on the basis of strong mineral reaction observed in the sample where early formed clinopyroxenes are progressively replacing by hornblende as well as serpentine minerals (Fig.3.4A). The proportion of pyroxene decreases while hornblende is produced coevally with intensive deformation shearing.

### 5.1.2 Metamorphism in Amphibole Gneiss (KS<sub>8</sub> &KS<sub>9</sub>)

#### Prograde Metamorphism ( $M_1$ )

The mineral assemblage in these rock samples Hbl + Pl + Qtz + Kfs ± Bt ± Chl ± Zircon ± opaque compose the total rock (Fig. 3.6). In the field, garnet (spessartine) minerals are abundant in the rock, but thin section study never showed any isotropic garnet. The amount of K-feldspar (3-10%) in the rock suggested that the metamorphic peak ( $M_1$ ) of this rock unit is reached upper amphibolite facies. The mineral assemblages Hbl + Pl + Grt (field observation) + Bt used to indicate the parent rock was igneous origin.

#### Retrograde Metamorphism ( $M_2$ )

The breaking down of biotite to a green colored mineral chlorite and replacement of pyroxene by hornblende manifested a retrograde metamorphism ( $M_2$ ) was happened in the rock (Fig. 3.6D &E). Zonations of composition are reported on the amphibole (sodium glaucophane amphibole) as a result of its alteration to actinolite. This zonation indicates there is reaction partitioning in composition of material to give changes in disequilibrium condition.

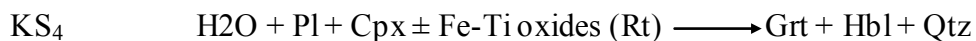
### 5.1.3 Metamorphism in Granulite Gneiss (KS<sub>3</sub>, KS<sub>4</sub>, KS<sub>10</sub>)

#### Prograde Metamorphism ( $M_1$ )

Mafic rocks have locally reached  $M_1$  in the high-pressure granulite facies evidenced by the association Grt + Cpx + Qtz + Pl + Rt in samples KS<sub>3</sub>, KS<sub>4</sub> and KS<sub>10</sub> (Fig. 3.7). The assemblage Qtz ± Grt ± Cpx + Pl ± Rt ± Ep ± Hbl ± Bt + opaque describes the whole rocks composition representing metamorphic peak condition. The presence of Cpx + Hbl + Pl ± Grt makes its characteristic assemblage of granulite facies. The characteristic assemblage also used as an indicative of the protolith (igneous parent) from which the metamorphic rocks are yielded.

## Retrograde Metamorphism (M<sub>2</sub>)

Alteration of biotite at its rims to chlorite and progressive replacement of clinopyroxene by hornblende (Fig. 3.7C) evidenced a temperature drop was occurred during the uplift of the area as a consequence of D<sub>3</sub> deformation. As the reaction proceeded, the neo-formed hornblende in filled the clinopyroxene grains but it also formed new single grains. Barink (1984) published a paper in which he investigated pyroxene replacement by hornblende in a metagabbro. The author described the replacement of pyroxene by hornblende, assumed to be isochemically balanced with replacement of plagioclase by garnet. As a conclusive metamorphic reaction he obtained the following equation:



The authors also noticed that this reaction is actually the reverse of one of the De Waard reactions (De Waard, 1965; Jen and Kretz, 1981) which are thought characteristic for the progressive amphibolite to granulite facies transition. During the thin section analysis, around 38 % of quartz is observed in KS<sub>4</sub> prohibiting the use of the term metagabbroic. The abundance of quartz however does not necessarily have an impact of the proposed reaction, and the other settings of this equation remain relevant with the observations. Fe-Ti oxides can be evidenced by accessory mineral rutile.

### 5.1.4 Metamorphism in Biotite-Hornblende Gneiss (KS<sub>7</sub>)

#### Prograde Metamorphism (M<sub>1</sub>)

The mineral assemblage (Fig. 3.8) in sample KS<sub>7</sub> Qtz + Pl + Opx + Bt + Hbl + Cpx + opaque describes the average modal rocks composition observed at the metamorphic peak but compositional variations are reported depending upon the field view in the sample. Locally, the highly sutured quartz boundaries highlight the high temperatures the samples have reached. The granulite facies assemblage Bt + Opx + Cpx + Hbl + Pl used as a characteristic equilibrium mineral assemblage where the rock has igneous origin.

#### Retrograde Metamorphism (M<sub>2</sub>)

Orthoclase series possesses stringer perthitic exsolved texture under crossed polarizer light (Fig. 3.8B). The orthopyroxene has being replaced by serpentine which developed a bastite texture (Fig. 5.1 below).

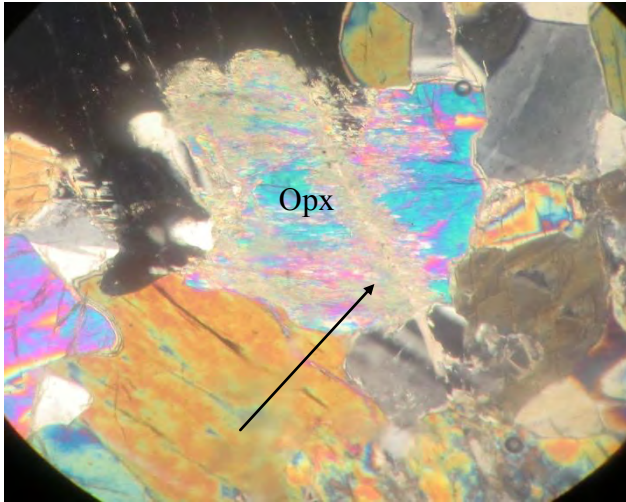


**Figure 5. 1 Photomicrograph showing bastite texture in orthopyroxene.**

### **5.1.5 Metamorphism in Granitic Gneiss (KS<sub>6</sub>)**

#### **Prograde Metamorphism (M<sub>1</sub>)**

The mineral assemblage of this rock (Fig. 3.9) is Qtz + Bt + Pl + Kfs + Ep + Hbl + Chl + opaque minerals describe the average rocks composition observed at the metamorphic peak. Low proportion of K-feldspar and the presence epidote in the rock, the assemblage cannot be used as a healthy characteristic of a granulite facies, but an upper amphibolite facies (hornblende + plagioclase + garnet (seen in field) + biotite) is certainly attained.

#### **Retrograde Metamorphism (M<sub>2</sub>)**

The laths of hornblende as well as broad flakes of biotite alter to green colored mineral called chlorite at their edges (Fig. 3.9A & C). Thin section studies show the opaque minerals in this granitic gneiss composition that pertained with biotite and hornblende (Fig. 3.9E & D) suggesting that both of them have undergone dissolution. These opaque minerals may be magnetite.

### **5.1.6 Metamorphism in Migmatite (KS<sub>5</sub>)**

#### **Prograde Metamorphism (M<sub>1</sub>)**

The migmatite rock shows flows of thin light bands appearing as a chaotic leucosome features as a result of partial melting at higher temperature. The assemblage Qtz + Bt + Pl + Kfs + Ep + Hbl + opaque illustrates the total rocks composition observed at the metamorphic peak (Fig. 3.12). K-feldspar + melt characterize metamorphic peak facies.

Partial melting, in migmatite is evidenced by the common occurrence of migmatite and leucosome (Fig. 3.11) volumes. In the first case, the rock itself is partially molten whereas leucosome volumes occur as intrusive dykes or chaotic pods composed of felsic minerals which segregated from the host rock during the partial melting. In this section focus was given on these mesosome volumes, especially on their composition.

#### Retrograde Metamorphism ( $M_2$ )

Melt shows evidences of a temperature drop in the migmatite; biotite and hornblende, as well as many perthite exsolution lamellae (orthoclase) are commonly observed (Fig. 5.2B).

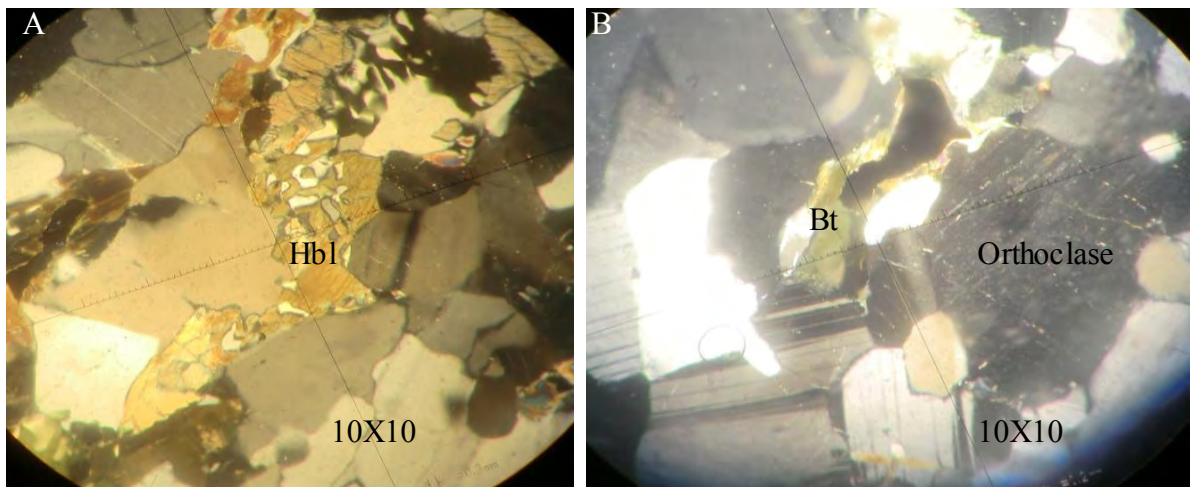


**Figure 5.2** Micropictures resulted as temperature drop. (A) Quartz and rare hornblende in a mesosome volume show graphic intergrowth texture. Crossed polar. (B) Biotite and orthoclase feldspar. Note orthoclase exhibits perthitic texture and dissolution of biotite precipitated by opaque. Crossed polar.

As the main catalyzer and reactant during partial melting,  $H_2O$  fluids have an important role in the whole rock chemistry. Close look of biotite under high power objective lens, its rims are altering hydrothermally to chlorite (Fig. 3.12B & E) through green biotite with magnetite (opaque). Serpentinization is an open-system (metasomatism) which must involve aqueous in order to create serpentine minerals (Best, 2003). So, it is believed that the replacement of and orthopyroxene by serpentine creating mesh and bastite textures resulted from fluid interaction (see Fig. 3.4A and Fig. 5.1).

#### 5.1.7 Metamorphism in Tremolite-Actinolite Schist ( $KS_1$ )

##### Prograde Metamorphism ( $M_1$ )

The assemblage Qtz + Tremolite + Act + Chl + Ep describes the average rocks composition observed at the peak of metamorphic equilibrium. Minerals such as chlorite, epidote and

actinolite are characterized the metamorphic peak to greenschist facies (Fig. 3.14). The absence of biotite in the rock assemblage manifests the metamorphic grade is to lower greenschist facies where the temperature is less than 400<sup>0</sup>C.

#### Retrograde Metamorphism (M<sub>2</sub>)

The petrographic study showed there is alteration of tremolite-actinolite series to chlorite mineral which revealed there was temperature drop in the metamorphic history (Fig.3.14).

## 5.2 Deformation Microstructures

In this section, deformation microstructures that encountered in the thin sections have been reviewed. As a rock undergoes increasing pressure-temperature metamorphic conditions, minerals are subjected to an increasing flow stress and the internal strain energy which also increases needs a counterpart to prevent the crystal lattice from breaking down. In order to reduce this flow stress, physical processes occur, among which dynamic recrystallization, which is reviewed here and quartz is taken as a good indicator in this paper because of its easily responding nature to stress.

Quartz easily been deformed by dynamic recrystallization which is a key mechanism for understanding deformation processes and the most important deformation mechanism in quartz. Three sub-processes commonly occur depending upon temperature conditions and strain rate. They originate from two physical mechanisms which are namely the migration of existing grain boundaries and the formation of new grain boundaries (Hirth and Tullis, 1992; Stipp et al., 2002).

Grain boundary migration recrystallization (GBM) is observed within high temperature conditions. This domain is characterized by highly amoeboid grain shapes (Fig. 5.3). Within GBM (1) Sub-domain, grain sizes and shapes are variable but contour of individual grains are still observable and grain boundary pinning commonly occurs (2) Grain boundary pinning is weak and for the highest temperature conditions, chessboard patterns are observed. They are evidences for even higher temperature where quartz grains are larger displaying even more amoeboid shapes and grain boundaries which are not always detectable (Fig. 5.3A). The transition from GBM (1) to (2) is suggested to be related to transition between quartz  $\alpha$  to quartz  $\beta$  while temperature elevates.

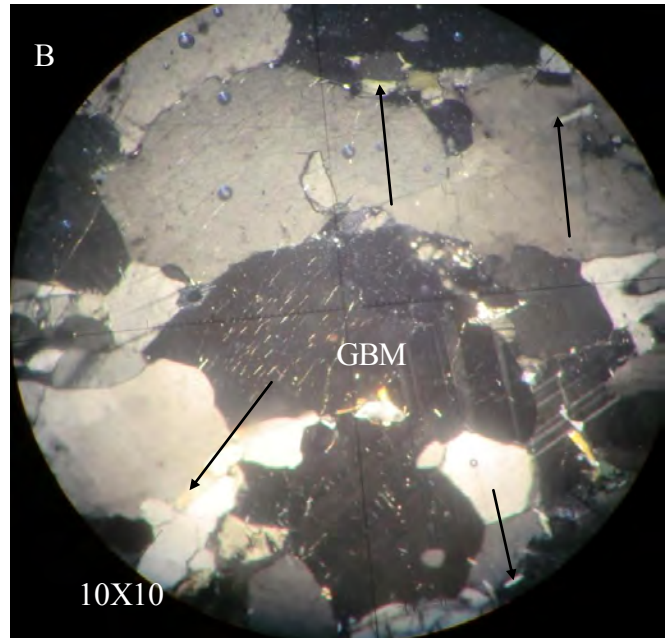
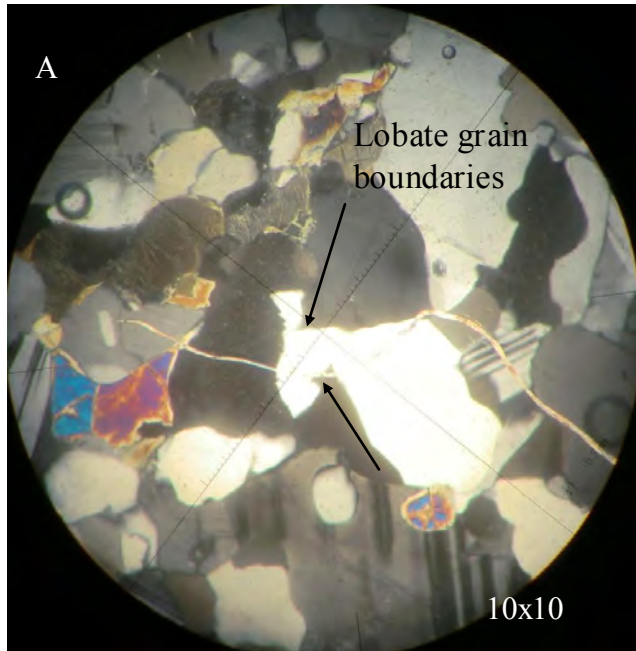


**Figure 5.3** Deformed quartz crystals due to dynamic recrystallization. (A) Close-up on lobate grain boundaries illustrating GBM mechanisms. Crossed polars. (B) Grain boundary migration in a granite gneiss. Crossed polars.

In the study area, the metamorphic evolution was investigated by field observation data and optical microscopic evidences. Throughout thin section study, the mineral reactions and microstructural evidences allowed defining two distinct metamorphic events. The first deformation event is believed to be Precambrian age because the metamorphic peak assemblage in  $M_1$  showed the same characteristics and structures orientations as it has been described in the literatures. The enhancement of progression metamorphism is terminated at a stage of post-colleSSIONAL ductile shearing (Shackleton and Ries, 1984; Shackleton, 1986) which resulted back retreatment of high temperature minerals to low temperature ones in  $M_2$  metamorphism.

### **6.1 Precambrian Metamorphic Assemblage ( $M_1$ )**

Progressive Path:

Mafic to ultramafic rocks have locally reached metamorphic peak assemblage  $M_1$  in the high-pressure and very high granulite facies evidenced by the association Grt + Cpx + Qtz + Pl and Grt + Qtz + Pl + Rt (described by Elvevold et al., 2003), in samples KS<sub>2</sub> and KS<sub>4</sub>, respectively.

In rock samples of (KS<sub>2</sub>, KS<sub>3</sub>, KS<sub>4</sub>, KS<sub>7</sub> and KS<sub>10</sub>) the mineral assemblages observed were indicated the metamorphic peak reached up to granulite facies conditions ( $M_1$ ) or in a retrograde and lower grade metamorphic stage (upper amphibolite facies). In these samples, the assemblage Grt + Cpx ± Rt defined the metamorphic peak and terminated the prograde path. The mineral assemblages of these rock samples are quartz ± orthopyroxene (hypersthene) ± clinopyroxene + hornblende ± biotite + plagioclase ± garnet ± rutile + opaque. This assemblage together with the observed inequigranular texture indicates the granulite facies metamorphism (Bucher and Grapes, 2011).

### **6.2 Precambrian Metamorphic Assemblage ( $M_2$ )**

Retrograde Path:

The main argument for a retrograde path is given by a set of granulite facies to amphibolite facies samples and by some reaction textures affecting the peak assemblage in the granulite facies samples. This retrograde path is somehow related to the onset of D<sub>3</sub> shear deformation episode. This late retrograded event is characterized by the gneisses in the area which is marked by mineral assemblages Hornblende + Plagioclase + Pyroxene + quartz + epidote ± opaque.

This metamorphic phase is characterized by regional retrogression that is observed in all high grade metamorphic units. Clinopyroxenes which are progressively replaced by hornblende amphibole (Fig. 6.1A) according to a mineral reaction retrogressing in the sample KS<sub>2</sub> from the granulite to the amphibolite facies is defined there was post-M<sub>1</sub> metamorphism. Serpentinization, epidotization, sercitzation and chloritization processes in pyroxenes, feldspar, and biotite are also some processes that manifest the occurrence of retrogression.

Late quartz inclusions in sample KS<sub>10</sub> (granulite) are locally suggested to be the result of late recrystallizations during retrograde metamorphism. Likewise, quartz annealing is often encountered and suggests late mineral re-equilibration (Fig. 6.1B).

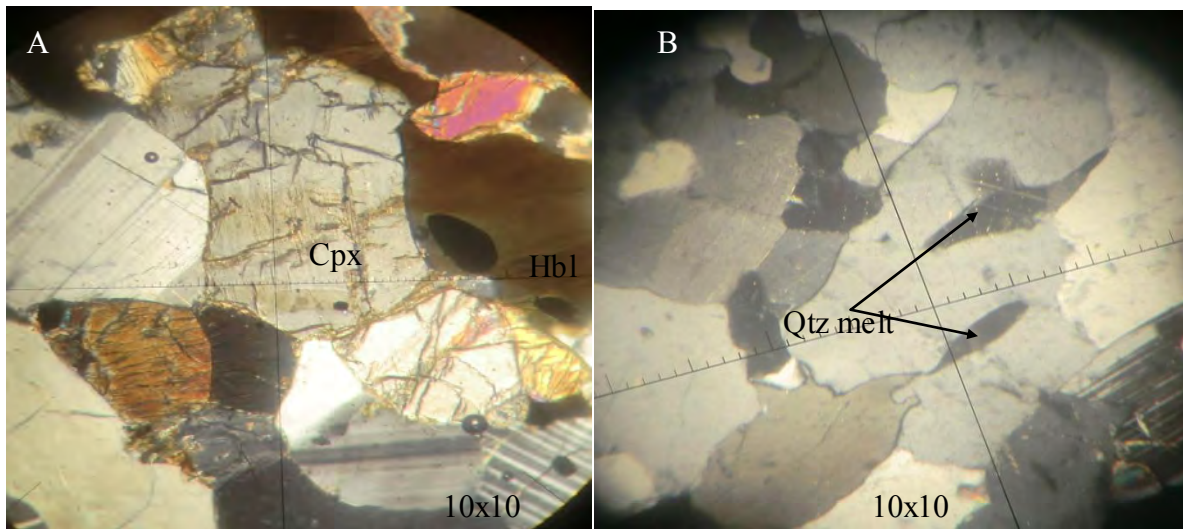


**Figure 6.1** Pictures showing recrystallization as result of temperature decline. (A) Microphotograph of a retrogressed focusing on a mineral reaction of a wide clinopyroxene crystal being replaced by hornblende, epidote minerals in charnockite rock. (B) Quartz melt in leucosome volume in migmatite. Both are in crossed polars.

**7.1 Conclusions**

The area of study Sorobo, in southern Ethiopia is covered by high grade metamorphic rocks which are classified as amphibole gneiss, biotite-hornblende gneiss, granulite gneiss, granitic gneiss, tremolite-actinolite schist, migmatite, and charnockite based on both field observation data and petrographic study. The amphibole gneiss rocks have covered the largest part of the study area followed by granitic and granulite rocks accordingly. Migmatitic rock patches are observed in amphibolite and granulite units and not mapped in this paper. It also comprises syn- to post-tectonic intrusive bodies that range from ultramafic to granitic in composition and various pre- to post- rift deposits.

The evolution aspect of the tectonic history is started with three ductile and a brittle-ductile which eventually lasted in brittle deformation. The data revealed that the first two phases of deformation folded and refolded the existing rock planar but the three one is accompanied with intensive shearing. Petrographic study of the rock samples of all lithologies from the area are shown that  $D_1$  and  $D_2$  deformations predate progressive upgrading of minerals to migmatization and high grade metamorphism and successive mineral paragenesis.  $D_3$  phase of deformation is evidenced by different small scale fold taken field data which might happen after collisional ductile shear environment. Brittle-ductile deformation is also taken place in the area where lots of its results (faults, joints, fractures, etc) in the field are recognized. Micro-veins supported this event (see Fig. 6.2A).

All the litho-units are extensively deformed and metamorphosed consequently possess gneiss texture. But relics of mafic to ultramafic origin rocks (xenoliths of amphibolite) can be noticed here and there during field survey (Fig. 3.9B).  $M_1$  metamorphism in rock units such as charnockite, granulite, and biotite-hornblende reached granulite facies, whereas in the other lithologies it reached upper amphibolites facies. The protolith and paragenesis of the rocks (metamorphic rocks) is recognized from the thin section analysis and generally, their origins were noticed as igneous rocks.

During the Precambrian path, petrographic evidences for a retrograde episode are reported, witnessing exhumation or thrust folding processes. This retrogression occurred in conjunction with a strong retrograde gneissosity textures produced by intensive shearing. Herein,

recrystallization of quartz is commonly observed. Furthermore, epidotization, chloritization, serpentization and mineral alterations are recognized in-situ (in field) and in lab investigation.

In the Konso Sorobo, particularly in charnockite rock, complete dehydration process is manifested by the coexistence of orthopyroxene and clinopyroxene. All the micas react-out with the evolution of metamorphic grade instead there is appearance of potassium feldspar in the rock. With increasing temperature, the importance of partial melting is outlined by the importance of migmatites as well as leucosome lenses and layers scattered in the rock (where the temperature could account 650<sup>0</sup>-1100<sup>0</sup>C).

In granulite, migmatite and amphibole gneisses, about 5-10% opaque minerals are reported, mostly they are concomitant to biotite and hornblende; and sometimes associated with pyroxene. These opaque minerals are precipitates of substrates where the minerals were dissociated with the temperature decline. Elsewhere, about 2% of rutile is identified in granulite rock.

The area is highly affected by different tectonic structures like folds, faults, joints, fractures and shear foliations. It is also affected by different intrusions including; pegmatite veins, quartz veins, felsite dikes, aplite and basalt dikes.

Orientation of foliation data on the entire map showed there is regional fold with parasitic folds on its limbs. Whereas, plot of pole to plane foliation data indicated the whole area is folded deeply and trends southwesterly.

## **7.2 Recommendation**

Even if the present research is considered as enough when the objectives and aims are concerned, further studies had better to recommend in next researches. Therefore, the following studies will be recommended:

- The present study is limited to field observation and thin section analyses, geochemical analysis is needed to know the major and trace elemental composition of the whole rock. This also will help to understand well the protolith of the rocks as well as the type of tectonism took place in the area. In the present work, relative aging is presented but the absolute aging is required.
- There are recrystallized quartzs seen during the petrologic examination, so, temperature ranges of these quartz dynamic recrystallizations should be accurately constructed.

Geothermobarometry study of P-T conditions prevailing during metamorphism using electron microprobe is needed.

- The presences of sulphide such as pyrite in the quartz veins and tourmaline bracketed together with coarse-grained pegmatite intrusions are good clue to be alert for the further exploration. In addition, from 5 to 10% of opaque minerals are reported in this research, but still it requires ore microscope/reflected light microscope study for the identification of these opaque minerals.

## Reference

- Abdelsalam, M. G. and Stern, R. J. (1996). Stures and shear zones in the Arabian-Nubian Shiel. *J. Afr. Earth Sci.* **23**: 289-510.
- Abdelsalam, M. G., and Stern, R. J. (1998). Formation of juvenile continental crust in the Arabian–Nubian shield: evidence from granitic rocks of the Nakasib suture, NE Sudan. *Geol Rundsch* **87**:150–160.
- Alene, M., & Barker, A. J. (1993). Tectonometamorphic evolution of the Moyale region, southern Ethiopia. *Precambrian research*, **62**(3), 271-283.
- Amenti, A. (1996). The Precambrian of southern Ethiopia. Unpublished Ep., EIGS, Addis Ababa, Note No. 397, 6pp.
- Amenti, A., Nassir, H., Tesfaye, Y., Woldegebriel, G., Getahun, S., Kiros, M. and Tadesse, A. (1992). Geological evolution of the proterozoic of southern Ethiopia. 29<sup>th</sup> Inter. Geol. Congr. Abstracts 2, Kyoto.
- Asrat, Asfawossen (1997). Geology and geochemistry of the Negash Pluton and their metallogenic significance, central Tigray. MSc Thesis, Addis Ababa University, Ethiopia.
- Asrat, A. and Pierre, B. (2003). Petrology, geochronology and Sr–Nd isotopic geochemistry of the Konso pluton, south-western Ethiopia: implications for transition from convergence to extension in the Mozambique Belt. *International journal of earth sciences*.
- Asrat, A., Barker, P. and Gleizes, G. (2001). The Precambrian Geology of Ethiopia: a Review. *African Geoscience Review* **8**: 271-288.
- Asrat, A.; Barbey, P.; Gleizes, G.; Reisberg, L. and Ludden, J. (2002). Structure, géochimie et âge du pluton Negash (nord Ethiopie): implications sur la nature du Bouclier Arabo-Nubien (ANS) et ses relations avec la Chaîne Mozambique (MB). RST-19, 9–12 April, Nantes, Résumés, 51–52.
- Ayalew, T. & Gichile, S. (1990). Preliminary U–Pb ages from southern Ethiopia. In: Rocci G.
- Ayalew, T., Bell, K., Moore, J.M., Parrish, R.R.(1990). U–Pb and Rb–Sr geochronology of the Western Ethiopian Shield. *Geol. Soc. Am. Bull.* **102**, 1309–1316.
- Barink, H., W. (1984). Replacement of pyroxene by hornblende, isochemically balanced with replacement of plagioclase by garnet, in a metagabbro of upper amphibolite grade. *Lithos* **17**: 247-58.
- Bedru Hussien (1999). The Geology Structure & geochemistry of the crystalline rocks of the Moyale area, southern Ethiopia: Implications for the tectogenesis of the precambrian basement. Geological Survey of Ethiopia, 114p.

- Behrmann, J. H. and Weldehaimanot, B. (1995). A study of metabasite and metagranite chemistry in the Adola region (south Ethiopia): Implications for the evolution of the East African Orogen. *J. Afr. Earth Sci.* **21**: 459-476.
- Berhe, S. M. (1990). Ophiolites in north east and east Africa, implication for Proterozoic crustal growth. *J. Geol. Soc. London* **147**: 41-56.
- Best, M., G. (2003). *Igneous and Metamorphic Petrology*- 2<sup>nd</sup> ed. Blackwell Science Ltd, Germany, 463 pp.
- Bonavia, F. F. and Chorowicz, J. (1992). Northward expulsion of the pan-African of north-east Africa guided by a re-entrant zone of the Tanzania craton. *Geology* **20**: 1023-1026.
- Brodie, K. H., & Rutter, E. H. (1985). On the relationship between deformation and metamorphism, with special reference to the behavior of basic rocks. *In Metamorphic reactions*, Springer, New York **4**: 138-179.
- Bucher, K. and R. H. Grapes (2011). "Petrogenesis of metamorphic rocks." Springer-Verlag Berlin Heidelberg.
- Burke, K.C., Sengör, A.M.C. (1986). Tectonic escape in the evolution of the continental crust. In: Baranzangi, M., Brown, L. (Eds.), *Reflection Seismology: The Continental Crust*. American Geophys. Union Geodyn. Ser. **14**: 41-53.
- Chater, A. M. (1971). The geology of the Megado area of southern Ethiopia. -PhD. thesis Univ. Leeds.
- Davidson, A. (compiler) (1983). The Omo River project: reconnaissance geology and geochemistry of parts of Illubabor, Keffa, Gemu Gofa, and Sidamo Ethiopia. – Ethiopian Institution of Geological Surveys.
- Davidson, A., Moore, J. M. and Davies, J. C. (1973). Preliminary report on the geology and geochemistry of parts of Sidamo, Gemu Gofa, and Kefa Provinces. Rept. Omo River Project 1, Ministry of Mines, Addis Abeba.
- De Waard, D. (1965). "The occurrence of garnet in the granulite-facies terrane of the Adirondack Highlands." *Journal of Petrology* **6**(1): 165-191.
- de Wit, M. J. and Chewaka, S. (1981). Plate tectonic evolution of Ethiopia and the origin of its mineral deposits: an overview. In: Chewaka, S. & de Wit, M.J. (eds) *Plate tectonics and metallogenesis: some guidelines to Ethiopian mineral deposits*. *Ethiopian Inst. Geol. Surv. Bull No.* **2**: 115-129.
- Eby, GN (1992). Chemical subdivision of the A-type granitoids: petrogenetic and tectonic implications. *Geology* **20**: 641-644. Ethiopia, Univ. Southampton, M.Phil. thesis, U.K.

- Ethiopian Institute of Geological Survey (EIGS) (2010). Geological Map of Ethiopia, 2<sup>nd</sup> ed., Unpublished technical report, EIGS, Addis Ababa, Ethiopia, 129 pp.
- Ghebreab, W. (1992). The geological evolution of the Adola Precambrian greenstone belt, southern Ethiopia. *J. Afr. Earth Sci.* **14**: 457-469.
- Gichile, S. (1992). Granulites in the Precambrian basement of southern Ethiopia: geochemistry, P–T conditions of metamorphism and tectonic setting. *J Afr Earth Sci.* **15**:251–263.
- Gilboy, C.F. (1970). The geology of the Garibbero region of southern Ethiopia. Phd . thesis. Leeds University, UK 176p.
- Hirth, G. and J. Tullis (1992). "Dislocation creep regimes in quartz aggregates." *Journal of structural geology* **14**(2): 145-159.
- Höhndorf, A.; Meinhold, K. D. and Vail, J. R. (1994). Geochronology of an orogenic igneous complexes in the Sudan: isotopic investigations in north Kordofan, the Nubian Desert and the Red Sea Hills. *J. Afr. Earth Sci.* **19**: 3–15.
- Jelenc, D.A. (1966). Mineral occurrences of Ethiopia. Ministry of mines, Addis Ababa, Ethiopia, 14p.
- Jen, L. and R. Kretz (1981). "Mineral chemistry of some mafic granulites from the Adirondack region." *The Canadian Mineralogist* **19**(3): 479-491.
- Kazmin, V. (1972). Some aspects of Precambrian Development in Africa. Unpublished Nature, **237**: 160.
- Kazmin, V. (1978). Geology of Ethiopian basement and possible relation between the Mozambique and Red Sea Belt. *Egypt. J. Geol.* **22**: No. 1, 73-86.
- Kazmin, V. Shiferaw, A. and Balcha, T. (1978). The Ethiopian Basement: Stratigraphy and possible manner of evolution. *Geol. Rundsch.* **67**: 531-546.
- Key, R. M., Charsly, T.J., Hackman, T.J., Wilkinson, A.F. and Rundle, C. C. (1989). Superimposed upperProterozoic collision controlled orogenies in the Mozambique Orogenic belt of Kenya. *Precambrian Research* **44**: 197-225.
- Kretz, R. (1981). Site-occupancy interpretation of the distribution of Mg and Fe between orthopyroxene and clinopyroxene in metamorphic rocks. *Can Mineral* **19**: 493-500
- Kroner, A., Stern, R. J., Linnebacker, P., Manton, W., Rischmann, T. and Hussein, I. M. (1991). Evolusion of Pan- African island arc assemblages in the south Red Sea Hills, Sudan, and

- in SW Arabia as exemplified by geochemistry and geochronology. *Precambrian Research* **53**: 99-118.
- Küster, D. (1993). Geochemistry and petrogenesis of Permo-Jurassic oversaturated alkaline complexes of northern Kordofan, central Sudan. In: Thorweihe U, Scheandelmeier H (eds) *Geoscientific research in NE Africa*, Rotterdam, pp 197–201.
- Küster, D. and Harms, U. (1998). Post-collisional potassic granitoids from the southern and northwestern parts of the Late Neoproterozoic East African Orogen: a review. *Lithos* **45**: 177–196.
- Meert, J. G. (2003). Asynopsis of events related to the assembly of Eastern Gondwana. *Tectonophysics* **362**: 1-40.
- Melesse, M. and Demerew, Y. (2003). Report on the Geology, geochemistry and Geophysics of Konso area, southwestern Ethiopia: Unpublished, Addis Ababa, Ethiopia.
- Mengesha, T., Tadiwos, C. and Workneh, H. (1996). The Geological Map of Ethiopia, 1:2,000,000 scale, (2<sup>nd</sup> eds), EIGS, Addis Ababa.
- Mohr, P. A. (1960). Report on a geological excursion through southern Ethiopia; Geophys. Observ., *Addis Ababa, Bull.*, **2**: 1.
- Mohr, P.A. (1962). The Geology of Ethiopia. Univ. Coll. Of Addis Ababa press (reprinted in 1971 by the Haile Selassie University Press) Asmara, 268p.
- Paquette, J.L. and Nédélec, A. (1998). A new insight into Pan-African tectonics in the east–west Gondwana collision zone by U–Pb zircon dating of granites from Central Madagascar. *Earth Planet Sci Lett.* **155**: 45–56.
- Shackleton, R. M. (1997). Precambrian tectonics of northeast Africa. In: Al Shanti AMS (ed) *Evolution and mineralization of the Arabian–Nubian Shield*, **2**. Pergamon, Oxford, p 1–6.
- Shackleton, R. M. and Ries, A. C. (1984). The relation between regionally consistent stretching lineations and plate motions. *J. Struct.geol.* **6**: 111-117.
- Shackleton, R. M. (1986). Precambrian collision tectonics in Africa. In: collision tectonics (edited by Coward . M. P. & Ries, A. C.). *Spec. publs geol. Soc. Lond.* **19**: 329-349.

- Stern, R. J. (1994). Arc assembly and continental collision in the Neoproterozoic East African Orogen: Implication for the consolidation of Gondwanaland. *Annual Review of Earth and Planetary Sciences* **22**: 319-351.
- Stern, R. J. and Dawoud, A. S. (1991). Late Precambrian (740 Ma) charnockite, enderbite, and granite from Jebel Moya, Sudan: a link between the Mozambique Belt and the Arabian–Nubian Shield? *Geology* **99**: 648–659.
- Stipp, M.; Stunitz, H.; Heilbronner, R. and Schmid, S.M. (2002). "The eastern Tonale fault zone: a 'natural laboratory' for crystal plastic deformation of quartz over a temperature range from 250 to 700°C. *Journal of structural geology* **24**(12): 1861-1884.
- Tadesse T, Hoshino M, Suzuki K, Iizumi S (2000). Sm–Nd, Rb–Sr and Th–U–Pb zircon ages of syn- and post- tectonic granitoids from the Axum area of northern Ethiopia. *J Afr Earth Sci.* **30**: 313–327.
- Tadesse Yihunie (2003). Chemical Th-U-total Pb Isochron Ages of Zircon & Monazite from Granitic Rocks of the Negele Area, Southern Ethiopia. Geological Survey of Ethiopia
- Tefera, M., Chernet, T. and Haro, W. (1996). Geological Map of Ethiopia, second edition. Regional Mapping Department of the Ethiopian Geological Survey.
- Teklay, M., Kroner, A., Mezger, K. and Oberhänsli, R. (1998). Geochemistry, Pb-Pb single zircon ages and Nd-Sr isotope composition of Precambrian rocks from southern and eastern Ethiopia: Implication for crustal evolution in east Africa. *J. Afr. Earth Sci.* **26**: 207-227.
- Temtme, S. (1955). Short report of preliminary investigation for copper S-W of Magie, Imperial Ethiopian Govt, Ministry of Mines. Unpubl, 11p.
- Vail, J. R. (1976). Outline of the geochronology and tectonic units of the basement complex of northeast Africa. - *Proc. Royal Soc. A* **350**: 127-141, London.
- Vail, J. R. (1985). Pan-African (late Precambrian) tectonic terrains and the reconstruction of the Arabian-Nubian shield. *Geology* **13**: 839-842.
- Vail, J. R. (1989). Ring complexes and related rocks in Africa. *J Afr Earth Sci.* **8**:19–40.

- Warden, A. J. & Horkel, A. D. (1984). The Geological evolution of north-east branch of the Mozambique Belt (Kenya, Somalia, Ethiopia). *Mitt. Oesterr. Geol. Ges.* **77**: 161-184.
- Warden, A. J. (1981). Correlation and Evolution of the Precambrian of the Horn of Africa and Southwestern Arabia. Unpublished. PhD. Thesis, Mont. Univ., Leoben.
- Worku Hailu (1996a). Geodynamic development of the Adola belt (southern Ethiopia) in the Neoproterozoic and its control on gold mineralization. PhD. Thesis, University of Giessen.
- Worku, H. (1996b). Structural control and metamorphic setting of the shear zone-related Au vein mineralization of the Adola Belt (southern Ethiopia) and its tectono-genetic development. *J. Afr. Earth Sci.* **23**: 383-409, Oxford.
- Worku, H. and Schendelmeier, H. (1996). Tectonic evolution of the Neoproterozoic Adola Belt of southern Ethiopia : evidence for a Wilson Cycle process and implications for oblique plate collision. *Precambrian Research* **77**: 179-210.
- Worku, H. and Yifa, K. (1992). The tectonic evolution of the Precambrian metamorphic rocks of the Adola belt (southern Ethiopia). *J. Afr. Earth Sci.* **14**: 37-55.
- Yibas, B. (2000). The Precambrian geology, tectonic evolution, and controls of gold mineralisations in southern Ethiopia. Unpublished PhD. Thesis, University of the Witwatersrand, Johannesburg, South Africa, 448 pp.
- Yibas, B., Reimold, W.U., Armstrong, R., Koeberl, C., Anhaeusser, C.R. and Phillips D. (2002). The tectonostratigraphy, granitoid geochronology and geological evolution of the Precambrian of southern Ethiopia. *J. Afr. Earth Sci.* **34**: 57-84.
- Yibas, B., Reimold, W.U., Koeberl, C., and Anhaeusser, C.R. (2003a). Geochemistry of the mafic rocks of the ophiolitic fold and thrust belts of southern Ethiopia: constraints on the tectonic regime during the Neoproterozoic (900–700 Ma), **121**: 157-183.
- Yibas, B., Reimold, W.U. and Anhaeusser, C.R. (2000). The geology of the Precambrian of southern Ethiopia: I—the tectonostratigraphic record. Information Circular **344**, Economic Geology Research Institute, University of the Witwatersrand, Johannesburg, 21 pp.
- Yibas, B., Reimold, W.U., Armstrong, R., Koeberl, C., Anhaeusser, C.R. and Phillips, D. (2003b). Evolution of the East African and related orogens, and the assembly of Gondwana. *Journal of African Earth Sciences* **123**: 81-85.

### **Bibliography**

- Adams, A. E. ; Mackenzie, W. S.; Guilford, C. (1988). Atlas of Sedimentary Rocks under the Microscope.

Brandon Browne (2007). Atlas of Common Rock-Forming Minerals in Thin Section

MacKenzie, W.S.; and Guilford, C. (1994). Atlas of Rock-Forming Minerals in Thin Section

MacKenzie, W.S.; Donaldson, C.H.; and Guilford, C. (1988). Atlas of Sedimentary Rocks under the Microscope.

MacKenzie, W.S.; Donaldson, C.H.; and Guilford, C. (1988). Atlas of Igneous Rocks and Their Texture.

Passchier and Trouw (2005). Observations of deformation microstructure.

Pramod K. Verma (2010). Optical Mineralogy.

## Annex

Sample	Mineral present %	Description	Rock name
KS <sub>1</sub>	Act =52 Qtz =20 Tremolite=17 Ep = 6 Chl =5	<p><b>Actinolite:</b> Occurs as highly stretched laths of crystals that accommodate foliation, showing 13-21<sup>0</sup> extinction. The mineral has two sets of cleavages lined with its longest axis itself parallel to foliation. Epidotization and chloritization processes are commonly seen.</p> <p><b>Quartz:</b> Occurs as elongated aggregates. Individual subhedral grains vary in size between 0.05 and 1.5 mm. Grain size often increases in ribbons. Quartz is colorless, with no cleavage, no relief, it has a low birefringence and shows an undulose extinction. Quartz also occurs as inclusions and is locally suggested to be the result of late recrystallizations during retrograde metamorphism. Likewise, quartz annealing is often encountered and suggests late mineral re-equilibration. Some of quartz crystals have hexagonal which might be the original form of it. It also has pseudomorphs of pyroxene shape in some cases. The quartz mineral fills the most fractures of plagioclase, and biotite.</p> <p><b>Tremolite:</b> occurs as euhedral to subhedral; subrounded grains of phenocrysts. It is colorless, non pleochroic showing second order of polarization colors and moderate to strong birefringence. Its internal fractures are filled by dark minerals like sulfides and the rims showing epidotization.</p> <p><b>Epidote:</b> occurring as subhedral elongated crystals. It is colorless to light grey and shows a low birefringence; showing high interference colors of green and blue. It also has a single cleavage and presents a straight extinction parallel to its length.</p> <p><b>Chlorite:</b> is seldom observed as shredded crystals, in association with actinolite minerals. It is pale green, biaxial, low birefringence and displays anomalous colors. It also has one set of perfect basal cleavage and parallel extinction to its cleavage.</p>	Tremolite-actinolite schist
	KS <sub>2</sub>	<p>Pl = 30 Opx =16 Qtz =14 Cpx =14 Op =4 Grt =2 Hbl =5 Kfs = 15</p> <p><b>Plagioclase:</b> occurring as anhedral large crystals with a low relief and two cleavages at 90 degrees. But in some crystals the two cleavages are not at right angle. It possesses albite twinning and perthite texture (rare), an oblique extinction and a first order birefringence. Manebach twinning is also observed in this thin section.</p> <p><b>Orthopyroxene:</b> Pale green mineral showing pleochroism from green to pink with a moderate relief, a single cleavage, non-parting and a low-birefringence; opaque included. It presents a parallel extinction.</p> <p><b>Quartz:</b> Occurs as subhedral grains vary in size between. Quartz is colorless, with no cleavage, no relief, it has a low birefringence and shows a wavy extinction. It also shows pseudomorph of plagioclase.</p> <p><b>Clinopyroxenes:</b> broad pale green with a moderate relief, a single cleavage and a low-birefringence. It shows right hand angle between 15<sup>0</sup> to 40<sup>0</sup> extinction. It associated with olivine and shows serpentinization process too.</p> <p><b>Opakes:</b> Occurs as hedral to subhedral sometimes having anhedral shape (&lt;0.01 to 0.2 mm), and are dark in both plane and crossed polarized light cases.</p> <p><b>Garnet:</b> Colorless mineral, euhedral to subhedral, with no cleavage and has a high relief. The mineral is locally porphyroclastic with cracks.</p> <p><b>Hornblende:</b> Occurs as laths or subhedral to anhedral and sheared pale green grains exhibiting pleochroism. It shows an oblique extinction ranging from 14<sup>0</sup> to 22<sup>0</sup> with its cleavage and has high relief and a moderate birefringence. The characteristic diamond shaped cleavages and partings are poorly defined but still observable. Small crystals of quartz and opaque minerals are seen as inclusions in the large grains of hornblende. Commonly, it alters to green colored mineral called chlorite. The hornblende and biotite surrounded the opakes which might be suggestible that they had dissolved into which cavities the opaque has been precipitated.</p>	

PI = 38  
Cpx = 10  
Qtz = 27  
KS<sub>3</sub> Kfs = 7  
Op = 1  
Hbl = 11  
Rt = 0.5

**Clinopyroxene:** Colorless with a moderate relief, a single cleavage, a low-birefringence and inclined extinction. Clinopyroxenes contain inclusion, zoned and replaced by amphibole.

**Quartz:** Occurs as elongated aggregates, colorless, with no cleavage, no relief, it has a low birefringence and shows undulose extinction. It also occurs as inclusions and is locally suggested to be the result of late recrystallizations during retrograde metamorphism. Like wise, quartz annealing is often encountered and suggests late mineral re-equilibration.

**Rutile:** occurring as small anhedral blebs (~0.05mm) glued to a mass of plagioclase feldspars. It has dark yellow-orange color and very high relief. It is usually accessory mineral but is locally found in relatively high proportions.

**Opagues:** occurs as hedral to subhedral sometimes having anhedral shape (<0.01 to 0.2 mm). The individual grains are all enclosed by biotite and hornblende. All are dark in both plane and crossed polarized light cases.

**Hornblende:** happens as very anhedral and sheared pale green grains. It shows an oblique extinction, high relief and has a low birefringence. The characteristic diamond shaped cleavages are poorly defined. Zonations are locally reported and the mineral can be observed replacing clinopyroxenes.

**Clinopyroxenes:** pale green with a moderate relief, a single cleavage and a low-birefringence. The mineral presents at inclined extinction. It replaces adjacent olivine minerals.

**Garnet:** colorless, euhedral to anhedral large grains. It is isotropic, with no cleavage and has a high relief. The grains are often cracked and included quartz and locally porphyroclastic and partially deformed.

**Opaque:** occurs as hedral to subhedral sometimes having elongated shape. The individual grains are dispersed as columnar aggregates overall the rock sample. This situation allowed suggesting that the rock has been retrogressively metamorphosed favoring the minerals are likely to force dissolution process within which cavities the opaque minerals precipitated. As exception, large euhedral shaped (~0.6 mm) showing deep red color in both PPL and XPL.

**Biotite:** Occurs as thin to broad flakes laths; subhedral to hedral of cluster biotite crystals that accommodating the cleavage. Biotite shows straight extinction. The mineral has a single cleavage lined with its longest axis itself parallel to foliation. The extinction lies within ranges of 0<sup>0</sup> to 9<sup>0</sup> and the minerals show 3<sup>rd</sup> to 4<sup>th</sup> order of birefringence.

**Quartz:** Occurs as elongated aggregates, colorless, with no cleavage, no relief, it has a low birefringence and shows undulose extinction. It also occurs as inclusions and is locally suggested to be the result of late recrystallizations during retrograde metamorphism. Like wise, quartz annealing is often encountered and suggests late mineral re-equilibration.

**Plagioclase:** occurring as anhedral large crystals with a low relief and two cleavages at 90 degrees. But in some crystals the two cleavages are not at right angle. It possesses albite twinning and perthite texture, an oblique extinction and a first order birefringence. Manebach twinning is also observed in this thin section.

**Quartz:** Occurs as columnar aggregates. Individual subhedral to anhedral grains vary in size. Quartz is colorless, with no cleavage, no relief, it has a low birefringence and shows a wavy extinction. Some smaller fragments of quartz crystals overlapped feldspar or even larger quartz crystals itself which might suggest that they have brown by deformation. Graphic intergrowth relationship between hornblende and quartz was developed in this rock.

**K-feldspars:** Mineral occurring as anhedral grains exhibiting low to moderate relief, colorless, low order of birefringence, non pleochroic with two sets of cleavages. Microcline and orthoclase alkali feldspars are observed under

Granitic  
Gneiss

PI = 40  
Qtz = 35  
Bt = 10  
KS<sub>4</sub> Op/Rt = 7  
Hbl = 6  
Cpx = 8  
Grt = 0.4

Granulite  
gneiss

Qtz = 26  
Kfs = 24  
Hbl = 16  
Bt = 15  
KS<sub>5</sub> Pl = 20  
Op = 8  
Ep = 1

the microscopic study. The microcline series has a typical cross-hatched, whereas the orthoclase series possesses stringer perthitic exsolved texture under crossed polarizer light. Carlsbad twin is here and there observed which can be the characteristic of sanidine.

**Biotite:** Occurs as highly stretched crystals braining around dark porphyroclasts and accommodating the foliation. The biotite mineral shows straight extinction with its long axis. The mineral has a single cleavage lined with its longest axis itself parallel to foliation. Quartz inclusions are commonly observed possessing graphic intergrowth with the mineral. The careful study under the high power showed its rims are altering to vermiculite through hydrobiotite. The vermiculite recognized by its anomalous blue birefringence colour.

**Plagioclase:** Mineral occurring as very large crystals with a low relief. It possesses albite twins, an oblique extinction and a first order birefringence. Polysynthetic and penetrative twins are not uncommon. Plagioclases occur as broken and strongly altered grains with frequent overlaps of growth twins.

**Opakes:** Occurs as hedral to subhedral sometimes having elongated shape (<0.01 to 0.2 mm). The individual grains are dispersed as columnar aggregates all enclosed by biotite minerals. This situation allowed suggesting that biotites tend to dissolution process within which cavities the opaque minerals precipitated. All are dark in both plane and crossed polarized light cases except one large euhedral shaped (~0.2 mm) showing deep red color in both cases.

**Clinozoisute-epidote:** Mineral occurring as euhedral eight sided crystals (<0.005 to 0.1 mm) or columnar aggregates. Epidote: is colorless, non pleochroic and shows a low birefringence. It has twinning plane and also showing strong birefringence greenish blue color. The mineral has a single cleavage and presents an oblique extinction parallel to its length. The mineral is lying parallel with the biotite fabric.

**Plagioclase:** The mineral occurring as very large crystals with a low relief, and two cleavages at 90 degrees. It possesses albite twins and most portions it is anorthite, an oblique extinction and a first order birefringence.

Qtz = 47  
Pl = 21  
Hbl = 16  
KS<sub>6</sub> Op = 7  
Bt = 5  
Kfs = 2  
Chl = 2

**K-feldspars:** Mineral occurring as subhedral to anhedral grains exhibiting low to moderate relief, colorless, low order of birefringence, non pleochroic with two sets of cleavages. The extinction position lies between 5<sup>0</sup> to 15<sup>0</sup> values. It also shows first order, maximum up to first order of gray polarization colors. Sanidine and orthoclase alkali feldspars are observed under the microscopic study. Orthoclase series possesses stringer perthitic exsolved texture under crossed polarizer light. Carlsbad twin is here and there observed which can be the characteristic of sanidine.

**Hornblende:** Occurs as laths and/or subhedral to anhedral and sheared pale green grains exhibiting pleochroism. The mineral shows an oblique extinction and has a high relief and a moderate birefringence. The characteristic diamond shaped cleavages and partings are poorly defined but still observable. The extinction ranges from 14<sup>0</sup> to 22<sup>0</sup> with its cleavage. Small crystals of quartz and opaque minerals are seen as inclusions in the large grains of hornblende. Commonly, it alters to green colored mineral called chlorite.

Migmatite

Ep =2

**Biotite:** Occurs as laths and subhedral crystals braining around dark porphyroclasts and accommodating the foliation. Biotite shows straight extinction with its long axis. The mineral has a single cleavage lined with its longest axis itself parallel to foliation. Quartz inclusions are commonly observed possessing equant grains with the mineral. Both biotite and hornblende edges is shown that they are altering to chlorite.

Granitic  
gneiss

**Chlorite:** The chlorite is seldom observed as shredded crystals, in association with biotite and hornblende minerals. The mineral is pale green, biaxial, low birefringence and displays anomalous colors. It has one set of perfect cleavage and parallel extinction to its cleavage.

**Epidote:** Mineral occurring as smaller euhedral to subhedral crystals (<0,005 to 0.3mm). Epidote is colorless to light grey and shows a moderate birefringence. The mineral has high interference colors of green, red and blue. The mineral has a single cleavage and presents a straight extinction parallel to its length. The mineral is frequently observed within biotite fabric implying that there was retrograde metamorphism in the area.

**Quartz:** Occurs as broad or elongated aggregates. Individual subhedral grains vary in size between 0.05 and 1.5 mm. Quartz is colorless, with no cleavage, no relief, it has a low birefringence and shows an undulose extinction. Quartz also occurs as inclusions and is locally suggested to be the result of late recrystallizations during retrograde metamorphism. Lobate grain boundaries are common.

**Opaques:** Occur as hedral to subhedral sometimes having anhedral shape (<0.01 to 0.2 mm). The individual grains are all enclosed by biotite and hornblende minerals.

Hbl = 30  
Kfs = 10  
Pl = 14  
Qtz = 10  
Cpx = 10  
Bt = 21  
Op = 4

KS<sub>7</sub>

**Hornblende:** Occurs as laths (<0.05 to 3 mm) pale green grains exhibiting pleochroism. The mineral shows an oblique extinction and has a high relief and a moderate birefringence. The characteristic diamond shaped cleavages and partings are well defined. The extinction ranges from 14<sup>0</sup> to 22<sup>0</sup> with its cleavage.

**Biotite:** Occurs as thin to broad flakes laths; subhedral to hedral of cluster biotite crystals that accommodating the cleavage. Biotite shows straight extinction. The mineral has a single cleavage lined with its longest axis itself parallel to foliation. The extinction lies within ranges of 0<sup>0</sup> to 9<sup>0</sup> and the minerals show 3<sup>rd</sup> to 4<sup>th</sup> order of birefringence.

Biotite-  
hornblende  
gneiss

**K-feldspars:** Mineral occurring as subhedral to anhedral grains exhibiting low to moderate relief, colorless, low order of birefringence, non pleochroic with two sets of cleavages. The extinction position lies between 5<sup>0</sup> to 15<sup>0</sup> values. It also shows first order, maximum up to first order of gray polarization colors. Sanidine and microcline alkali feldspars are observed under the microscopic study with respective Carlsbad twinning and perthitic texture. Orthoclase series possesses stringer perthitic exsolved texture under crossed polarizer light.

**Clinopyroxene:** The mineral occurs as subhedral form, colorless, non pleochroic showing second order of polarization colors and moderate birefringence.

**Plagioclasem:** this mineral occurring as anhedral large crystals with a low relief and two cleavages at 90 degrees. But in some crystals the two cleavages are not at right angle. It possesses albite twinning and perthite texture, an oblique extinction and a first order birefringence. Manebach twinning is also observed in this thin section

**Quartz:** Occurs as big crystals aggregates. Some varying in size (<0.01-0.05) subhedral to anhedral equant individual grains of aggregates are dispersed in crystals as independent. Quartz is colorless, with no cleavage, no relief, it has a low birefringence and shows a wavy extinction and infrequently twinning.

**Opagues:** Occur as very small sized rarely having anhedral shape (<0.01 to 0.2 mm). The individual grains are seen as inclusion in all minerals. All are dark in both plane and crossed polarized light cases.

**Hornblende:** Occurs as anhedral- prismatic laths clusters pale green and yellow grains (Fig. 3.4F). The mineral shows an oblique extinction and has a high relief and a low birefringence. The characteristic cross-section shaped cleavages are clearly defined but some of the crystals lack this characteristics. Zonations of composition are locally reported on the amphibole as a result of its alteration to actinolite. Therefore, this amphibole is sodium glaucophane amphibole. The mineral also observed by replacing epidote where the epidote minerals are totally pseudomorphed by blue amphibole except rare cores. The hornblende itself is being replaced by pyroxene. Very non-ratable deep red non pleochroic and unextincting opaque minerals crystals are seen inclusions in hornblende.

**Plagioclase:** The mineral occurring as very large crystals with a low relief, and two cleavages at 90 degrees. It possesses albite, Bavena twins, and simple contact twinning, an oblique extinction and a first order birefringence. Pseudomorphs of plagioclase are seen in some parts the rock after replacement of calcic amphibole; hornblende (Fig. 3.4F).

**Quartz:** Occurs as big crystals clustered together. Some varying in size subhedral to anhedral equant individual grains of aggregates are dispersed in hornblende and biotite crystals as inclusions. Grain size often increases in ribbons. Quartz is colorless, with no cleavage, no relief, it has a low birefringence and shows a wavy extinction. Some smaller fragments of quartz crystals overlapped feldspar or even larger quartz crystals itself which might suggest that they have brown by deformation. Microstructures in the mineral crystals are filled by quartz microveins. Its rims show yellow colour. Opaque minerals are seen in the quartz crystals as inclusive. Some quartz crystals have pseudomorphs of epidote.

**K-feldspar:** Low relief mineral, small subhedral grains occur uncommonly mostly likely identified as microcline which is colorless with perthitic texture and a first order birefringence.

**Orthopyroxene:** Pale green mineral showing pleochroism from green to pinkish with a moderate relief, a single cleavage, partings and a low-birefringence. The mineral presents a parallel extinction. Some parts of its rims are show serpentinization. Hornblende mineral is replacing it. Euhedral to anhedral quartz ribbons present as overprints.

Hbl = 46

Pl = 24

Qtz = 15

Kfs = 10

Opx = 5

KS<sub>8</sub>

Amphibole  
gneiss

	Pl = 30	<p><b>Chlorite:</b> Occurs as laths of crystal clusters, in association with biotite micas. The mineral is pale green, and displays an anomalous birefringence. Chlorite is observed lying with the biotite fabric and occurs in late retrograde stages. Strong variations (from light green to blue) in the interference color of the mineral indicate that compositional changes locally occurred in the mineral.</p> <p><b>Quartz:</b> Occurs as elongated aggregates. Individual subhedral grains vary in size. Quartz is colorless, with no cleavage, no relief, it has a low birefringence and shows an undulose extinction. Quartz also occurs as inclusions of six sided and is locally suggested to be the result of late recrystallizations during retrograde metamorphism.</p> <p><b>K-feldspar:</b> Low relief mineral, small subhedral grains occur uncommonly mostly likely identified as microcline which is colorless with perthitic texture and a first order birefringence.</p> <p><b>Hornblende:</b> Occurs as anhedral- prismatic laths clusters pale green and yellow grains. The mineral shows an oblique extinction at <math>32^{\circ}</math> and has a high relief and a low birefringence. Like biotite, zircon and opaque minerals are associated with it.</p> <p><b>Zircon:</b> Occur as very small blebs including biotite and calcic amphibole. The mineral is colorless with a high relief and is easily identified by its dark halos, resulting from its radioactive decay. The characteristic color zoning in it might be formed as a result of more than one metamorphism phases.</p> <p><b>Opaque:</b> Occurs as hedral to subhedral sometimes having elongated shape. The individual grains are dispersed as columnar aggregates all enclosed by biotite and hornblende minerals. This situation allowed suggesting that both biotites and hornblende tend to dissolution process within which cavities the opaque minerals precipitated. All are dark in both plane and crossed polarized light cases.</p>	Amphibole gneiss
	Bt = 10		
KS <sub>9</sub>	Chl = 21		
	Qtz = 7		
	Op = 5		
	Kfs = 3		
	Hbl = 23		
	Zr = 1		
	Plagioclase = 40		
	Quartz = 10		
KS <sub>10</sub>	Biotite = 9	<p><b>Plagioclase:</b> occurs as very large crystals anhedral to subhedral with a low relief, and two cleavages at right angle. It possesses albite, Baveno twins, an oblique extinction and a first order birefringence. It shows granular texture with other grains. Inclusions of dark minerals (opaques) are commonly observed in the crystals. In some crystals, late deformation cleavages are developing.</p> <p><b>Quartz:</b> Occurs as elongated aggregates. Subhedral to anhedral individual grains vary in size. Quartz is colorless, with no cleavage, no relief, it has a low birefringence and shows undulose extinction. It replaces biotite and plagioclase locally which suggested to the result of late retrograde metamorphism.</p> <p><b>Biotite:</b> Occurs as highly stretched crystals braining around opaque porphyroclasts and accommodating the foliation that shows straight extinction. It has a single cleavage lined with its longest axis itself parallel to foliation. Its laths are altering to chlorite.</p> <p><b>Clinopyroxene:</b> pale green mineral with a moderate relief, a single cleavage and a low-birefringence. The mineral presents at inclined extinction. It replaces adjacent olivine minerals.</p> <p><b>Opaque:</b> Occurs as hedral to subhedral sometimes having elongated shape. The individual grains are dispersed as columnar aggregates in the rock suggesting that the rock has been retrogressively metamorphosed. All are dark in both plane and crossed polarized light cases.</p>	Granulite gneiss
	Cpx = 20		
	Op = 17		

## DECLARATION

I hereby declare that the thesis entitled "Metamorphism and Deformation History of Precambrian Rocks of Konso Area, Southern Ethiopia" has been carried out by me under the supervision of Mulugeta Alene (PhD), Department of Geology, Addis Ababa University, Addis Ababa during the year 2015 as partial fulfillment of MSc Degree program in Petrology. I further declare that this work has not been submitted to any other university or institution for the award of any degree or diploma, and also that all sources of materials used during the thesis work have been properly acknowledged.

.....  
Aspiron Hangibayna (Candidate)

.....  
Date

This is to certify that the above declaration made by the candidate is correct to the best of my knowledge and it has been submitted for examination with my approval as a university advisor.

.....  
Dr. Mulugeta Alene (Advisor)

.....  
Date